

49650

CENTRAL LIBRARY	
TEZPUR UNIVERSITY	
Accession No. <u>49650</u>	CENTRAL LIBRARY T U
Date <u>14/9/11</u>	ACC. NO. ... <u>T154</u>

REFERENCE BOOK  
NOT TO BE ISSUED  
TEZPUR UNIVERSITY LIBRARY

# **PREPARATION OF $\pi$ - CONJUGATED POLYMERS AND EVALUATION OF THEIR PHOTOVOLTAIC PROPERTIES**

**A thesis submitted  
in partial fulfillment of the requirements for the degree of**

***Doctor of Philosophy***

**By**

***Binod Pokhrel***

***Registration No. 107 of 2003***



**School of Science and Technology**

**Department of Chemical Sciences**

**Tezpur University**

**Napaam, Tezpur - 784028**

**Assam, India**

**November, 2010**

*Dedicated  
to my Parents  
With love and gratitude*

# PREPARATION OF $\pi$ -CONJUGATED POLYMERS AND EVALUATION OF THEIR PHOTOVOLTAIC PROPERTIES

## ABSTRACT

The present thesis deals with synthesis, characterization and evaluation of thermal, electrochemical, photoluminescence properties of a few new 1,1'-bis-2-naphthol based polyurethanes, side chain and main chain azomethine linkage containing polythiophenes and polycarbazole derivatives. A considerable effort has been devoted to the synthesis of polymers with special emphasis on the solubility, optical and electrochemical properties of  $\pi$ -conjugated polymers. The thesis also provides an account of photovoltaic performances exhibited by the polymers. The contents of the thesis have been compiled into five chapters.

**Chapter 1** deals with the general introduction of  $\pi$ -conjugated polymers and their application in photovoltaic devices. A brief review of synthetic procedures, optical properties, electrochemical properties of conjugated polymers is presented. General aspects of the device, device characterization and different types of device architectures for polymeric photovoltaic cells have been described in this chapter. This chapter also describes objectives along with the plan and methodology.

**Chapter 2** describes the synthesis and characterization of monomers and polymers and thermal properties of polymers. We have synthesized the following polymers.

- i) Poly [N,N-bis -(2-thienylmethylene)-o-dianisidine] (PBSD)
- ii) Poly [(3-phenyl azomethine ethyl) thiophene] (PPAET)
- iii) Poly [(3-phenyl azomethine butyl) thiophene] (PPABT)
- iv) Poly[(9-dodecylcarbazole)] (PDDC)
- v) Poly[(9-dodecylcarbazole)-co-thiophene] (PDDCT)
- vi) Poly(tolyl-1,1'-binaphthyl carbamate) (PU<sub>1</sub>)
- vii) Poly(hexamethylene-1,1'-binaphthyl carbamate) (PU<sub>2</sub>)

The synthetic procedures of monomers and polymers are discussed in this chapter. The monomers were characterized by FTIR, <sup>1</sup>H NMR and CHN analyzer. The synthesized polymers

were also thoroughly characterized by FTIR,  $^1\text{H}$  NMR, and molecular weights of polymers were determined by GPC analysis. The physical parameters and thermal properties of the polymers were also evaluated and are discussed in detail.

**Chapter 3** reports the electrochemical and the optical properties of synthesized polymers. The oxidation and reduction potential of polymers were assessed in cyclic voltammetry method. Furthermore, band gap of polymers was measured by electrochemically and compared with the optical method. The relative PL quantum yield of polymers with respect to Rhodamine B dye was measured. The PL quenching of the polymers in the presence of  $\text{TiO}_2$  nanoparticles in solution have been observed. This explains the suitability of  $\text{TiO}_2$  nanoparticles as electron acceptor in hybrid photovoltaic devices indicating ultrafast electron transfer from donor polymer to acceptor.

**Chapter 4** includes the study of photovoltaic performance of the synthesized polymers. Single layer, bulk heterojunction, hybrid organic-inorganic and host-guest approach of solar cells for the developed conjugated polymers have been reported. The polymers show the power conversion efficiency in the range 0.019-0.38%.

**Chapter 5**, the last chapter of the thesis includes the concluding remarks, highlights of the findings and future scopes of the present investigation. 1,1'-bis-2-naphthol based polyurethanes, side chain and main chain azomethinic linkage containing polythiophenes, and polycarbazole derivatives have been synthesized using condensation and oxidative coupling methods. The polymers are soluble in organic solvents and found thermally stable. The optical and electrochemical properties showed that the polymers bear the potentiality to be used in photovoltaic devices. The optical band gap of the polymers calculated was in the range of 2.1-3.4 eV. The utility of the polymers as photovoltaic materials has been studied by fabricating the devices with different structural approaches and showed significant performance.

## **DECLARATION BY THE CANDIDATE**

The thesis entitled "*Preparation of  $\pi$ - conjugated polymers and evaluation of their photovoltaic properties*" is being submitted to the Tezpur University in partial fulfillment for the award of the degree of Doctor of Philosophy in *Chemical Sciences* is a record of bonafide research work accomplished by me under the supervision of Prof. S. K. Dolui.

All helps received from various sources have been duly acknowledged.

No part of this thesis has been submitted elsewhere for award of any other degree.

Date: 30/11/2010

Place: Tezpur

*Binod pokhrel*  
Binod Pokhrel

Department of Chemical Sciences

Tezpur University



**TEZPUR UNIVERSITY**  
(A Central University established by an Act of Parliament)  
NAPAAM, TEZPUR - 784028  
DISTRICT : SONITPUR :: ASSAM :: INDIA

Ph : 03712 - 267004  
03712 - 267006  
Fax : 03712 - 267006  
03712 - 267005

e-mail : adm@agnigarh.tezu.ernet.in

## **CERTIFICATE OF THE PRINCIPAL SUPERVISOR**

This is to certify that the thesis entitled "*Preparation of  $\pi$ -conjugated polymers and evaluation of their photovoltaic properties*" submitted to the School of Science and Technology, Tezpur University in partial fulfillment for the award of the degree of Doctor of Philosophy in *Chemical Sciences* is a record of research work carried out by *Mr. Binod Pokhrel* under my supervision and guidance.

All help received by him from various sources have been duly acknowledged.

No part of this thesis has been submitted elsewhere for award of any other degree.

**Date:** 30 Nov. 2010

**Place:** Tezpur

**S. K. Dolui**

**Professor**

**School of Science and Technology**

**Department of Chemical Sciences**



# TEZPUR UNIVERSITY

(A Central University established by an Act of Parliament)

NAPAAM, TEZPUR - 784028

DISTRICT : SONITPUR :: ASSAM :: INDIA e-mail : adm@agnigarh.tezu.ernet.in

Ph 03712 - 267004

03712 - 267005


Fax 03712 - 267006

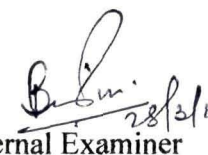
03712 - 267005

## Certificate of the External Examiner and ODEC

This is to certify that the thesis entitled “**Preparation of  $\pi$ -conjugated polymers and evaluation of their photovoltaic properties**” submitted by **Mr. Binod Pokhrel** to Tezpur University in the Department of **Chemical Sciences** under the school of **Science and Technology** in partial fulfillment of the requirement for the award of the degree of Doctor of Philosophy in **Chemical Sciences** has been examined by us on 28/03/2011 and found to be satisfactory.

Signature of:

  
Principal Supervisor 28/3/11

  
External Examiner 28/3/11

Associate Supervisor

Co-Supervisor

Date: \_\_\_\_\_



## Preface

Conjugated polymers are valuable material for scientists to design electronic devices like light emitting diode (LED) to generate light, photovoltaic cell to generate power, sensor to detect materials etc. The advancement made in this field is so rapid that almost every day a new polymer or a modification of existing polymer is appearing in the journals.

Conjugated polymers offer several advantages over inorganic and organic molecules such as flexibility, relative ease of processing by common techniques (spin and blade coating, ink – jet printing), or the ability to architect a compound for efficient energy conversion in solar cells. A large number of different classes of conjugated polymers have been developed such as polyaniline, polypyrroles, poly(*N*-vinylcarbazole)s, poly(fluorene)s (PFs), poly(*p*-phenylene vinylene)s (PPVs), and poly(thiophenes) (PTs) etc. While polythiophene derivatives are still the leading materials for organic solar cells. Utilization of solar energy as alternative of fossil fuel is a promising option and hence receiving impetus in research field. Polymer based organic photovoltaic systems hold the promise for a cost-effective, light weight solar energy conversion platform.

The major problem encountered in conjugated polymer is its solubility. A considerable effort has been devoted to the synthesis of  $\pi$ -conjugated polymers with special emphasis on the improvement in solubility. The present thesis deals with synthesis, characterization and evaluation of thermal, electrochemical, and photovoltaic properties of a few new 1,1'-bis-2-naphthol based polyurethanes, side chain and main chain azomethine linkage containing polythiophenes and polycarbazole derivatives. The thesis also provides an account of fluorescence quenching and sensor application of ester substituted polythiophenes. The contents of the thesis have been compiled into five chapters. Chapter 1 deals with the general introduction of  $\pi$ -conjugated polymers and their application in photovoltaic devices. Chapter 2, describes the synthesis and characterization of monomers and polymers and their thermal properties. In Chapter 3, electrochemical and optical properties of synthesized polymers have been discussed. Chapter 4 includes the study of photovoltaic properties of the polymers. Chapter 5, the last chapter of the thesis includes the concluding remarks, high lights of the findings and future scopes of the present investigation.

We hope that this study contributes a little knowledge to the rapidly advancing field of conjugated polymers and also opens up the possibilities of further research on the subject.

This research was carried out in the Department of Chemical Sciences, Tezpur University with financial assistance from the Defence Research and Development Organisation (DRDO) and Council of Scientific and Industrial Research (CSIR) under sponsored research scheme.

Bimod Pokhrel

## Acknowledgement

*I would like to express my deep sense of profound gratitude and indebtedness to my respected teacher and supervisor, Prof. S. K. Dolui for his inspiring guidance, endless patience, and work of freedom and the opportunity to work in his laboratory. It would have not been possible for me to bring out this thesis without his help, fatherly care, and constant encouragement throughout the research work.*

*I am grateful to Dr. R. K. Dutta, Prof. N. Karak and Prof. A. Kumar, Tezpur University, for their suggestions and discussions. I am grateful to all the faculty members of Department of Chemical Sciences for their help and suggestions.*

*I would like to acknowledge the sophisticated instrument facilities received for Dept of Chemical Sciences and other Departments of Tezpur University.*

*I am thankful to Prof. B. Ghosh, Jadavpur University, Kolkata for giving me opportunity to do solar cell fabrication work in his laboratory. I am also thankful to Dr. P. Banerjee and staff of School of Energy Studies, Jadavpur University for their constant support and help in fabricating the photovoltaic device.*

*My sincere thanks go to Dr N. SenSarna and Mr Samuil Islam, IASST, Guwahati, for providing GPC data. I thank Dr. Dibyendu Bag, DMSRDE, Kanpur for his help. I am really thankful to Sadhan Sir, Sibdasda, Abuda, Ganeshda, Dipuda, for their constant help to get the literature.*

*My special thanks go to Mr. B. Gohain, Dr. B. Saikia, Mr. N. Dutta, Mr. P. Nath, Mr. R. Borah, Mr S. Phukan, Mr. P. S. Barua, Mr S. Das, Mr. R. Boruah, Mr. J. Borah, Mr. H. Gogoi, Mr. H. Das, Mr. G. B. Chhetry for their timely help in many situations.*

*I would like to thank my friends Ashok, Mrinal and Roshan for their valuable support and help. I am thankful to all well wisher especially, Partoshda, Tapasiba, Nandimidi, Illiusda, Rashmiba, Digantada, Rabiulda, Rajuda, Suvangshuda, Jyotishmoyda, Parashaba, Kausikda, Hiranyada, Manashiba, Nilkamalda, Chandanda for their help.*

*I am truly thankful to my lab mates and friends Jatin, Anamika, Lakhya, Muhsina, Surajit, Isha, Amar, Binoy, Monalisha and Chandramika, who have taught and helped me in many aspect of life. It has been a great adventure. I will remember forever for their friendship and help.*

*I am also thankful to all my friends especially Nirmala, Kalyan, Pubalee, Bulamani, Ajantaba, Lakshmath, Subrata, Suresh, Barnali, Shremayee, Harekrishna, Srvaprasad, Buddha, Uday, Goutam, Mrdula, Mandakini, Jeenajyoti, Dhruva. Bijoy, Biplab, Ankur, Rashmi, Satya, Upamanyuda, Madhurjya, Subasit, Debasish, Sovan, Soumik, Smrutimala, Nabanita, Madhurjya, Sanjeebda, Jyotiprasad, Praveen, Ranjan, sudhir, Nabanath, Prasenjtda, Narayan, Dipak, Bimalendu, Kunal, Bidyut for their support and help.*

*I am grateful to Mrs. Sutapa Dolui for her motherly care, kindness and encouragement and Swapnil for his brotherly affection and support. I thank the Defence Research and Development Organisation (DRDO) and Council of Scientific and Industrial Research (CSIR) for funding the projects to complete this research. I would like to convey my pranams to my parents for their blessing, love and affection. I would like to express my respect and gratitude to all my family members for their constant encouragement, inspiration and support throughout my studies to fulfill my dream.*

*Most of all, I would like to convey my deep regards and profound respect to my Uncle, Mr. Tikaram Pokhrel and Mr. Surajit Choudhury and his family for their advice, unwavering support, constant source of inspiration. It would have not been possible for me to accomplish the research without his timely support and well wish.*

*Finally, I thank the authorities of Tezpur University for granting me the permission to do this work. Last but not least I would like to thank almighty for everything.*

*Binod Pokhrel*

# Contents

---

<b>Abstract</b>	<b>i</b>
<b>Preface</b>	<b>vi</b>
<b>Acknowledgement</b>	<b>vii</b>
<b>Table of Contents</b>	<b>ix</b>
<b>List of Tables</b>	<b>xi</b>
<b>List of Figures</b>	<b>xii</b>
<b>List of Schemes</b>	<b>xv</b>
<b>Abbreviations</b>	<b>xvi</b>

## **Chapter 1: Introduction**

1.1	Conjugated polymers	1
1.2	Synthesis of conjugated polymers	2
1.3	Synthesis of Conjugated Polymers by Chemical Methods	2
1.4	Electrochemical polymerization	8
1.5	Characterization of luminescent conjugated polymers	11
1.6	Conjugated polymer in photovoltaic devices	15
1.7	Background of organic photovoltaic cells	18
1.8	Photovoltaic device characterization	19
1.9	Different types of photovoltaic cells	20
1.10	Conditions for photovoltaic materials	25
1.11	Solubility of conjugated polymers	26
	References	30

## **Chapter 2: Synthesis and characterization of soluble conjugated polymers**

2.1	Introduction	41
2.2	Materials	42
2.3	Instrumentations	43
2.4	Experimental	44
2.5	Results and discussions	50

2.6	Conclusions	71
	References	72
<b>Chapter 3: Study of electrochemical and optical properties of conjugated polymers</b>		
3.1	Introduction	77
3.2	Experimental	79
3.3	Results and discussions	81
3.4	Conclusion	101
	References	103
<b>Chapter 4: Photovoltaic property evaluation of conjugated polymers</b>		
4.1	Introduction	108
4.2	Experiment	110
4.3	Results and discussions	113
4.4	Comparison of power conversion efficiency of devices based on the synthesized polymers	129
4.5	Conclusion	130
	References	132
<b>Chapter 5: Conclusion and future scopes</b>		
5.1	Conclusions	138
5.2	Future scopes	142
	Publication	143

## List of Tables

---

Chapter	Table	Title	Page No.
2	2.1	Physical properties of polymers	62
	2.2	Molecular weights and degree of polymerization of polymers	63
	2.3	Thermal characteristics of the polymers	68
3	3.1	Electrochemical parameters and energy levels of the polymers	87
	3.2	Summary of the optical characteristic exhibited in UV-visible absorption spectra	94
	3.3	Absorption, emission and relative quantum yield values of polymers in solution	101
4	4.1	Summary of the photovoltaic performance for the solar cells based on PBTD	114
	4.2	Photovoltaic properties of PPAET and PPABT based hybrid devices	118
	4.3	Photovoltaic properties of PDDC and PDDCT based photovoltaic devices before and after annealing at 150°C for 30 minutes	121
	4.4	Photovoltaic parameters of devices based on PU <sub>1</sub> and PU <sub>2</sub> with Rhodamine B	127

## List of Figures

---

Chapter	Figure	Title	Page No.
1	1.1	Possible diad linkages for 3-alkylthiophene	5
	1.2	Jablonski diagram	12
	1.3	A voltammogram of an ideal system for forward scan	15
	1.4	Specific conversion steps and loss mechanisms in an organic solar cell	16
	1.5	Pictorial description of photovoltaic cell	17
	1.6	<i>I-V</i> characteristics of a typical photovoltaic device	20
2	2.1	<sup>1</sup> H NMR spectrum of BTD	50
	2.2	<sup>1</sup> H NMR spectrum of PAET	51
	2.3	<sup>1</sup> H NMR spectrum of PABT	51
	2.4	<sup>1</sup> H NMR spectrum of DDC	52
	2.5	<sup>1</sup> H NMR spectrum of BINOL	53
	2.6	<sup>1</sup> H NMR spectrum of PBTB	55
	2.7	<sup>1</sup> H NMR spectrum of PPAET	56
	2.8	<sup>1</sup> H NMR spectrum of PPABT	57
	2.9	<sup>1</sup> H NMR spectrum of PDCC	59
	2.10	<sup>1</sup> H NMR spectrum of PDDCT	59
	2.11	<sup>1</sup> H NMR spectrum of PU <sub>1</sub>	61
	2.12	<sup>1</sup> H NMR spectrum of PU <sub>2</sub>	61
	2.13	TGA curve of polymer PBTB	64

	2.14	TGA curves of (a) PPAET (b) PPABT	65
	2.15	TGA curves of (a) PDDC (b) PDCCT	66
	2.16	TGA curves of PU <sub>1</sub> and PU <sub>2</sub>	67
	2.17-2.20	DSC thermograms of polymers	69
3	3.1	Standard three electrode electrochemical cell	80
	3.2	Measurement of onset in CV	82
	3.3-3.6	Cyclic Voltammogram of polymer films on ITO coated glass at a scanning rate of 50 mV/S	83
	3.7-3.9	Anodic peak current density vs. scan rate plots of polymers	88
	3.10-3.13	UV-visible absorption spectra of polymer in solution	91
	3.14-3.20	PL spectra of polymer and blend of polymer and TiO <sub>2</sub> (or PCBM) in THF	96
4	4.1	<i>I-V</i> Measurement configuration	111
	4.2	Typical <i>I-V</i> curve of a photovoltaic cell	112
	4.3	<i>I-V</i> characteristics of PBTD based photovoltaic devices	114
	4.4	Schematic energy level diagram for PBTD based bulk heterojunction device	115
	4.5	<i>I-V</i> characteristics of PPAET and PPABT based photovoltaic devices	117
	4.6	Schematic energy level diagram for PPAET and PPABT based hybrid devices	118
	4.7-4.8	<i>I-V</i> characteristics of PDDC and PDDCT based photovoltaic devices before and after annealing	122



4.9	Schematic energy level diagram for PDDC and PDDCT based devices	124
4.10	<i>I-V</i> Characteristics of (a) PU <sub>1</sub> + Rhodamine B (b) PU <sub>2</sub> + Rhodamine B based photovoltaic devices	127
4.11	Schematic energy level diagram for the host-guest system based hybrid heterojunction device	128

## List of Schemes

---

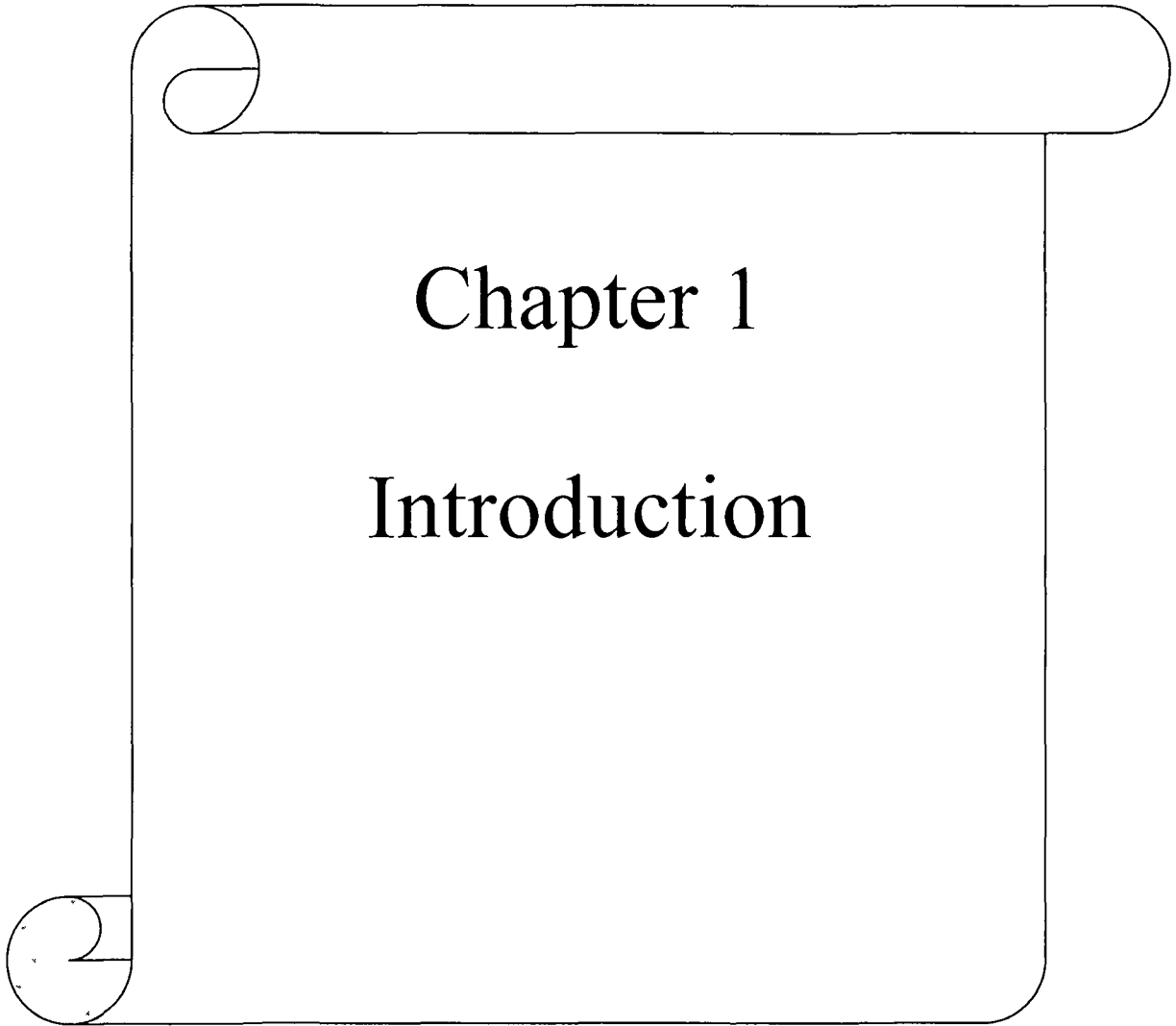
Chapter	Scheme	Title	Page No.
1	1.1	Free radical mechanism of oxidative coupling of polythiophene	3
	1.2	Curtis synthesis of P3AT	3
	1.3	Synthesis of poly(9,9-dialkylfluorene) via Yamamoto coupling	4
	1.4.1	Grignard synthesis of poly(3-alkylthiophene)	5
	1.4.2	Regio-regular P3AT synthesis	6
	1.5	Reike synthesis of PATs and catalyst specificity	7
	1.6	Suzuki coupling of conjugated polymers, where Ar is an aromatic group	8
	1.7	Stille polycondensation of conjugated polymers, where Ar is an aromatic group	8
	1.8	Mechanism of electropolymerization	10
2	2.1	Reaction scheme for synthesis of BTD and PBT	54
	2.2	Reaction scheme for synthesis of PAET, PABT and PPAET, PPABT	56
	2.3	Reaction scheme for synthesis of DDC and polymers PDDC, PDDCT	58
	2.4	Reaction scheme for synthesis of BINOL and PU <sub>1</sub> , PU <sub>2</sub>	60

## Abbreviations used in the thesis

---

CP	Conjugated polymer
CV	Cyclic voltammetry
DCE	Dichloroethene
DDTA	Dodecyl 2-(thiophene-3-yl) acetate
DMAc	Dimethyl acetamide
DMAP	Dimethylamino pyridine
DMF	<i>Dimethyl formamide</i>
DMSO	Dimethyl sulfoxide
DP	Degree of polymerization
DSC	Differential scanning calorimetry
EL	Electroluminescence
FET	Field effect transistor
FTIR	Fourier transform infrared spectroscopy
GPC	Gel permeation chromatography
HOMO	Highest occupied molecular orbital
ITO	Indium tin oxide
LED	Light emitting diode
LUMO	Lowest unoccupied molecular orbital
MEH-PPV	poly [2-methoxy-5-(2-ethylhexyloxy)-1,4-phenylenevinylene]
NMR	Nuclear magnetic resonance spectroscopy
PA	Polyacetylene
PAT	Polyalkylthiophene
PBTD	Poly [N,N-bis -(2-thienylmethylene)-o-dianisidine]
PCBM	[6,6]-phenyl C <sub>61</sub> -butyric acid methyl ester
PDDC	Poly[(9-dodecylcarbazole)]
PDDCT	Poly[(9-dodecylcarbazole)-co-thiophene]

PEDOT:PSS	Poly (ethylene dioxythiophene): polystyrene sulphonate
PHTA	Poly (hexyl-2-(thiophene-3-yl) acetate)
PL	Photoluminescence
PLED	Polymer light emitting diode
PPABT	Poly [3-phenyl azomethine butylthiophene]
PPAET	Poly [(3-phenyl azomethine ethyl) thiophene]
PPP	Poly (p-phenylene)
PPV	Poly (phenylenevinylene)
PSS	Poly (styrene sulfonate)
PT	Polythiophene
PU <sub>1</sub>	Poly(tolyl-1,1'-binaphthyl carbamate)
PU <sub>2</sub>	Poly(hexamethylene-1,1'-binaphthyl carbamate)
PV	Photovoltaic
ROMP	Ring opening metathesis polymerization
T <sub>g</sub>	Glass transition temperature
TGA	Thermogravimetric analysis
THF	Tetrahydrofuran
T <sub>m</sub>	Melting temperature
UV	Ultra violet
XRD	X-ray diffraction
Φ	Quantum yield
λ	Wave length



# Chapter 1

## Introduction

### 1.1. Conjugated polymers

Since the discovery of metallic conductivities in polyacetylene doped with various electron acceptors or electron donors,<sup>1</sup> the field of conducting polymers has developed very rapidly. Conjugated polymers (CPs), also known as conducting polymers, are polyunsaturated compounds in which a continuous electron path extends along the entire backbone. Conjugated polymers contain a backbone consisting of alternating single and double bonds between carbon-carbon or carbon-nitrogen atoms. Even though conjugated polymers are known as *linear or rigid rods*, they are *not completely straight and flat*, but twisted along their backbones. Polymer chains consist of  $sp^2$ -hybridized carbons and p-electrons. These p-electrons form a delocalized pi-system, which gives rise to the polymer's semiconducting properties. Conjugated polymers are currently very important materials and are used widely for the development of devices such as light-emitting diodes,<sup>2-6</sup> thin film transistors,<sup>7-12</sup> photovoltaic cells,<sup>13-19</sup> sensors,<sup>20-23</sup> lasers,<sup>24-26</sup> and nonlinear optical systems.<sup>27-30</sup>

Unique microelectronic, optical, and photonic applications are emerging in which  $\pi$ -conjugated polymers and oligomers complement, or even replace conventional inorganic and metallic components. As a result, these materials are under intense chemical, physico-chemical, and electronic scrutiny. One of the potential applications of  $\pi$ -conjugated polymers includes the use in photovoltaic device due to low cost module. Solar cells or PV cells absorb sunlight and change it directly and continuously into electricity. They do this noiselessly without generating pollution, and without using any moving part.

Recent progress achieved using organic crystals, multilayered thin film and interpenetrated network technologies, permit one to expect a very fast increase in the conversion yield of organic solar cells. This will possibly make them a competitive alternative to the various forms of silicon cells. Indeed, in last two years it has been observed a significant jump in the conversion yield of organic photovoltaic (PV) solar cells, passing from a 1% yield achieved many years ago, to a 5-6% yield achieved recently.<sup>15, 31-33</sup> This opens the perspective of seeing very soon, on a typical 5 years time-scale, organic PV cell with solar efficiencies in excess of 10%. The long term objective of such very active research is to reduce the cost of PV modules.

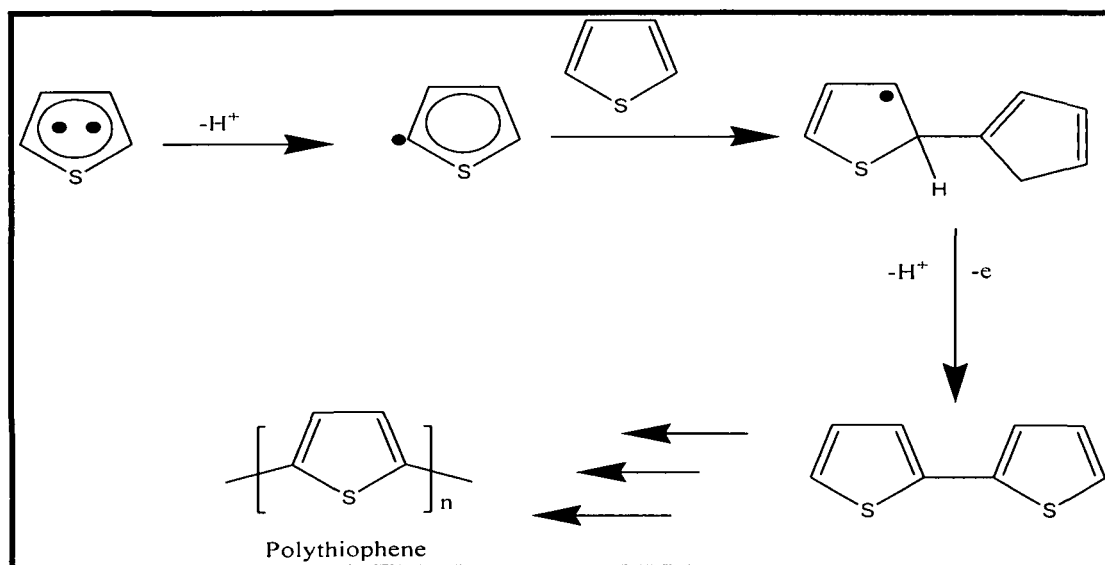
## **1.2. Synthesis of conjugated polymers**

The first challenge in studying conjugated polymers is their synthesis. The two methods for obtaining conjugated polymers are electrochemical and chemical polymerization means.<sup>34</sup> Electrochemical polymerization is usually carried out in oxidative anodic conditions and yields a polymer film. This method allows a facile route to prepare conducting polymers but yields a limited amount of the desired polymer<sup>34-36</sup> and, as a consequence, chemical synthesis appears more desirable. There are several chemical synthesis approaches to obtain conjugated polymers.

## **1.3. Synthesis of conjugated polymers by chemical methods**

### **1.3.1. Oxidative coupling**

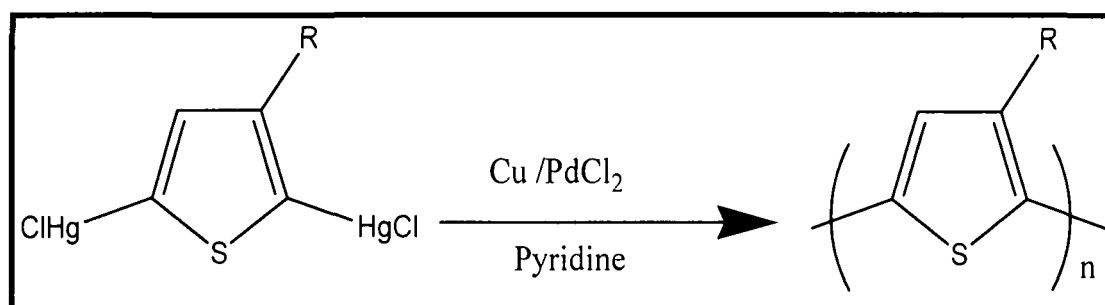
Oxidative coupling is a simple, straightforward and versatile method to synthesize conjugated polymers.<sup>37-43</sup> Polyanilines, polypyrroles, poly(9,9-dialkylfluorene)s (PAFs) and poly(3-alkylthiophene)s (PATs) are a few classes of conjugated polymers where oxidative coupling method is extensively used to their synthesis.<sup>12,34,38,43</sup> In this method, the monomer is dissolved in a suitable solvent and oxidatively polymerized with FeCl<sub>3</sub>. Ferric chloride oxidizes the 3-alkylthiophene monomer to produce radical cations with spin-density, predominantly in the 2 and 5- positions of the thiophene, which is subsequently coupled to form a polymer. This procedure yields polymers with reasonably high molecular weights. However, they contain many structural defects that may lead to undesirable properties. The free radical mechanism of oxidative coupling is shown in Scheme 1.1. It has been reported that these defects can be minimized by performing the reactions at lower temperatures. However, the inability to remove the oxidant completely from the final product can still dramatically influence its performance in devices such as FETs, LEDs, PV cells etc.



**Scheme 1.1:** Free radical mechanism of oxidative coupling of polythiophene

### 1.3.2. Curtis' demercuration polymerization

Curtis and co-workers have developed a new preparation method for P3ATs based on the Pd-catalyzed, reductive coupling reaction of 2,5-bis-(chloromercurio)-3-alkylthiophenes as shown in Scheme 1.2. The Curtis method ensures only  $\alpha, \alpha'$ -coupling between thienylene moieties. The most appealing feature of this method is its tolerance to electrophilic groups, such as carbonyls, esters, and nitriles. This method has also been extended to prepare poly(3-alkylthienyl ketones).<sup>44</sup>

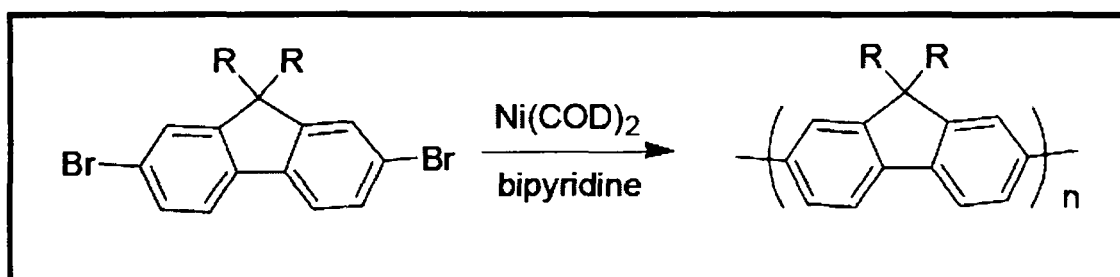


**Scheme 1.2:** Curtis synthesis of P3AT



### 1.3.3. Yamamoto coupling

The Yamamoto coupling method (Scheme 1.3) is an effective route to synthesize conjugated polymers. This route has been successful in polymerizing several classes of conjugated polymers which include thiophene, fluorene, thiazole and phenylene. The use of a large quantity of  $\text{Ni}(\text{COD})_2$  (COD= 1,3-cyclooctadiene) and the instability of the nickel complex, however, makes this reaction undesirable.<sup>41,45</sup>



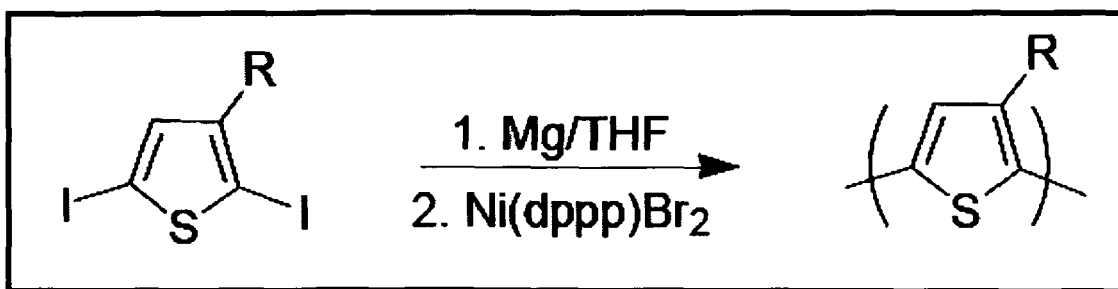
Scheme 1.3: Synthesis of poly(9,9-dialkylfluorene) via Yamamoto coupling

### 1.3.4. Metal-catalyzed cross coupling

Metal-catalyzed cross coupling has been proven to be a versatile route to synthesize conjugated polymers. The catalyzed reaction mechanisms are essentially the same regardless of the reaction type, and follow three key steps: (i) oxidative addition of an aryl halide to the metal catalyst, (ii) transmetalation between the aforementioned catalyst complex and the organometallic reagent to form a diorganometallic, (iii) reductive elimination to give an aryl-aryl bond and a regenerated catalyst. The use of this method with different catalysts is discussed in the next subsection.

#### 1.3.4.1. Kumada coupling

Kumada cross coupling, illustrated in Scheme 1.4.1, was first used to prepare soluble and processable poly(3-alkylthiophene)s (when alkyl chains are greater than propyl) by Elsenbaumer and co-workers. In this method, 2,5-diiodo-3-alkylthiophene was treated with one mole equivalent of magnesium to form the Grignard species. When  $\text{Ni}(\text{dppp})\text{Br}_2$  (dppp = diphenylphosphinopropane) catalyst was introduced, a polymer formed.



**Scheme 1.4.1:** Grignard synthesis of poly(3-alkylthiophene)

Since poly(3-alkylthiophene)s (P3ATs) are non-centrosymmetric, regio-regularity is a factor. PATs may couple as: head-to-head, head-to-tail, and tail-to-tail (Figure 1.1). These linkages have a pronounced effect on their properties. The PATs synthesized by Elsenbaumer and co-workers were regio-random.<sup>46</sup>

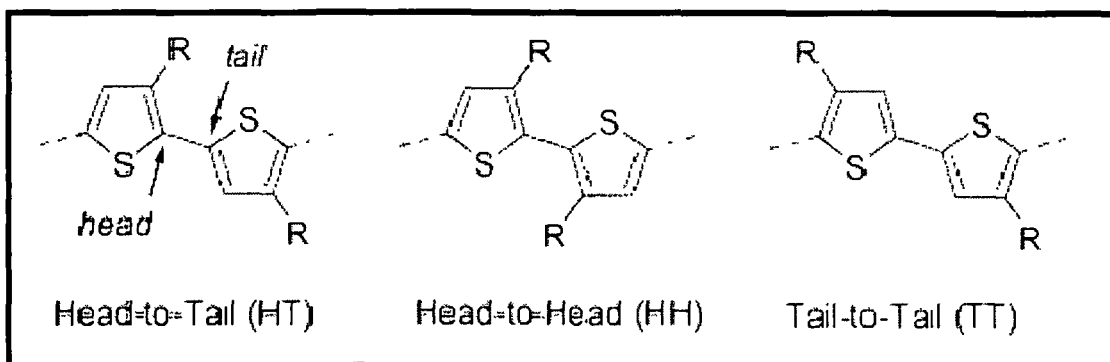


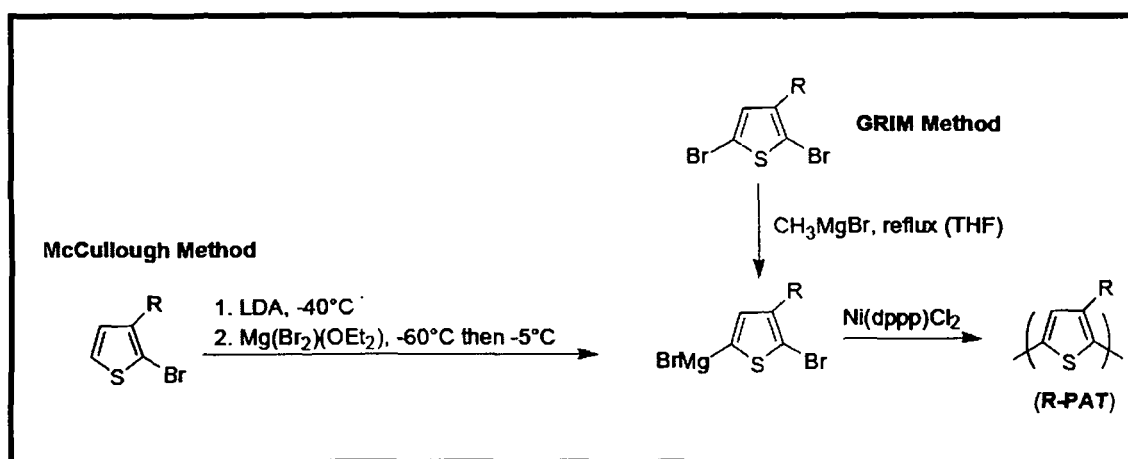
**Figure 1.1:** Possible diad linkages for 3-alkylthiophene

McCullough and co-workers discovered two methods to produce regioregular (>98% head-to-tail coupling) P3ATs: McCullough and Grignard Metathesis (GRIM) methods. These methods are illustrated in Scheme 1.4.2 and are both based on the Kumada cross coupling of 2-bromo-5-(magnesiobromo)-3-alkylthiophene.

#### 1.3.4.2. McCullough method

In the McCullough method (Scheme 1.4.2), high purity 2-bromo-3-alkylthiophene (free from the 2-bromo-4-alkylthiophene isomer) is selectively lithiated at the 5-position with lithium diisopropylamine (LDA) at low temperatures ( $-40^{\circ}\text{C}$ ) to afford 2-bromo-3-alkyl-5-lithiothiophene. This organolithium intermediate is converted to a

Grignard reagent by reacting with  $\text{MgBr}_2 \cdot \text{Et}_2\text{O}$  to yield 2-bromo-5-(magnesiobromo)-3-alkylthiophene and subsequent addition of  $\text{Ni}(\text{dppp})\text{Cl}_2$  catalyst results in regio-regular poly(3-alkylthiophene).<sup>39,47</sup>



Scheme 1.4.2: Regio-regular P3AT synthesis

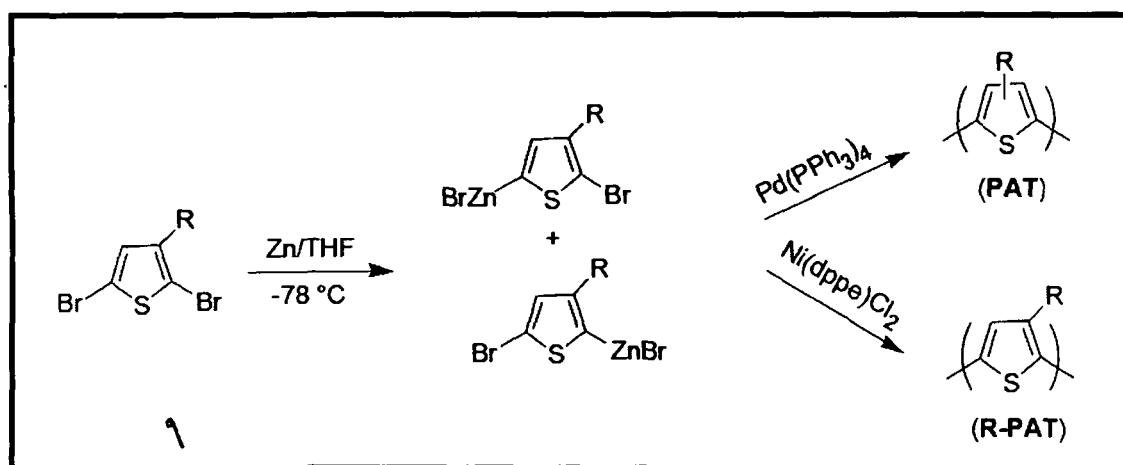
#### 1.3.4.3. GRIM method

The Grim method is a facile route to make regio-regular P3ATs. In this method, 2,5-dibromo-3-alkylthiophene monomer is used, rather than 2-bromo-3-alkylthiophene. The former is easier to purify due to the large differences in volatility of the reactants and the side products. The 2-bromo-5-(magnesiobromo)-3-alkylthiophene is easily formed by reacting 2,5-dibromo-3-alkylthiophene with methyl magnesium bromide, followed by introduction of the nickel catalyst to yield a regio-regular poly(3-alkylthiophene) in high yields (60-70%).<sup>39,48</sup>

#### 1.3.5. Reike method

Reike and co-workers discovered a method to produce regio-regular PATs. This method is illustrated in Scheme 1.5. This polymerization method is a one pot reaction in which reactive Reike zinc undergoes a regio-selective oxidative addition on the 5-position of 2,5-dibromo-3-alkylthiophene to form 2-bromo-5-bromozincio-3-alkylthiophene. With the addition of  $\text{Ni}(\text{dppe})\text{Cl}_2$  (dppe =diphenylphosphinoethane), regio-regular PAT (R-PAT) is formed. Alternatively, with the addition of  $\text{Pd}(\text{PPh}_3)_4$

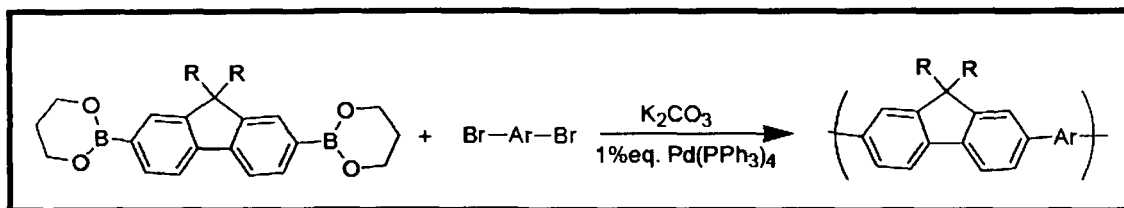
(PPh<sub>3</sub> = triphenylphosphine), a regio-random polymer is obtained. It is rationalized that the size of the catalyst (both metal and ligands) controls the regio-specificity of the resulting polymer.<sup>39,49</sup>



**Scheme 1.5:** Reike synthesis of PATs and catalyst specificity

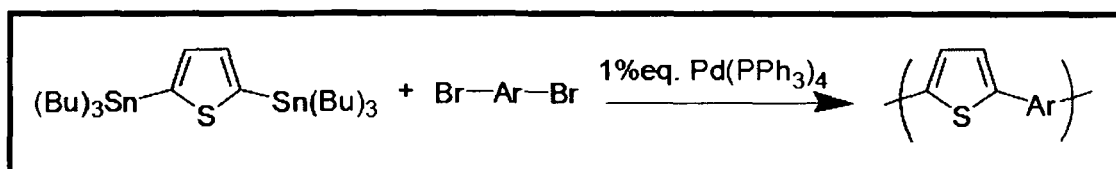
### 1.3.6. Suzuki and Stille polycondensation

Pd-Catalyzed cross coupling is a convenient method for aryl-aryl coupling and provides a route to synthesize a wide variety of conjugated polymers, and copolymers. Two common Pd-catalyzed cross coupling methods are Suzuki and Stille type reactions. The advantages of these methods are water insensitivity, commercial availability of many monomers (and precursors), and the yield of high molecular weight polymers. In Suzuki coupling (Scheme 1.6), a diboronic acid (or ester) is coupled with a dibrominated aryl group in the presence of a base (e.g. K<sub>2</sub>CO<sub>3</sub>). This procedure was first adopted in 1989 by Wegner and coworkers for the synthesis of well-defined processable poly(*p*-phenylene)s. This method is quite versatile, especially for the synthesis of alternating copolymers, and can tolerate a large number of functional groups. Fluorene type polymers are commonly synthesized by this method.<sup>50</sup>



**Scheme 1.6:** Suzuki coupling of conjugated polymers, where Ar is an aromatic group

Stille coupling (Scheme 1.7) is also a versatile, polycondensation reaction to form conjugated polymers. The use of toxic tin compounds is the main drawback concomitant to this method.<sup>51</sup>



**Scheme 1.7:** Stille polycondensation of conjugated polymers, where Ar is an aromatic group

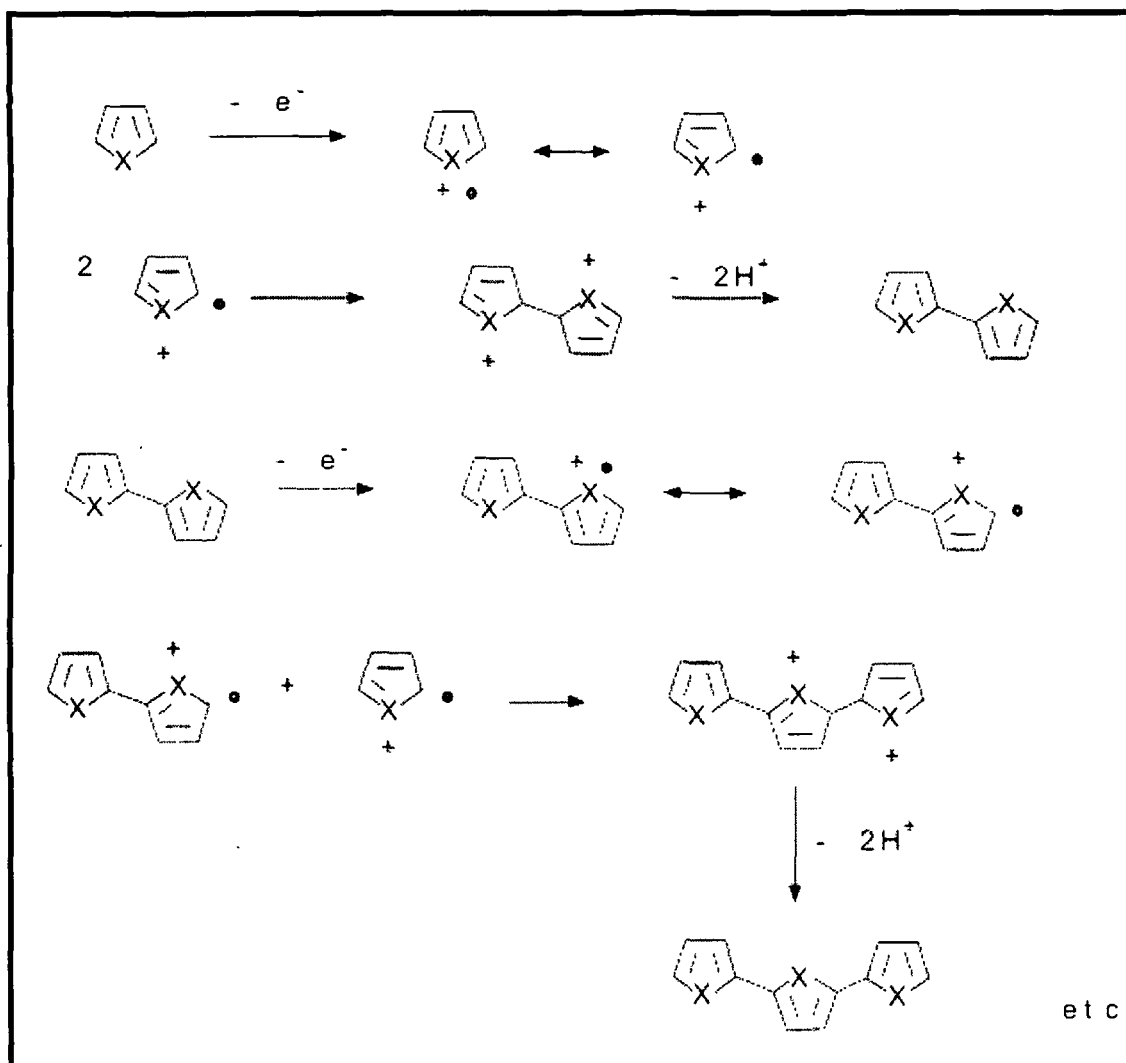
Conjugated polymer synthesis in general differs from other chemical reactions in many ways. The most stringent requirement for polymerization reaction is the high purity of the monomers and chemicals. A trace amount of impurity might even stop polymerization or lead to undesirable products. The reaction conditions (i.e., catalysts, temperature, time of reaction, etc) must be strictly controlled. Isolation and purification of conjugated polymers becomes a problem because a trace amount of an ionic or catalyst impurities present in the polymer will result in a large error in end use application. The presence of moisture and air is highly undesirable in polymerization reactions, particularly in oxidative polymerization. In most of the polymerization processes, the requirement of an inert and dry atmosphere is essential. This can be ensured by the passage of dry and pure nitrogen or argon gas through the polymerization chamber.

#### 1.4. Electrochemical polymerization

Electrochemical polymerization to form conjugated polymers is the widely used process as it offers certain advantages over other processes. The main advantage of this

technique is the direct synthesis of the polymer in the form of a thin film. The other advantages include rapidity, absence of catalyst, precise control of polymer film thickness and morphology, direct formation of the polymer in the oxidized conducting form. Electrochemical polymerization is normally carried out in a single or dual compartment cell by adopting a standard three-electrode configuration in a supporting electrolyte, both dissolved in an appropriate solvent. Electrochemical polymerisation can be carried out potentiometrically by using a suitable power supply (potentiostat, galvanostat). Generally, Potentiostatic conditions are recommended to obtain thin films, while galvanostatic conditions are recommended to obtain thick films.<sup>34,35</sup>

Electrochemical polymerization involves radical cationic mechanism as shown in scheme 1.8.<sup>34</sup> The initiation step proceeds by radical cation generation from monomer via electrochemical oxidation. In the propagation step, two radical cations undergo recombination followed by formation of dimer by loss of two protons from radical-radical intermediate species. Electrochemical oxidation of the dimer and subsequent process generates 'oligomeric' radical cation which on combination with similar oligomeric radical cation or with monomer radical cation repeatedly builds up the polymer. The termination step occurs via exhaustion of reactive radical species in vicinity of the electrode. It is noteworthy in case of electropolymerization that once the initiating electrochemical potential is applied, the population of radical cations is likely to far exceed that of neutral monomer in the vicinity of electrode surface. Thus, a generated radical cation is far more likely to be surrounded by other radical cations than by neutral monomers, or oligomers or other species. Among the several determinant causes for this is the usually rapid electron transfer kinetics for electro-oxidation of the monomer, in comparison with the slower diffusion of monomer from bulk of reaction medium to electrode, thus causing a rapid depletion of monomer at the electrode.



**Scheme 1.8:** Mechanism of electropolymerization

Although electropolymerization is nearly generic technique for quick and rapid production of conjugated polymers, but all organic monomers do not undergo electropolymerization. The reason why certain monomers electro-polymerize at all to yield conjugated polymers lie in a combination of stability factors of the radical ions generated in the first step and the oxidation potential for generation of these radical ions. In nearly all the cases of successful electropolymerization, the radical ions are found to be highly stabilized via charge delocalization, and electrochemical oxidation was reasonably facile.

Despite the facile nature of electrochemical polymerization, the major limitations of this process viz. insoluble material, problem in large scale production, inability for primary structure elucidation due to insolubility of products, poor quality of films leaves little use of the technique for different applications.<sup>34,37</sup> Utility of chemical polymerization process with enhanced solubility of conjugated polymerization attracts much attention to the chemist.

### **1.5. Characterization of luminescent conjugated polymers**

Characterization techniques discussed in the following sections are those used to examine the optical properties of conjugated polymers. These characterization tools are important for understanding the role of the chemical structure on the properties of these materials.

#### **1.5.1. Absorption and emission spectroscopy**

Generally, the observed transitions in absorption spectroscopy of conjugated polymers are attributed to electronic excitation from  $\pi$  to  $\pi^*$  states and emission from  $\pi^*$  to  $\pi$  states. Upon electronic excitation of the polymer, a number of photo-physical processes, shown in Figure 1.2, may occur: fluorescence, phosphorescence, or radiationless decay.<sup>52</sup> Fluorescence is observed after singlet relaxation from the first excited state. If intersystem crossing occurs, a triplet excited state is generated whose relaxation will result in phosphorescence. If emission does not occur, then a non-radiative pathway is dominant and the electronic excitation is converted into rotational or vibrational motion within the polymer and its surroundings. The difference between the absorption and emission maxima of the spectra is called the Stokes shift, and it occurs when emission from the lowest vibrational excited state relaxes to various vibrational levels of the electronic ground state.



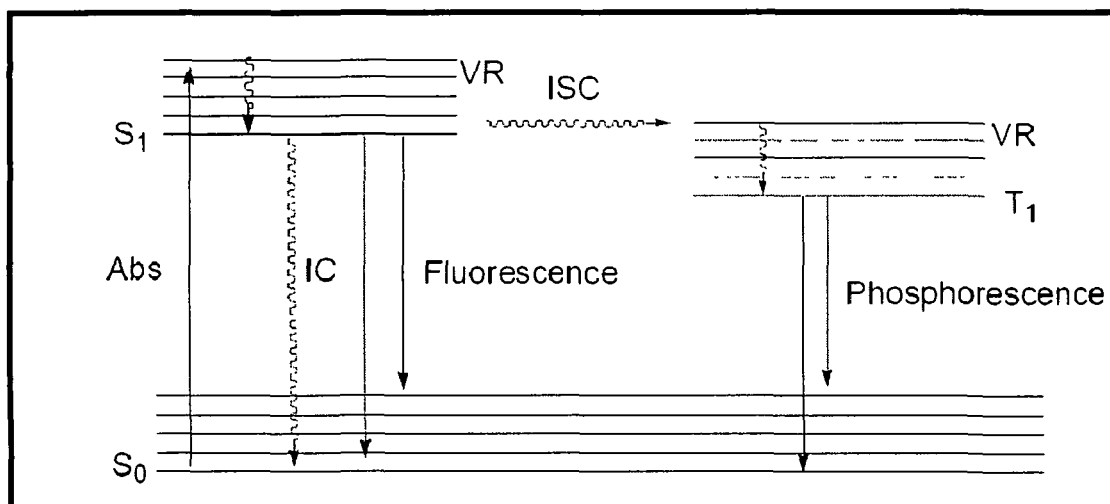


**Figure 1.2:** Jablonski diagram. Abs = absorption, VR = vibrational relaxation, ISC = intersystem crossing, IC = internal conversion, S<sub>0</sub> = ground state singlet, S<sub>1</sub> = first singlet excited state, T<sub>1</sub> = first triplet excited state.

Quantitative analysis of the emission efficiency of the polymer is characterized by its quantum yield of luminescence ( $\Phi_{PL}$ ). The  $\Phi_{PL}$  is the ratio of the number of photons emitted to the number of photons absorbed, as shown in Equation (1).

$$\text{Quantum Yield } (\Phi_{PL}) = \text{Photons emitted} / \text{Photons absorbed} \quad (1)$$

According to the law of conservation of energy, the maximum  $\Phi_{PL}$  must be 1. The value of  $\Phi_{PL}$  is related to the rates of radiative ( $\tau_r$ ) and non-radiative ( $\tau_{nr}$ ) decays, as described in Equation (2).<sup>53</sup>

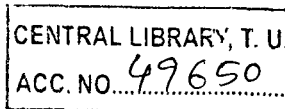
$$\text{Quantum Yield } (\phi_{PL}) = \frac{\tau_r}{\tau_r + \tau_{nr}} \quad (2)$$

As  $\tau_{nr}$  approaches 0, the quantum yield of luminescence approaches unity. Generally,  $\Phi_{PL}$  is highest in dilute solutions, where the emitting species are isolated from each other. In most cases, increasing the concentration of the polymer in solution

decreases the quantum yield of luminescence due to concentration quenching, which follows the Stern-Volmer relationship.<sup>52</sup>

The interchain interactions of the CPs lead to formation of tight aggregates, which results in fluorescence quenching because of  $\pi$ -stacking between main chains of the CPs.<sup>54,55</sup> The quenching efficiency increases with increasing tendency of the polymer to associate with the quencher in solution. This association can occur either through the formation of a nonluminescent complex between the polymer and the quencher (static quenching) or due to collisions between the photoluminescent macromolecule and the quencher (dynamic quenching). For both mechanisms, the quantitative measure of the luminescence quenching efficiency is given by the Stern-Volmer constant,  $K_{SV}$  defined by equation (3).<sup>56</sup>

$$\phi^0/\phi = 1 + K_{sv}[\text{quencher}]$$



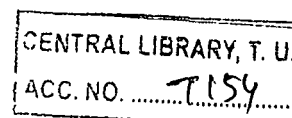
(3)

Where,  $\phi^0$  is the intensity of fluorescence in the absence of the quencher and  $\phi$  is the intensity of fluorescence in the presence of the quencher. The equation reveals that  $\phi^0/\phi$  increases in direct proportion to the concentration of the quenching moiety, and the constant  $K_{sv}$  defines the efficiency of quenching. When all the other variables are held constant, higher the  $K_{sv}$ , lower is the concentration of quencher required to the luminescence.

The quantum yield of luminescence can be determined either by secondary or primary methods. In the secondary method, the quantum yield is related to that of a known standard as shown in equation (4).<sup>57</sup>

$$\phi_s = \phi_r \left( \frac{A_r}{A_s} \times \frac{I_s}{I_r} \right) \quad (4)$$

In this equation,  $\phi_s$  represents quantum yield of a sample in solution and  $\phi_r$  represents known quantum yield of reference sample in solution.  $A_s$  and  $A_r$  are the absorbance of the sample and reference solution respectively at the excitation



wavelength,  $I_r$  and  $I_s$  are the corresponding relative integrated fluorescence intensities. In order to obtain reliable results, it is important to match as closely as possible the optical absorption properties of the sample with those of the references. Typical standards are 9,10-diphenylanthracene in cyclohexane ( $\Phi_{PL} = 0.90$ ), quinine sulfate in 1 N  $H_2SO_4$  ( $\Phi_{PL} = 0.546$ ), rhodamine 101 in ethanol ( $\Phi_{PL} = 1$ ) and rhodamine B in water ( $\Phi_{PL} = 0.31$ ). This method assumes that the emission from the sample is isotropic (equal in all directions), as is the case in dilute solutions. Measuring the  $\Phi_{PL}$  of an anisotropic sample, such as a film, is quite difficult since its emission intensity has an angular dependence

The quantum yield of luminescent polymer largely depends on effective conjugation length of conjugated polymers. The solution quantum yield of luminescence increases with increasing conjugation length, indicating that the rate of non-radiative decay decreases with conjugation length. This increase in  $\Phi_{PL}$  with higher conjugation lengths can be explained by: (a) an increased structural stability of an unspecified origin<sup>58</sup> or (b) the lack of singlet fission (process where two triplet excitons are produced from the fission of one singlet excited state).<sup>59</sup>

### 1.5.2. Electrochemical properties

Electrochemical properties can be studied through cyclic voltammetric method. In cyclic voltammetry (CV), the potential is increased linearly from an initial potential to a peak potential and back to the initial potential again, while the current response is measured (Figure 1.3). For freely diffusing species, as the potential is increased, easily oxidized species near the electrode surface react, and a current response is measured. When the direction of the scan is reversed, the oxidized species near the electrode surface are reduced, and again a current response is measured.

The electrochemical properties of conjugated polymers offer the information of oxidation and reduction potential, and stability of synthesized polymer. Moreover, it gives the range of electrochemical potential window which is essential for end use application. The oxidation potential is a measure of how much energy is needed to withdraw electrons from the HOMO level of polymer and the reduction potential is at the same time a characteristic of the LUMO level. Therefore, the onset oxidation and reduction potentials are closely related to the energies of the HOMO and LUMO levels of

polymer and thus can provide important information regarding the magnitude of the energy gap.<sup>60,61</sup>

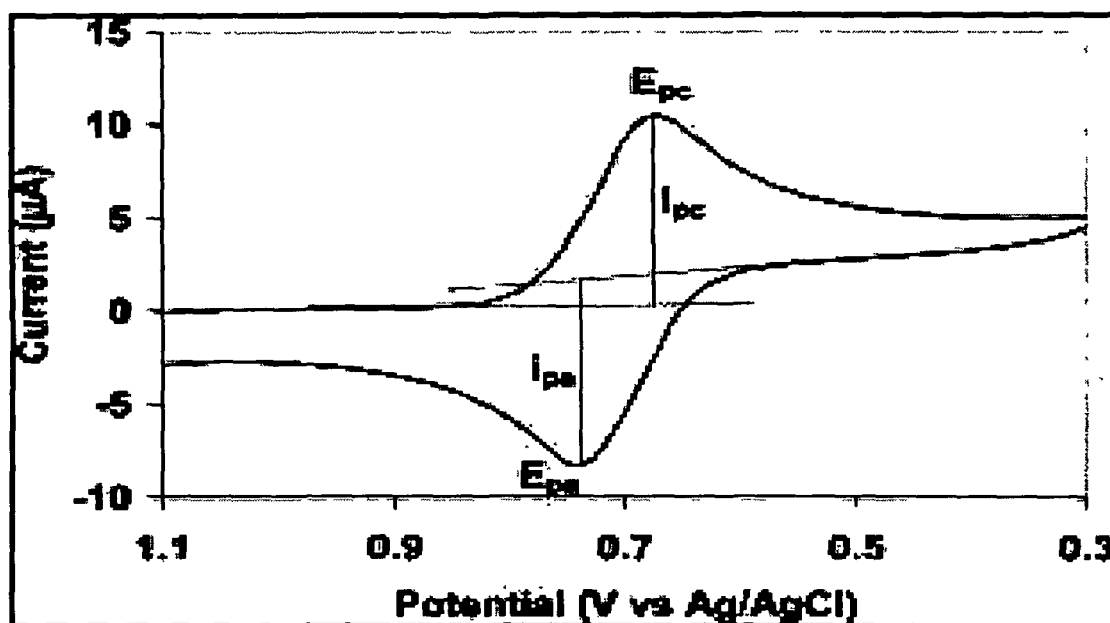


Figure 1.3: A voltammogram of an ideal system for forward scan

The oxidation and reduction potential of conjugated polymer films increases with increasing alkyl side chain length. Introduction of an electron donating group, such as an alkoxy or alkyl thio –group results in reducing band gaps, lowering oxidation potentials and stabilizing of conducting state. Fluoroalkyl substituents on the polymer backbone lead to a higher oxidation potential. Electron withdrawing substituents in conjugated polymers lower the HOMO and LUMO energies and increase the electron affinity of the polymer.<sup>62-76</sup>

### 1.6. Conjugated polymer in photovoltaic devices

The photovoltaic (PV) energy technologies can contribute to environmentally friendly, renewable energy production, and the reduction of the carbon dioxide emission associated with fossil fuels and biomass. Plastic solar cell technology is based on conjugated polymers. Conjugated polymers and active organic molecules have the immense advantage of facile, chemical tailoring to alter their properties, such as the band

gap. Conjugated polymers combine the electronic properties known from the traditional semiconductors and conductors with the ease of processing and mechanical flexibility of plastics. Therefore, this new class of materials has attracted considerable attention owing to its potential of providing environmentally safe, flexible, lightweight and inexpensive electronics.<sup>77-80</sup>

Various architectures for organic solar cells have been investigated in recent years. In general, for a successful organic photovoltaic cell four important processes have to be optimized to obtain a high conversion efficiency of solar energy into electrical energy (Figure 1.4).<sup>81</sup>

- Absorption of light
- Charge generation and separation of the opposite charges
- Charge transport
- Charge collection

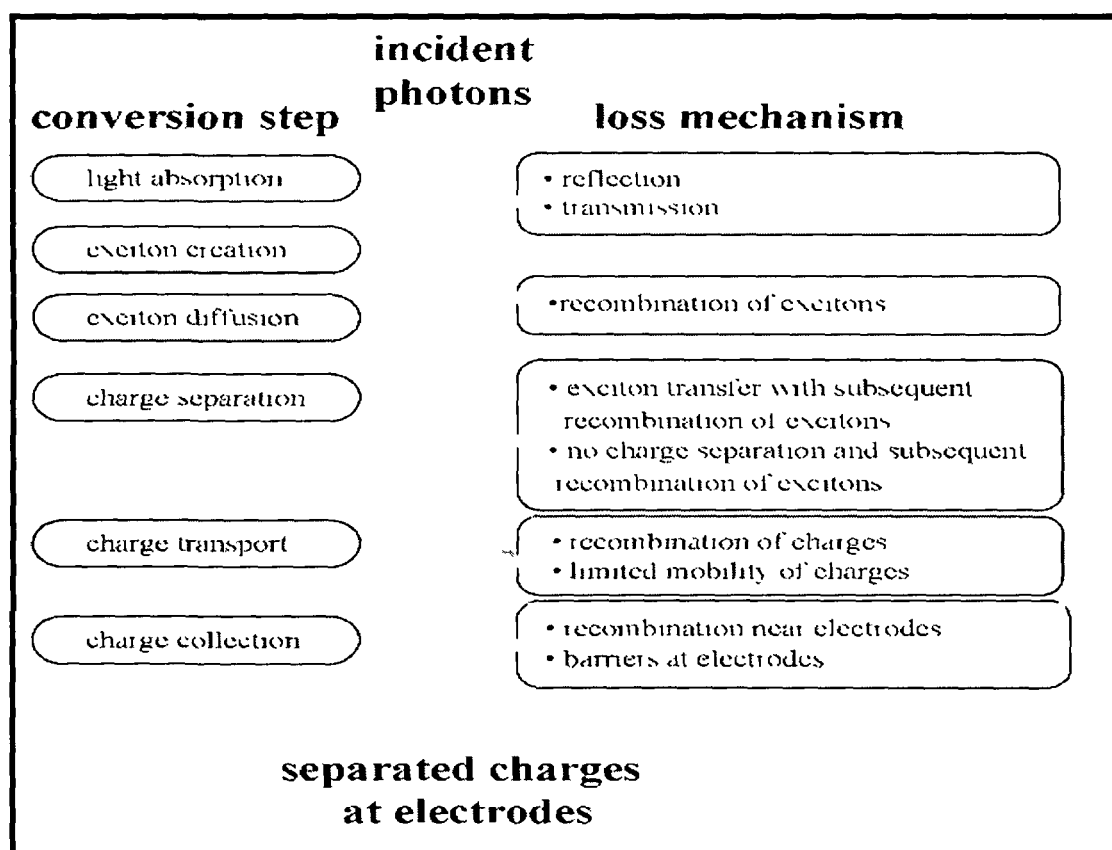


Figure 1.4: Specific conversion steps and loss mechanisms in an organic solar cell

For an efficient collection of photons, the absorption spectrum of the photoactive organic layer should match the solar emission spectrum and the layer should be sufficiently thick to absorb all incident light. A better overlap with the solar emission spectrum is obtained by lowering the band gap of the organic material, but this will ultimately have some bearing on the open-circuit voltage. Increasing the layer thickness is advantageous for light absorption, but burdens the charge transport. Creation of charges is one of the key steps in photovoltaic devices in the conversion of solar light into electrical energy. In most organic solar cells, charges are created by photoinduced electron transfer. In this reaction, an electron is transferred from an electron donor (D), a p-type semiconductor, to an electron acceptor (A), an n-type semiconductor, with the aid of the additional input energy of an absorbed photon ( $h\nu$ ).<sup>82-90</sup>

For an efficient charge generation, it is important that the charge-separated state is the thermodynamically and kinetically most favorite pathway after photoexcitation. Therefore, it is important that the energy of the absorbed photon is used for generation of the charge separated state and it should not be lost via competitive processes like fluorescence or non-radiative decay. In addition, the charge-separated state should be stabilized, so that the photogenerated charges can migrate to the electrodes. Therefore, the back electron transfer should be slowed down as much as possible. This can be explained in Figure 1.5.

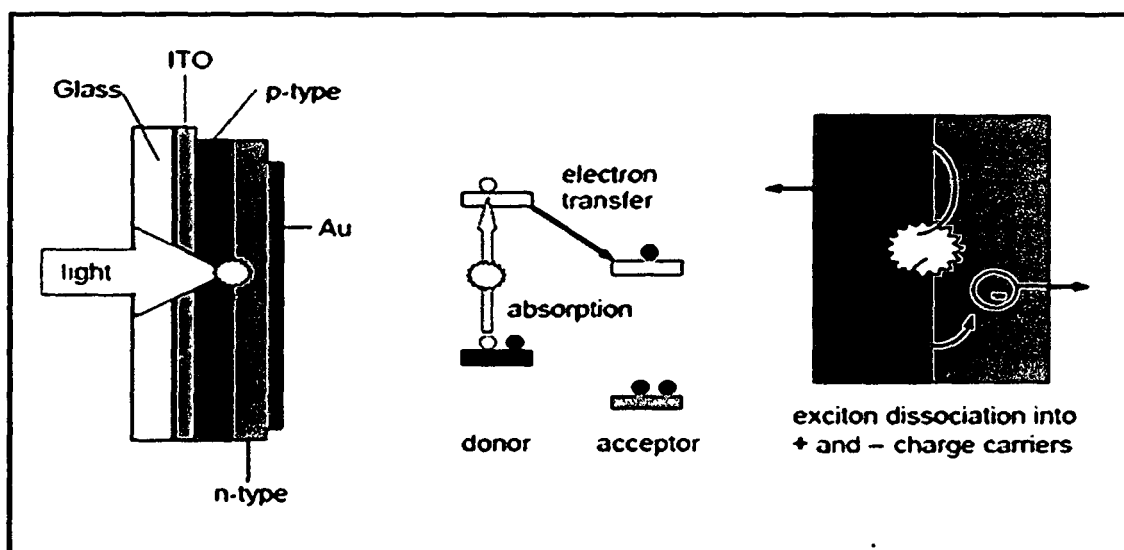


Figure 1.5: Pictorial description of photovoltaic cell

### 1.7. Background of organic photovoltaic cells

Photoconductivity was first observed on anthracene in the beginning of the 20th century. From the 1950s anthracene was intensively studied, partly because the crystal structure was accurately determined and high-purity single crystals were readily available.<sup>91</sup> The first real PV investigations were done on porphyrins and phthalocyanines. These classes of compounds remain among the most investigated dyes as PV materials.<sup>91-92</sup>

One of the most studied photoconducting polymers is poly(vinyl carbazole) (PVK). The first report came in 1958 by Hoegel *et al* who proposed its practical use as an electrophotographic agent.<sup>93</sup> In the 1970s it was discovered that certain conjugated polymers, notably poly(sulphur nitride) and polyacetylene could be made highly conducting in the presence of certain dopants.<sup>94</sup> In 1982 Weinberger *et al.*<sup>95</sup> investigated polyacetylene as the active material in an Al/ polyacetylene/graphite cell. The cell had a low open-circuit voltage ( $V_{OC}$ ) of only 0.3 V and a low QE of only 0.3%. Later Glenis *et al.* investigated different polythiophenes.<sup>96</sup> Again the systems suffered low efficiencies and low open-circuit voltages in the 0.4 V range. The low open-circuit voltages has been ascribed to the formation of polarons (delocalised excitons) that energetically relax in the energy gap, which then becomes smaller than the  $\pi$ - $\pi^*$  gap. This relaxation results in a large spectral shift when the luminescence spectra are compared to the absorption spectra (Stokes' shift). The result of the relaxations is that it limits the attainable voltage and the maximum power conversion efficiency(PCE). Different electrode materials have been used but not with success. A major breakthrough in cell performance came in 1986 when C.W. Tang showed that much higher efficiencies are attainable by producing a double layered cell using two different dyes.<sup>31</sup>

Followed by the poly(alkyl-thiophenes) (PATs), PPV and its derivatives, polyfluorene, polycarbazoles are the most investigated conjugated polymer in PV cells. The breakthrough in device architecture and development in efficient conjugated polymers have led the new arena of polymer based solar cells.<sup>13,16,80,82,97-98</sup> The highest efficiency achieved for polymeric solar cells is 5-6% recently.<sup>15</sup>

### 1.8. Photovoltaic device characterization

Accurate efficiency measurements for fabricated solar cells are crucial to evaluate new material systems or processing technologies. This behaviour can be seen in the fourth quadrant of the Current-Voltage ( $I$ - $V$ ) characteristic as shown in Figure 1.6. Considering the voltage dependence of the  $I$ - $V$  curve the maximum power is the maximum product of  $I$  and  $V$  that can be found amongst the data points in the fourth quadrant. This maximum area is larger the more the  $I$ - $V$  curve resembles a rectangle with the area  $V_{OC} \times I_{SC}$ . The ratio between these two areas represents a measure of the quality of the shape i.e. fill factor (FF) of the  $I$ - $V$  characteristics.

$$\text{Fill factor (FF)} = (I.V)_{\text{Max}} / I_{SC} \cdot V_{OC}$$

Thus:

$$\text{Maximum power } (P_{\text{Max}}) = (I.V)_{\text{Max}} = I_{SC} \cdot V_{OC} \cdot \text{FF}$$

Where  $V_{OC}$  is the open-circuit voltage (When  $I = 0$ ),  $I_{SC}$  is the short-circuit current (when  $V = 0$ ), FF is the fill factor and  $P_{\text{Max}}$  corresponds to maximum power point.

Higher the fill factor (FF), more is the  $I$ - $V$  characteristics resembling a constant current source with a maximum voltage electric power. In order to describe the power conversion efficiency ( $\eta_e$ ) of a solar cell the maximum output power  $P_{\text{Max}}$  has to be related to the power of the incident light ( $P_{\text{in}}$ ).

$$\eta_e = I_{SC} \cdot V_{OC} \cdot \text{FF} / P_{\text{in}}$$



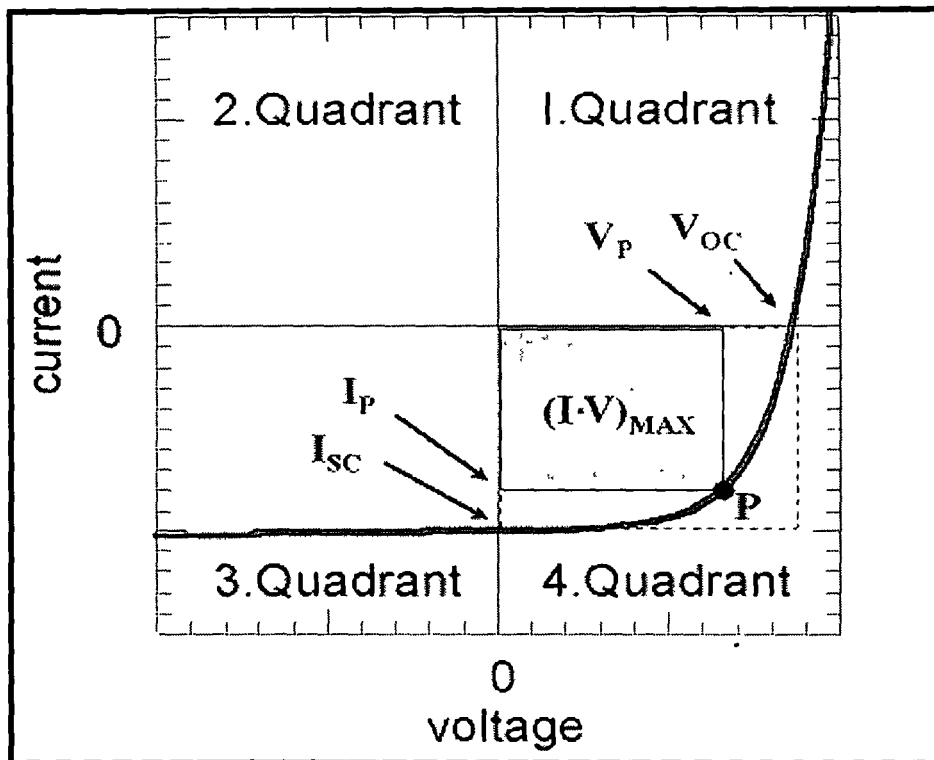


**Figure 1.6:**  $I$ - $V$  characteristics of a typical photovoltaic device

In order to compare efficiencies of solar cells, solar radiation standards have been defined in the past. The most common standard at present is the AM1.5 spectrum which can be approached by commercial solar simulators. If international recognition of a solar power conversion efficiency number of a cell is desired, the cell should be measured by one of the internationally recognised institutions that offer solar cell efficiency measurements such as the National Renewable Energy Laboratories (NREL) in USA or the Fraunhofer Institute for Solar Cell research in Freiburg (Germany).

## 1.9. Different types of photovoltaic cells

### 1.9.1. PV cells made from single layers of conjugated polymers

Single layer organic photovoltaic cells are the simplest form amongst the various organic photovoltaic cells. These cells are made by sandwiching a layer of organic electronic materials between two metallic conductors, typically a layer of indium tin oxide (ITO) with high work function and a layer of low work function metal such as Al, Mg and Ca.<sup>80,99</sup> The basic structure of such a cell is illustrated in Figure 1.7.

The difference of work function between the two conductors sets up an electric field in the organic layer. When the organic layer absorbs light, electrons will be excited to LUMO orbital and forms excitons with the holes left in HOMO. The electric field is responsible to separate the electrostatic bounds excitons which then pull electrons to the positive electrode (an electrical conductor used to make contact with a nonmetallic part of a circuit) and holes to the negative electrode. The current and voltage resulting from this process can be utilized. Weinberger et al. used polyacetylene as the organic layer, Al and graphite as electrodes to fabricate a cell, which had an open circuit voltage of 0.3 V and a charge collection efficiency of 0.3%.<sup>95</sup> Glenis et al. reported a Al/poly(3-nethylthiophene)/Pt cell had an external quantum yield of 0.17%, an open circuit voltage of 0.4 V and a fill factor of 0.3.<sup>96</sup> Karg et al. fabricated an ITO/PPV/Al cell, showing an open circuit voltage of 1V and a power conversion efficiency of 0.1% under white-light illumination.<sup>100</sup>

### 1.9.2. Double layer cells

This type of organic photovoltaic cell contains two different layers in between the conductive electrodes (Figure 1.7). These two layers of materials have differences in electron affinity and ionization energy. Therefore electrostatic forces are generated at the interface between the two layers. The materials are chosen properly to make the differences large enough, so that these local electric fields are strong, which may break up the excitons much more efficiently than the single layer photovoltaic cells do. The layer with higher electron affinity and is the electron acceptor, and the other layer with higher ionization potential is the electron donor. This structure is also called planar donor-acceptor heterojunctions.<sup>80,91</sup>

In 1986, a major breakthrough was realized by Tang, who introduced a double-layer structure of a p-and n-type organic semiconductor.<sup>31</sup> A 70 nm thick two-layer device was made using copper phthalocyanine as the electron donor, and a perylene tetracarboxylic derivative as the electron acceptor. The photoactive material was placed between two dissimilar electrodes, indium tin oxide (ITO) for collection of the positive charges and silver (Ag) to collect the negative charges. A power conversion efficiency of about 1% was achieved under simulated AM2 illumination (691 W/m<sup>2</sup>). Important aspect

in this concept is that the charge generation efficiency is relatively independent of the bias voltage.

In the double-layer structure, the photoexcitations in the photoactive material have to reach the p-n interface, where charge transfer can occur before the excitation energy of the molecule is lost via intrinsic radiative and non-radiative decay processes to the ground state. Because the exciton diffusion length of the organic material is in general limited to 5-10nm, only absorption of light within a very thin layer around the interface contributes to the photovoltaic effect. This limits the performance of double-layer devices, because such thin layer can impossibly absorb all the light. C<sub>60</sub> has high electron affinity, making it a good material as electron acceptor in photovoltaic cells. Sariciftci et al. first fabricated a C<sub>60</sub>/MEH-PPV double layer cell,<sup>101</sup> which had a relatively high fill factor of 0.48 and a power conversion efficiency of 0.04% under monochromatic illumination. For PPV/C<sub>60</sub> cells, Halls et al. reported a monochromatic external quantum efficiency of 9%, a power conversion efficiency of 1% and a fill factor of 0.48.<sup>102</sup>

### 1.9.3. Bulk heterojunction cells

In combining electron donating (*p*-type) and electron accepting (*n*-type) materials in the active layer of a solar cell, care must be taken that excitons created in either material can diffuse to the interface, to enable charge separation. Due to their short lifetime and low mobility, the diffusion length of excitons in organic semiconductors is limited to about ~10 nm only. This imposes an important condition to efficient charge generation. Anywhere in the active layer, the distance to the interface should be in the order of the exciton diffusion length. Despite their high absorption coefficients, exceeding 10<sup>5</sup> cm<sup>-1</sup>, a 20 nm double layer of donor and acceptor materials would not be optical dense, allowing most photons to pass freely. The solution to this dilemma is elegantly simple. By simple mixing the *p* and *n* type materials and relying on the intrinsic tendency of polymer materials to phase separate on a nanometer dimension, junctions throughout the bulk of the material are created that ensure quantitative dissociation of photogenerated excitons, irrespective of the thickness (Figure 1.7). Polymer-fullerene solar cells were among the first to utilize this bulk-heterojunction principle.<sup>13,103</sup> Nevertheless, this attractive solution poses a new challenge. Photogenerated charges must

be able to migrate to the collecting electrodes through this intimately mixed blend. Because holes are transported by the *p*-type semiconductor and electrons by the *n*-type material, these materials should be preferably mixed into a bicontinuous, interpenetrating network in which inclusions, cul-de-sacs, or barrier layers are avoided. C<sub>60</sub> and its derivatives are used as electron acceptor in the dispersed heterojunction photovoltaic cells.<sup>103-108</sup> In 1994 Yu et al. made the first dispersed polymer heterojunction PV cell by spincoating on ITO covered glass from a solution of MEH-PPV and C<sub>60</sub> in a 10:1 weight ratio.<sup>109</sup> The cell showed a photosensitivity of 5.5 mA/W. In 1996 Kohler also used this approach for fabricating PV cells with success.<sup>110</sup> One limitation of this approach is the relative low solubility of fullerenes in normal solvents. This problem was solved when Hummelen et al. synthesized a number C<sub>60</sub>-derivatives with increased solubility, which allowed the fullerene content to be as high as 80% in the prepared films.<sup>111</sup> Using a methano-functionalised fullerene derivative Yu et al. repeated the fabrication procedure with a polymer/fullerene ratio of 20/80, the contacts were made of ITO and Ca, and the cell had a quantum efficiency (QE) of 29% and a PCE of 2.9% under monochromatic light, intensity at 20 mW/cm<sup>2</sup>.<sup>112</sup>

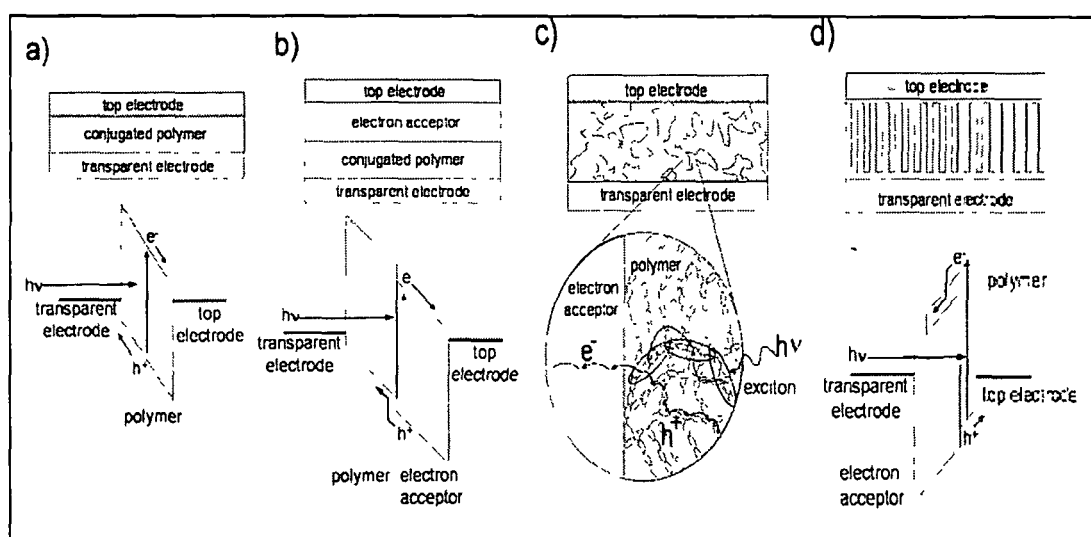


**Figure 1.7:** Four device architectures of conjugated polymer-based photovoltaic cells: (a) single-layer PV cell; (b) bilayer PV cell; (c) disordered bulk heterojunction; (d) ordered bulk heterojunction

#### 1.9.4. Hybrid solar cells

In order to overcome certain drawbacks of organic semiconductors, the idea of the hybrid solar cells using simultaneously organic and inorganic materials has been proposed.<sup>113-118</sup> Crystalline and nanocrystalline inorganic semiconductors have several attributes as electron acceptors, including relatively high electron mobility, high electron affinities, and good chemical and physical stability. Solution-processible nanocrystalline semiconductors that can be prepared in different morphologies offer the potential for a large area interface when combined with a solution-processed organic component. Hybrid polymer-inorganic structures can be prepared in different ways: a planar bilayer structure where an organic layer is deposited on top of an inorganic semiconductor layer; nanostructured porous structures where a connected semiconductor layer is filled with a conjugated polymer; and blends of nanocrystals with polymer where semiconductor nanoparticles and polymer are deposited from the same solution.<sup>119</sup> Greenham et al. reported PL quenching in MEH-PPV after mixing 5nm diameter CdS and CdSe nanoparticles.<sup>120</sup> Sun *et al* achieved 45% external quantum efficiency (EQE) at 480 nm with 86% branched nanoparticle of CdSe blended in PPV.<sup>115</sup> PV cells with conjugated polymer-TiO<sub>2</sub> heterojunction are also explored as hybrid organic-inorganic photovoltaic devices. TiO<sub>2</sub> does not absorb visible light like CdSe, it has some advantage over CdSe and PCBM as electron acceptor.<sup>13</sup> In PV cells made from conjugated polymer and TiO<sub>2</sub>, electron is transported to ITO and hole is transported to Al top electrode. PV cells are made with nanocrystalline TiO<sub>2</sub> and polythiophene derivative.<sup>116,117,119</sup>

#### 1.9.5. The guest-host approach

One of the promising approaches for organic solar cells includes the guest–host approach. The basic idea is to form a system composed of three components: donor component, acceptor component, and the polymeric matrix. The embedding of the photoactive conjugated polymer–acceptor blend into a conventional polymer matrix i.e. guest-host approach is a sound and promising methods to improve photoactive sample quality for the following reasons: less interchain interaction, possibility of ordering in the matrix, the stability of the photoactive polymer, possibility of tuning of charge transfer by changing intermolecular distance or dielectric permittivity of the host matrix.<sup>121-123</sup> In the

guest-host approach, the conjugated polymers are better encapsulated against environmental influences. A set of systems based on conjugated polymer–metal–fullerene networks in polystyrene matrix may serve as an example. Solar cell based on a soluble derivative of *p*-phenylene vinylene (MDMO-PPV), and a highly soluble methanofullerene, [6,6′]-phenyl C<sub>61</sub>-butyric acid methyl ester (PCBM), embedded into a conventional polymer, polystyrene was found to be 1.5%.<sup>121</sup>

### 1.10. Conditions for photovoltaic materials

The photovoltaic materials must possess good solubility in certain organic solvents so that these polymers can be cast from solution using wet-processing techniques such as spin casting, dip coating, ink jet printing, screen printing, and micromolding. These techniques represent an enormously attractive route for producing large-area photovoltaic cells cheaply because they can perform at ambient temperature and pressure. Most of these techniques can also be applied to systems that require flexible substrates, such as roll-to-roll coaters. A few conjugated polymers poly(3-hexylthiophene) (P3HT), poly[2-methoxy-5-(2′-ethylhexoxy)-1,4-phenylenevinylene] (MEH-PPV), and poly[2-methoxy-5-(3′,7′-dimethyloctyloxy)-*p*-phenylenevinylene] (OC<sub>1</sub>C<sub>10</sub>-PPV) are good photovoltaic donor materials containing alkyl and alkoxy side chains that make them soluble in common organic solvents.<sup>13,16</sup>

A second major requirement for the active layer in a PV cell is that it should absorb a significant fraction of the sun's light. The high (10<sup>5</sup> cm<sup>-1</sup>) peak optical absorption coefficient of many conjugated polymers makes them excellent candidates in this regard. The crystalline silicon PV cells must be made 100 nm thick to effectively absorb incident light, while organic semiconductors have a direct band gap and generally must only be 100-500 nm thick to absorb most of the light at their peak absorption wavelength. Moreover, Organic photovoltaic materials have many advantages compared to inorganic semiconductors:

(1) Organic materials can be made via various synthetic pathways, which make them inexhaustible in supply and always available for use.

(2) Via structure tuning and different functionalizations, organic compounds can fulfill the requirements of an efficient photovoltaic device, for example, broad absorption

spectra, suitable redox energies, and self-organization abilities facilitating efficient exciton and charge transport.

(3) Most organic compounds can be dissolved in common organic solvents. They can, hence, be processed not only via vacuum evaporation/sublimation but also by means of other low-cost manufacturing technologies, such as roll-to-roll or inkjet printing, drop-casting, spin- or dip-coating, doctor-blading, and other solution casts. These printing techniques render organic solar cells potentially manufacturable in a continuous printing process with large area coating.

(4) In solutions or in thin films, organic materials often show high absorption coefficients, which allow organic solar cells to still be efficient in very thin films and under low sunlight irradiation. In such thin films (around 100 nm), organic materials can absorb almost all incoming light (within their absorption range). In comparison, a standard silicon wafer would need a thickness of around 300  $\mu\text{m}$  to absorb the same amount of photons.

(5) Solar cells based on organic materials can be structurally flexible, and most of them are semitransparent. Organic solar cells, therefore, have a much larger application potential than conventional solar cells. They can be used not only as electricity providers on roof tops, like common inorganic solar cells, but can also be used for decoration in fashion, windows, toys, and mobile applications, e.g. charging for mobile phones or laptops.

### **1.11. Solubility of conjugated polymers**

From the beginning of their history, conjugated polymers have been found as intractable and insoluble due to their rigid backbone. It was an important goal in basic research as in application-oriented material science to develop techniques by which they could be processed.

A number of general techniques have been developed for improving the solubility of the polymers.<sup>61-71,124</sup> These include the following

- i) Copolymerization
- ii) Chain flexibility incorporation
- iii) Polymer blending
- iv) Chain substitution

#### **1.11.1. Copolymerization**

The rigidity of the conjugated chain may be reduced and thereby its solubility improved by copolymerization technique. Block copolymerization of 3- methyl thiophene and methyl methacrylate produces polymers soluble in THF. Poly (3-octylthiophene –co- N-(3-thenyl)-4-amino-2-nitrophenol) develops polymer highly soluble in solvents such as THF, chlorinated solvents, dioxane, toluene, etc.<sup>123</sup> Block copolymers containing thiophene units of several lengths alternating with aliphatic spacers and polyesters have been found to be highly soluble polymers.

#### **1.11.2. Chain Flexibility Incorporation**

Chain flexibility can be improved by incorporation of flexible centres or flexible linkages like sulphur, nitrogen, phosphorous etc in the side chain. Polymers of 3-(ethylmercapto)- and 3,4-bis(ethylmercapto)thiophenes are soluble in common organic solvents such as methylene chloride, chloroform, and THF.

#### **1.11.3. Polymer blending**

Blending of rigid conducting polymers with processable polymers is reported to have improved solubility. The success of blends depends on the mutual adhesion or compatibility of the polymers.

#### **1.11.4. Chain substitution**

Appropriate chain substitution leads to enhanced solubility due to reduction of close packing of the chains in the crystal lattice. Substitution of a long alkyl chain as the side groups gives rise to a soluble conjugated polymers. The introduction of alkyl groups



longer than butyl yields the materials soluble in common organic solvents. For example, replacement of a long alkyl sulfonate group in the 3- position of the thiophene molecule leads to a water soluble polythiophene. Alkoxy side groups on polythiophenes backbone increase the solubility of the polymer. Short alkoxy chains on polythiophenes lead to insoluble materials but long chain alkoxy substituents led to large increase in solubility. Polythiophene derivatives with fluoroalkyl, ether, hydroxyl, carboxylic acid, amide, urethane groups in side chain have improved the solubility. The presence of bulky phenyl, cyclohexyl substituents in polythiophene makes it soluble in typical organic solvents.

### **1.12. Objectives and plan of the work**

During the past two decades, intensive studies have been devoted to the synthetic methodology, structure characterization, electrochemical properties, and stability of conjugated polymers. The greater part of the work on heterocyclic conjugated polymers has centered on polythiophenes and its derivatives, mainly because, by the introduction of a suitable side group, a variety of soluble derivatives of the polymer can be made. By a proper choice of the side group, solubility and optical properties such as band gap, the photovoltaic performance of the conjugated polymers can be tailored. The length of the alkyl side group affects solubility. Low band gap conjugated polymers with higher solar radiation absorption are required for solar cell applications. For this purpose azomethine linkage containing thiophene in the main chain and side chain linkages serves the great role. This will provide higher absorption range of the visible light. Moreover, polycarbazole derivatives are of great importance because of its various useful properties; such as easy formation of relatively stable radical cations (holes), high thermal and photochemical stability. On the other hand, polyurethanes are an attractive area of study because of their metal-ion free synthetic pathway which is very useful for high performance polymers. So, polycarbazole derivatives with improved solubility and few soluble polyurethanes as host material in host-guest approach serves the purpose of photovoltaic materials.

### **Objectives of the present investigation**

- To synthesize  $\pi$ - conjugated soluble polymers.
- To characterize monomers and polymers by UV-Vis, FTIR, NMR, TGA/DSC, GPC, XRD techniques.
- To investigate electrochemical, thermal, and photoluminescence properties of synthesized polymers.
- To study photovoltaic performance of the synthesized polymers with respect to different device structures.

### **Plan of the work**

To fulfill the above objectives the following plans of work have been adopted.

- Preparation of soluble thiophene derivative with side chain and main chain azomethinic linkages.
- Preparation of carbazole derivative and its co-polymer with thiophene as photovoltaic materials.
- Preparation of 1,1'-bis-2 naphthol based polyurethanes.
- Characterization of monomers and polymers by UV-Vis, FTIR,  $^1\text{H}$  NMR.
- Study of thermal properties of polymers by TGA/ DSC. .
- Investigation of electrochemical behavior of polymers by cyclic voltametry.
- Study of photoluminescence properties of polymers using fluorescence spectrophotometer.
- Fabrication of photovoltaic devices considering different device parameters.
- Testing of devices.
- Evaluation of photovoltaic performance of the conjugated polymer based devices.

## References

1. Chiang, C.K.; Drury, M.A.; Gau, S.C.; Heeger, A.J.; Louis, E.J.; MacDiarmid, A.G.; Park, Y.W.; Shirakawa, H. Synthesis of Highly Conducting Films of Derivatives of Polyacetylene, (CH)<sub>x</sub>. *J. Am. Chem. Soc.*, **100**, 1013-1015 (1978).
2. Burroughs, J.H.; Bradley, D.D.C.; Brown, A.R.; Marks, R.N.; Mackay, K.; Friend, R.H.; Burn P.L.; Holmes, A.B. Light emitting diodes based on conjugated polymers. *Nature* **347**, 539-541 (1990)
3. Gupta, D.; Singh, S.; Katiyar, M.; Deepak; Hazra, T.; Verma, A; Manoharan S.S. Polymer light emitting diode using a new electrophosphorescent cyclometalated iridium complex. *Materials and Manufacturing Processes* **21**, 285–289 (2006)
4. Grimsdale, A.C.; Chan, K.L.; Martin, R.E.; Jokisz, P.W.; Holmes, A.B. Synthesis of light emitting conjugated polymers for applications in electroluminescent devices. *Chem. Rev.* **109**, 897-1091 (2009)
5. Akcelrud L. Electroluminescent polymers. *Prog. Polym. Sci.* **28**, 875-962 (2003)
6. Zhang Y. *et al* Polymer light emitting diodes based on a bipolar transporting luminescent polymer. *J. Mater. Chem.* **13**, 773-777 (2003)
7. Bao, Z.; Lovinger, A.J. Soluble regioregular polythiophene derivative as semiconducting materials for field-effect transistors. *Chem. Mater.* **11**, 2607-2612 (1999)
8. Zou, Y.; Sang, G.; Wu, w.; Liu, Y.; Li, Y. A polythiophene derivative with octyloxyl triphenylamine-vinylene conjugated side chain: synthesis and its applications in field-effect transistor and polymer solar cell. *Synth. Met.* **159**, 182-187 (2009)
9. Salleo, A.; Chabinyc, M.L.; Yang, M.S.; Street, R.A. Polymer thin-film transistors with chemically modified dielectric interfaces. *Appl. Phys. Lett.* **81**, 4383-4385 (2002)
10. Lee, J. *et al* Ion gel gated polymer thin-film transistors. *J. Am. Chem. Soc.* **129**, 4532-4533 (2007)
11. Li, J. *et al* Organic thin-film transistors processed from relatively nontoxic, environmentally friendlier solvents, *Chem. Mater.* **22**, 5737-5753 (2010)

12. Skotheim, T.A.; Elsenbaumer, R.L.; Reynolds J.R. *Handbook of conducting polymers* (Marcel Dekker Inc., New York, 1998)
13. Coakley, K.M.; McGehee, M.D. Conjugated polymer photovoltaic cells. *Chem. Mater.* **16**, 4533-4542 (2004)
14. Bundgaard, E.; Krebs, F.C. Low band gap polymers for organic photovoltaics. *Sol. Energy Mater. Sol. Cells* **91**, 954-985 (2007)
15. Kim, J.Y. *et al* Efficient tandem polymer solar cells fabricated by all-solution processing. *Science* **317**, 222-225 (2007)
16. Cheng, Y.J.; Yang, S.H.; Hsu, C.S. Synthesis of conjugated polymer for organic solar cell applications. *Chem. Rev.* **109**, 5868-5923 (2009)
17. Baran, D.; Balan, A.; Celebi, S.; Esteban, B.M.; Neugebauer, H.; Sariciftci, N.S.; Toppare, L. Processable multipurpose conjugated polymer for electrochromic and photovoltaic applications. *Chem. Mater.* **22**, 2978-2987 (2010)
18. Boucle, J.; Ravirajan, P.; Nelson, J. Hybrid-polymer metal oxide thin film for photovoltaic applications. *J. Mater. Chem.* **17**, 3141-3153 (2007)
19. Dennler, G.; Scharber, M.C.; Brabec, C.J. Polymer-fullerene bulk-heterojunction solar cells. *Adv. Mater.* **21**, 1-16 (2009)
20. Dai, L.; Soundarrajan, P.; Kim, T. Sensors and sensor arrays based on conjugated polymers and carbon nanotubes. *Pure Appl. Chem.* **74**, 1753-1772 (2002)
21. Maiti, J.; Pokhrel, B.; Baruah, R.; Dolui, S.K. Polythiophene based fluorescence sensors for acids and metal ions. *Sensors and Actuators B* **141**, 447-451 (2009)
22. Rahman, A.; Kumar, P.; Park, D.-S.; Shim, Y.-B. Electrochemical sensors based on organic conjugated polymers. *Sensors* **8**, 118-141 (2008)
23. Mcquade, D.T.; Pullen, A.E.; Swager, T.M. Conjugated polymer-based chemical sensor. *Chem. Rev.* **100**, 2537-2574 (2000)
24. Samuel, D.W. Laser physics: Fantastic plastics. *Nature* **429**, 709-711 (2004)
25. Rogers, J. A.; Tate, J.; Li, W.; Bao, Z.; Dodabalapur, A. Printed organic transistors and molded plastic lasers. *Israel Journal of Chemistry*, **40**, 139-146 (2000)
26. Díaz-García, M.A. *et al* Plastic lasers: Semiconducting polymers as a new class of solid-state laser materials. *Synthetic Metals* **84**, 455-462 (1997)

27. Craig, I.M.; Tassone, C.J.; Tolbert, S.H.; Schwartz, B.J. Second-harmonic generation in conjugated polymer films: A sensitive probe of how bulk polymer crystallinity changes with spin speed. *J. Chem. Phys.* **133**, 044901-11 (2010)
28. Lindsay, G.A.; Singer, K.D. *Polymers for Second-Order Nonlinear Optics* (American Chemical Society: Washington DC, 1995)
29. Manjunatha, M.G.; Adhikari, A.V.; Hegde, P.K.; Sandeep, C.S.S.; Philip, R. Synthesis and characterization of a new NLO-active donor-acceptor-type conjugated polymer derived from 3,4-diphenylthiophene. *J. Polym. Res.* **17**, 495-502 (2009)
30. Li, Z. *et al* An attempt to modify nonlinear optical effects of polyurethanes by adjusting the structure of the chromophore moieties at the molecular level using “click” chemistry. *Macromolecules* **39**, 8544-8546 (2006)
31. Tang, C.W. Two-layer organic photovoltaic cell. *Appl. Phys. Lett.*, **48**, 183-185 (1986)
32. Park, S.H. *et al* Bulk heterojunction solar cells with internal quantum efficiency approaching 100%. *Nat. Photonics*, **3**, 297-302 (2009)
33. Heremans, P; Cheyns, D.; Rand, B.P. Strategies for increasing the efficiency of heterojunction solar cells: Material selection and device architecture. *Acc. Chem. Res.* **42**, 1740-1747 (2009)
34. Chandrasekhar, P. *Conducting polymers, fundamental and applications: A practical approach* (Kluwer Academic Publishers, London, 1999)
35. Bargon, J.; Mohmand, S.; Waltman, R.J. Electrochemical synthesis of electrically conducting polymers from aromatic compounds. *IBM J. Res. Develop.* **27**, 330-341 (1983)
36. O. Olabisi (Ed.) *Hand book of thermoplastic* (Marcel Dekker, New York, 1997)
37. Kumar, D.; Sharma, R.C. Advances in conducting polymers. *Eur. Polym. J.* **34**, 1053-1060 (1998)
38. Roncali, J. Conjugated poly(thiophenes): synthesis, functionalization, and applications. *Chem. Rev.* **92**, 711-738 (1992)
39. McCullough, R.D. The chemistry of conducting polythiophenes. *Adv. Mater.* **10**, 1-23 (1998)

40. Scherf, U. Oligo- and polyarylenes, oligo- and polyarylenevilylenes. *Top Curr. Chem.* **201**, 163-222 (1999)
41. Yamamoto, T. Conjugated polymers with electronic and optical functionalities: Preparation by organometallic polycondensation, properties, and applications. *Macromol. Rapid Comm.* **23**, 583-606 (2002)
42. Cheng, Y.J.; Luh, T.Y. Synthesizing optoelectronic heteroaromatic conjugated polymers by cross-coupling reactions. *J. Organomet. Chem.* **689**, 4137-4148 (2004)
43. Hadziioannou, G.; Malliaras, C.G. *Semiconducting polymers: Chemistry, physics and engineering* (Second edition, 1<sup>st</sup> Vol., Wiley-VCH, Germany, 2007)
44. Curtis, M.D.; McClain, M.D. Synthesis of poly(3-alkylthienylene ketone)s by the Pd-catalyzed copolymerization of carbon monoxide with thienyl mercuric chlorides. *Chem. Mater.* **8**, 945-951 (1996)
45. Yamamoto, T.; Uemura, T.; Tanimoto, A.; Sasaki, S. Synthesis and chemical properties of  $\pi$ -conjugated poly(imidazole-2,5-diyl)s. *Macromolecules* **36**, 1047-1053 (2003)
46. Elsenbaumer, R.L.; Jen, K.Y.; Oboodi, R. Processible and environmentally stable conducting polymers. *Synth. Met.* **15**, 169-174 (1986)
47. McCullough, R.D.; Lowe, R.D. Enhanced Electrical Conductivity in Regioselectively Synthesized Poly(3-alkylthiophenes). *J. Chem. Soc. Chem. Commun.*, 70-72 (1992)
48. Loewe, R.S.; Ewbank, P.C.; Liu, J.; Zhai, L.; McCullough, R.D. Regioregular, head-to-tail coupled poly(3-alkylthiophenes) made easy by the GRIM method: Investigation of the reaction and the origin of regioselectivity. *Macromolecules* **34**, 4324-4333 (2001)
49. Chen, T.A.; Reike, R.D. The first regioregular head-to-tail poly(3-hexylthiophene-2,5-diyl) and a regiorandom isopolymer: nickel versus palladium catalysis of 2(5)-bromo-5(2)-(bromozincio)-3-hexylthiophene polymerization. *J. Am. Chem. Soc.* **114**, 10087-10088 (1992)
50. Rehahn, M.; Schluter, A.D.; Wegner, G.; Feast, W.J. Soluble poly(*para*-phenylene)s. 2. Improved synthesis of poly(*para*-2,5-di-n-hexylphenylene) via

- Pd-catalysed coupling of 4-bromo-2,5-di-n-hexylbenzeneboronic acid. *Polymer* **30**, 1060-1062 (1989)
51. Bao, Z.; Chan, W.; Lu, L. Synthesis of conjugated polymer by the Stille Coupling Reaction. *Chem. Mater.* **5**, 2-3 (1993)
52. Guillet, J. *Photophysics and photochemistry* (Cambridge University Press, London, 1985)
53. Lakowitz, J.R. *Principles of fluorescence spectroscopy* (Kluwer Academic, New York, 2<sup>nd</sup> Edition, 1999)
54. Kim, J. Assemblies of conjugated polymers: Intermolecular and intramolecular effects on the photophysical properties of conjugated polymers. *Pure Appl. Chem.* **74**, 2031-2044 (2002)
55. Scheblykin, I.G.; Yartsev, A.; Pullerits, T.; Gulbinas, V.; Sundström, V. Excited state and charge photogeneration dynamics in conjugated polymers. *J. Phys. Chem. B.* **111**, 6303-6321 (2007)
56. Cabarcos, E.L.; Carter, S.A. Effect of the molecular weight and the ionic strength on the photoluminescence quenching of water-soluble conjugated polymer sodium poly[2-(3-thienyl)ethoxy-4-butylsulfonate]. *Macromolecules* **38**, 4409-4415 (2005)
57. Davey, A.P.; Elliott, S.; O'Connor, O.; Blau, W. New rigid backbone conjugated organic polymers with large fluorescence quantum yields. *J. Chem. Soc. Chem. Comm.* 1433-1434 (1995)
58. Chosrovian, H. *et al* Time-resolved fluorescence studies on thiophene oligomers in solution. *Synth. Met.* **60**, 23-26 (1993)
59. Beljonne, D.; Cornil, J.; Friend, R.H.; Janssen, R.A.J.; Bredas, J.L. Influence of chain length and derivatization on the lowest singlet and triplet states and intersystem crossing in oligothiophenes. *J. Am. Chem. Soc.* **118**, 6453-6461 (1996)
60. Johansson, T.; Mammo, W.; Svensson, M.; Andersson, M.R.; Inganäs, O. electrochemical bandgaps of substituted polythiophenes. *J. Mater. Chem.* **13**, 1316-1323 (2003)

61. Bredas, J.L.; Silbey, R. Bourdreaux, D.S.; Chance, R.R. Chain-length dependence of electronic and electrochemical properties of conjugated systems: polyacetylene, polyphenylene, polythiophene, and polypyrrole. *J. Am. Chem. Soc.* **105**, 6555-6559 (1983)
62. Hu, X.; Xu, L. Structure and properties of 3-alkoxy substituted polythiophene synthesized at low temperature. *Polymer* **41**, 9147-9154 (2000)
63. Fichou, D. Structural order in conjugated oligothiophenes and its implications on opto-electronic devices. *J. Mater. Chem.* **10**, 571-588 (2000)
64. Leclerc, M.; Faid, K. Electrical and Optical Properties of Processable Polythiophene Derivatives: Structure-Property Relationships. *Adv. Mater.*, **9**, 1087-1094 (1997)
65. Zhao, X.; Hu, X.; Gan, L.H. Photoluminescent behavior of poly(3-hexylthiophene) derivatives with a high azobenzene content in the side chains, *Polym. Adv. Technol.*, **16**, 370-377 (2005)
66. Anderson, M.R.; Beggren, M.; Inganas, O.; Gustafsson, G. Electroluminescence from substituted poly(thiophenes)-from blue to nearinfrared. *Macromolecules*, **28**, 7525-7529 (1995)
67. Anderson, M.R. *et al* Substituted polythiophenes designed for optoelectronic devices and conductors. *J. Mater. Chem.*, **9**, 1933-1940 (1999)
68. Daoust, V.; Leclerc, M. Structure-property relationships in alkoxy-substituted polythiophenes. *Macromolecules*, **24**, 455-459 (1991)
69. Pomerantz, M.; Yang, H.; Cheng, Y. Poly(alkyl thiophene-3-carboxylates). Synthesis and Characterization of Polythiophenes with a Carbonyl Group Directly Attached to the Ring. *Macromolecules* **28**, 5706-5708 (1995)
70. Pomerantz, M.; Chang, Y.; Kasim, R.K.; Elsenbaumer, R.L. Poly(alkyl thiophene-3-carboxylates). Synthesis, properties and electroluminescence studies of polythiophenes containing a carbonyl group directly attached to the ring. *J. Mater. Chem.*, **9**, 2155-2163 (1999)
71. Lanzi, M.; Bizzarri, P.C.; Paganin, L.; Cesari, G. Highly processable ester-functionalized polythiophenes as valuable multifunctional and post-functionalizable conjugated polymers *Eur. Polym. J.* **43**, 72-83 (2007)



72. Murphy, A.R. *et al.*, Synthesis, Characterization, and Field-Effect Transistor Performance of Carboxylate-Functionalized Polythiophenes with Increased Air Stability. *Chem. Mater.* **17**, 4892-4899 (2005).
73. Kang, T.K.; Kim, J.Y.; Kim, K.J.; Lee, C.; Rhee, S.B. Photoluminescence properties of various polythiophene derivatives. *Synth. Met.* **69**, 377-378 (1995).
74. Lee, C.; Kim, K.J.; Rhee, S.B. The effects of ester substitution and alkyl chain length on the properties of poly(thiophene)s. *Synth. Met.*, **69**, 295-296 (1995).
75. Lee, S.; Hong, S.I.; Lee, C.; Rhee, S.B.; Kang, T.J. Luminescence study of poly(3-alkyl ester thiophene)s. *Mol Cryst. Liq Cryst.*, **295**, 19-22 (1997)
76. Bolognesi, A.; Botta, C.; Geng, Z.; Flores, C.; Denti, L. Modified poly(3-alkylthiophene) for LED preparation. *Synth. Met.*, **71**, 2191-2192 (1995).
77. Liao, K.-S.; Yambem, S. D.; Haldar, A.; Alley, N.J.; Curran, S.A. Designs and architectures for the next generation of organic solar cells. *Energies* **3**, 1212-1250 (2010)
78. Rockett, A.A. The future of energy-photovoltaics. *Curr. Opin. Solid State Mater. Sci.* **14**, 117-122 (2010)
79. Kippelen, B.; Bredas, J.-L. Organic photovoltaics. *Energy Environ. Sci.* **2**, 251-261 (2009)
80. Chamberlain, G.A. Organic solar cells: A review. *Solar Cells* **8**, 47-83 (1983)
81. Nunzi, J.-M. Organic photovoltaic materials and devices. *C. R. Physique* **3**, 523-542 (2002)
82. Hoppe, H.; Sariciftci, N.S. Organic solar cells: an overview. *J. Mater. Res.* **19**, 1924-1945 (2004)
83. Roncali, J. Molecular bulk heterojunctions: An emerging approach to organic solar cells. *Acc. Chem. Res.* **42**, 1719-1730 (2009)
84. Brabec, C.J. *et al* Origin of the open-circuit voltage of plastic solar cells. *Adv. Funct. Mater.* **11**, 374-380 (2001)
85. Bredas, J.-L.; Norton, J.E.; Cornil, J.; Coropceanu, V. Molecular understanding of organic solar cells: The challenges. *Acc. Chem. Res.* **42**, 1691-1699 (2009)

86. Morteani, A.C.; Sreearunothai, P.; Herz, L.M.; Friend, R.H. Silva, C. Exciton regeneration at polymeric semiconductor heterojunctions. *Phys. Rev. Lett.* **92**, 247402 (2004)
87. Helgesen, M.; Søndergaard, R.; Krebs, F.C. Advanced materials and processes for polymer solar cell devices. *J. Mater. Chem.* **20**, 36-60 (2010)
88. Bredas, J.L.; Cornil, J.; Heeger, A.J. The exciton binding energy in luminescent conjugated polymers. *Adv. Mater.* **8**, 447-452 (1996)
89. Nelson, J. Organic photovoltaic films. *Curr. Opin. Solid State Mater. Sci.* **6**, 87-95 (2002)
90. Hung, Y.S. *et al* Electronic structures of interfacial states formed at polymeric semiconductor heterojunctions. *Nat. Mater.* **7**, 483-489 (2008)
91. Spanggaard, H.; Krebs, F.C. A brief history of the development of organic and polymeric photovoltaics. *Sol. Energy Mater. Sol. Cells* **83**, 125-146 (2004)
92. Tang, C.W.; Albrecht, A.C. Transient photovoltaic effects in metal-chlorophyll-a-metal sandwich cells. *J. Chem. Phys.* **63**, 953-961 (1975)
93. Seanor, D.A. (Ed) *Electrical properties of polymers* (Academic Press, New York, 1982)
94. Skotheim, T.A. *Handbook of conducting polymers* (Marcel Dekker, New York, 1986)
95. Weinberger, B.R.; Akhtar, M.; Gau, S.C. Polyacetylene photovoltaic devices. *Synth. Met.* **4**, 187-197 (1982)
96. Glenis, S.; Tourillon, G.; Garnier, F. Influence of the doping on the photovoltaic properties of thin films of poly-3-methylthiophene. *Thin. Solid Films* **139**, 221-231 (1986)
97. Marks, R.N.; Halls, J.J.M.; Bradley, D.D.C.; Friend, R.H.; Holmes, A.B. The photovoltaic response in poly(p-phenylene vinylene) thin-film devices. *J. Phys. Condens. Matter* **6**, 1379-1394 (1994)
98. Moze, A.J.; Sariciftci, N.S.; Conjugated polymer photovoltaic devices and materials. *C.R. Chimie* **9**, 568-577 (2006)
99. Wöhrle, D.; Meissner, D. Organic solar cells. *Adv. Mater.* **3**, 129-138 (1991)

100. Karg, S.; Riess, W.; Dyakonov, V.; Schwoerer, M. Electrical and optical characterization of poly(phenylene-vinylene) light emitting diodes. *Synth. Met.* **54**, 427-433 (1993)
101. Sariciftci, N.S.; Smilowitz, L.; Heeger, A.J.; Wudl, F. Photoinduced electron transfer from a conducting polymer to Buckminsterfullerene. *Science* **258**, 1474-1476 (1992)
102. Halls, J.J.M.; Pichler, K.; Friend, R.H.; Moratti, S.C.; Holmes, A.B. Exciton dissociation at a poly(*p*-phenylenevinylene)/C<sub>60</sub> heterojunction. *Synth. Met.* **77**, 277-280 (1996)
103. Thompson, B.C.; Frechet, J.M. Polymer-fullerene composite solar cells. *Angewandte Chemie* **47**, 58-77 (2008)
104. Chen, J.; Cao, Y. Development of novel conjugated donor polymers for high-efficiency bulk-heterojunction photovoltaic devices. *Acc. Chem. Res.* **42**, 1709-1718 (2009)
105. Hope, H. *et al* Efficiency limiting morphological factors of MDMO-PPV:PCBM plastic solar cells. *Thin Solid Films* **511**, 587-592 (2006)
106. D. Sukeguchi, *et al* New diaryl-methanofullerene derivatives and their properties for organic thin-film solar cells. *Beilstein J. Org. Chem.* **5**, No. 7 (2009); DOI: 10.3762/bjoc.5.7
107. Gao, J.; Hide, F.; Wang, H. Efficient photodetectors and photovoltaic cells from composites of fullerenes and conjugated polymers: photoinduced electron transfer *Synth. Met.* **84**, 979-980 (1997)
108. Riedel, I. *et al* Polymer solar cells with novel fullerene-based acceptor. *Thin Solid Films* **451**, 43-47 (2004)
109. Yu, G.; Pakbaz, K.; Heeger, A.J. Semiconducting polymer diodes: Large size, low cost photodetectors with excellent visible-ultraviolet sensitivity. *Appl. Phys. Lett.* **64**, 3422-3424 (1994)
110. Köhler, A.; Wittmann, H.F.; Friend, R.H.; Khan, M.S.; Lewis, J. Enhanced photocurrent response in photocells made with platinum-poly-yne/C<sub>60</sub> blends by photoinduced electron transfer. *Synth. Met.* **77**, 147-150 (1996)

111. Hummelen, J.C. *et al* Preparation and characterization of fulleroid and methanofullerene derivatives. *J. Org. Chem.* **60**, 532-538 (1995)
112. Yu, G.; Gao, J.; Hummelen, J.C.; Wudl, F.; Heeger, A.J. Polymer photovoltaic cells: Enhanced efficiencies via a network of internal donor-acceptor heterojunctions. *Science* **270**, 1789-1791 (1995)
113. Beek, W.J.E.; Wienk, M.M.; Kemerink, M.; Janssen, R.A.J. Hybrid zinc oxide conjugated polymer bulk heterojunction solar cells. *J. Phys. Chem. B* **109**, 9505-9516 (2005)
114. Huynh, W.U.; Dittmer, J.J.; Alivisatos, A.P. Hybrid Nanorod-Polymer Solar Cells. *Science* **295**, 2425-2427 (2002)
115. Sun, B.; Marx, E.; Greenham, N.C. Photovoltaic Devices Using Blends of Branched CdSe Nanoparticles and Conjugated Polymers. *Nano Lett.* **3**, 961-963 (2003)
116. Lin, Y.T. *et al* Efficient photoinduced charge transfer in TiO<sub>2</sub> nanorod/conjugated polymer hybrid materials. *Nanotechnology*, **17**, 5781-5785 (2006)
117. Wu, M.-C. *et al* Nanostructured polymer blends (P3HT/PMMA): Inorganic titania hybrid photovoltaic devices. *Sol. Energy Mater. Sol. Cells* **93**, 961-965 (2009)
118. Beek, W.J.E.; Wienk, M.M.; Janssen, R.A.J. Efficient Hybrid Solar Cells from Zinc Oxide Nanoparticles and a Conjugated Polymer. *Adv. Mater.* **16**, 1009-1013 (2004)
119. Boucle, J.; Ravirajan, P.; Nelson, J. Hybrid polymer-metal oxide thin films for photovoltaic applications. *J. Mater. Chem.* **17**, 3141-3153 (2007)
120. Greenham, N.C.; Peng, X.; Alivisatos, A.P. Photoinduced electron transfer from conjugated polymers to CdSe nanocrystals. *Phys. Rev. B* **59**, 10622-10629 (1999)
121. Brabec, C.J.; Padinger, F.; Sariciftci N.S., Hummelen, J.C. Photovoltaic properties of conjugated polymer/methanofullerene composites embedded in a polystyrene matrix. *J. Appl. Phys.* **85**, 6866 (1999)
122. Hadziioannou G, van Hutten PF (ed.) *Semiconducting Polymers: Chemistry, physics and engineering*, (WILEY-VCH, Germany, pp554, 2000)

123. Gao, J.; Hide, F.; Wang, H. Efficient photodetectors and photovoltaic cells from composites of fullerenes and conjugated polymers: photoinduced electron transfer *Synth. Met.* **84**, 979-980 (1997)
124. Chittibabu, K.G.; Li, L.; Kamath, M.; Kumar, J.; Tripathy, S K. Synthesis and properties of a novel polythiophene derivative with a side-chain NLO chromophore. *Chem. Mater.* **6**, 475-480 (1994)



## Chapter 2

# Synthesis and characterization of soluble $\pi$ -conjugated polymers

## 2.1 Introduction

Conjugated polymers are receiving great research interest due to their unique electronic and optical properties and they offer many possibilities in terms of their potential applications in light emitting diodes (LED), sensors, photovoltaic devices, electrochromic devices etc.<sup>1-23</sup> The creative design and development strategies for conjugated polymers have led to new materials and enhanced performance. In determining the physical properties of conjugated polymers, more research has been focused on the structure and function of these materials. The different synthetic approaches can help to achieve the magnitude of  $\pi$  overlap along the backbone and choice of suitable side chains influences the properties like band gap, ionic conductivity, morphology and miscibility with other substances.<sup>1,3,14,24</sup> Chemical architecture to receive improved property and performance of conjugated polymer is hence being carried out in research with high impetus.

Generally, functional conjugated polymers are prepared through electrochemical and chemical methods.<sup>3,4,24-27</sup> The limitation in producing large amount of polymers by electrochemical process has restricted its utility. Therefore, chemical polymerization methods have attained popularity for synthesizing the large scale and soluble polymer. The chemical polymerization methods include oxidative coupling, Yamamoto coupling, McCullough method, Grignard Metathesis (GRIM) method, Reike method, Suzuki and Still method.<sup>28-33</sup>  $\text{FeCl}_3$  oxidative coupling is a straightforward, simple, versatile, and least expensive method among other chemical polymerization techniques. 3- substituted polythiophenes with alkyl, fluoroalkyl, alkoxy, ester groups in side chain have been synthesized by  $\text{FeCl}_3$  based oxidative coupling.<sup>34-42</sup> Moreover, solution condensation polymerization to form polyazomethines, polyurethanes (PUs) etc. is also employed extensively.<sup>43-46</sup>

In this chapter, an effort has been made to synthesize conjugated polymers with special emphasis on the solubility and tailor made band gap for application in photovoltaic devices. 1,1'-bis-2-naphthol based polyurethanes, side chain and main chain azomethinic linkage containing polythiophenes and polycarbazole derivatives have been synthesized with improved solubility using condensation and oxidative coupling methods.

This chapter describes the synthesis and characterization of monomers and polymers and thermal properties of polymers. We have synthesized the following polymers.

- i) Poly [N,N-bis -(2-thienylmethylene)-o-dianisidine] (PBTD)
- ii) Poly [(3-phenyl azomethine ethyl) thiophene] (PPAET)
- iii) Poly [(3-phenyl azomethine butyl) thiophene] (PPABT)
- iv) Poly[(9-dodecylcarbazole)] (PDDC)
- v) Poly[(9-dodecylcarbazole)-co-thiophene] (PDDCT)
- vi) Poly(tolyl-1,1'-binaphthyl carbamate) (PU<sub>1</sub>)
- vii) Poly(hexamethylene-1,1'-binaphthyl carbamate) (PU<sub>2</sub>)

The synthetic procedures of monomers and polymers are discussed below. The monomers were characterized by FTIR, <sup>1</sup>H NMR and CHN analyzer. The synthesized polymers were also thoroughly characterized by FTIR, <sup>1</sup>H NMR, UV-Vis and GPC analyses. Thermal properties of the polymers were studied using TGA and DSC techniques.

## 2.2 Materials

2-Thiophenecarboxyldehyde (Aldrich), o-dianisidine (Aldrich), 3-thiophene carboxyldehyde (Aldrich), 4-ethyl aniline (Merck), 4-butyl aniline (Merck), p-toluenesulphonic acid (PTSA) (Aldrich), Carbazole (Aldrich), 3-thiophene carboxyldehyde (Aldrich), thiophene (Aldrich), do-decyl bromide (Merck), 2,4-Toluenediisocyanate(TDI) (Merck), Hexamethylenediamine (HMDI) (Merck), Iron(III)chloride (Aldrich) were highly pure commercial product and used as received. . 2-Naphthol (Merck Ltd., Mumbai) was recrystallized from methanol. All the solvents were distilled before use and the reactions were performed under nitrogen atmosphere.



### **2.3. Instrumentations**

#### **2.3.1. Fourier Transform Infrared Spectrophotometer (FTIR )**

FTIR is a useful method for the characterization of monomer and polymers. It is primarily used for the detection of functional groups, but analysis of spectra in the lower frequency finger print region can give evidence of degree of polymerization and the effect of substituents on the electronic properties of the polymer backbone. FTIR spectra were recorded on a Nicolet, Impact 410 by using KBr pallet.

#### **2.3.2. Nuclear Magnetic Resonance Spectrometer ( $^1\text{H}$ NMR)**

NMR spectroscopy is one of the principal techniques used to obtain structural information about molecules. Structure of compound can be determined by studying the peaks of NMR spectra. It is a very selective technique, distinguishing among many atoms within a molecules or collection of molecules of the same type but which differ only in terms of their local chemical environment. In proton NMR spectroscopy, structure of molecules is ascertained with respect to hydrogen nuclei within the molecule of a substance.  $^1\text{H}$  NMR spectra were obtained on a Bruker AMX 400 MHz with deuterated  $\text{CHCl}_3$  ( $d_3$ ), and DMSO ( $d_6$ ) solvents having TMS as internal standard.

#### **2.3.3. Elemental Analysis**

Elemental analysis of the samples gives % composition of constituent elements viz, C, H, N, O, S indicating structural identification of the same. Elemental analysis was carried out in Perkin Elmer-2400 Series-II CHNS/O analyzer.

#### **2.3.4. Inherent Viscosity Measurements**

Viscosity is an important characteristic for all materials, especially polymers. Inherent viscosity for polymer is defined as the flow time of a polymer solution through a narrow capillary relative to the flow time of the pure solvent through the capillary. It gives an idea of the extent of polymerization and molecular weight. The inherent viscosity ( $\eta_{\text{inh}}$ ) was determined using an Ubbelohde viscometer in N,N'-dimethylacetamide (DMAc) at  $30 \pm 0.1$  °C with 0.5 g/dl polymer solution.

### **2.3.5. Gel Permeation Chromatography (GPC)**

Gel permeation chromatography (GPC) is used to determine the relative molecular weight of polymer samples as well as the distribution of molecular weights. Generally, GPC measures the molecular volume and shape function as defined by the intrinsic viscosity of polymer sample. Molecular weights of polymers were measured by gel permeation chromatography (410 Waters Model). Flow rate is maintained at 1 ml/min. Polymers were dissolved in THF solvent. Molecular weights were determined on the basis of polystyrene standards.

### **2.3.6. Thermogravimetric Analysis (TGA)**

Thermogravimetric analysis (TGA) reveals the thermal characteristics of polymers including degradation temperature, absorbed moisture content the level of oligomer in polymer etc. It determines the weight loss with respect to temperature. Thermogravimetric analysis (TGA) was conducted on a Shimadzu TG50 thermogravimetric analyzer with a heating rate of 10 °C/min under a nitrogen atmosphere. Analysis was performed at 0- 650 °C temperature ranges.

### **2.3.7. Differential Scanning Calorimetry (DSC)**

Differential scanning calorimetry (DSC) is used widely for polymers. It evaluates glass transition temperature ( $T_g$ ), melting temperature ( $T_m$ ) and purity of polymers. The result of a DSC experiment is a curve of heat flux versus temperature or versus time. Differential scanning calorimetry (DSC) of the polymers was accomplished on DSC-60 (Shimadzu) with a heating rate of 10 °C/ min under a nitrogen atmosphere. Analysis was performed at 0- 500 °C temperature ranges.

## **2.4. Experimental**

### **2.4.1. Monomer Synthesis**

#### **2.4.1.1. $N,N'$ -bis -(2-thienylmethylene)-o-dianisidine (BTD)**

In a 100 ml three necked round bottom flask equipped with a nitrogen inlet, a condenser and a Dean-Stark trap, 1.82 g (16.1 mmol) thiophene-2-carboxyldehyde and

1.95 g (8.0 mmol) o-dianisidine were introduced in 30 ml of methanol. P-toluenesulphonic acid was used as the catalyst. Nitrogen gas was purged into the flask and the reaction mixture was allowed to reflux for six hours under stirring. The yellow precipitate obtained after completion of the reaction was filtered out and washed with ethanol and hot water repeatedly and dried in vacuum. The monomer thus obtained was purified by recrystallization in acetone.

Yield 79%, mp: 207°C.

FTIR (KBr): 1250, 1443, 1617, 2821, 2964  $\text{cm}^{-1}$ .

$^1\text{H}$  NMR (400 MHz,  $\text{CDCl}_3$ )  $\delta$  (ppm): 3.73, 7.08, 7.23, 7.34-7.82, 8.76

Elemental analysis: Cal: C, 66.66%, H, 4.63%, N, 6.48%, O, 7.40%, S, 14.81%

Found: C, 66.21%, H, 4.93%, N, 6.16%, O, 7.63%, S, 14.27%

#### 2.4.1.2. 3-Phenyl azomethine ethylthiophene (PAET)

In a 100 ml three necked round bottom flask equipped with a nitrogen inlet, a condenser and a Dean-Stark trap, 1.82 g (16.1 mmol) thiophene-3-carboxyldehyde and 1.95 g (16.1 mmol) 4-ethyl aniline was introduced in 30 ml of methanol. P-toluenesulphonic acid was used as the catalyst. Nitrogen gas was purged into the flask and the reaction mixture was allowed to reflux for six hours under stirring. The yellow precipitate obtained after completion of the reaction was filtered out and washed with ethanol and hot water repeatedly and dried in vacuum. The monomer thus obtained was purified by recrystallization in acetone.

Yield 73%, m.p. 87 °C.

FTIR (KBr): 1250, 1443, 1607, 2821, 2964, 3021  $\text{cm}^{-1}$ ;

$^1\text{H}$  NMR (400 MHz,  $\text{CDCl}_3$ )  $\delta$  (ppm): 1.26-2.61, 7.08, 7.19 -7.38, 7.51, 8.27

Elemental analysis: Cal: C, 72.55%, H, 6.04%, N, 6.51%, S, 14.88%

Found: C, 72.14%, H, 6.26%, N, 6.63%, S, 14.69%

#### 2.4.1.3. 3-phenyl azomethine butylthiophene (PABT)

The 3-phenyl azomethine butyl thiophene was synthesized employing the same procedure that for monomer PAET with 1.82 g (16.1 mmol) of thiophene-3-carboxyldehyde and 2.40 g (16.1 mmol) of 4-butyl aniline.

Yield 76%, m.p. 83 °C

FTIR (KBr): 1258, 1441, 1605, 2832, 2951, 3029  $\text{cm}^{-1}$ ;

$^1\text{H}$  NMR (400 MHz,  $\text{CDCl}_3$ )  $\delta$  (ppm): 0.92-2.72, 7.06, 7.20, 7.34-7.48, 8.23

Elemental analysis: Cal: C, 74.07%, H, 6.99%, N, 5.76%, S, 13.17%

Found: C, 74.18%, H, 7.06%, N, 5.63%, S, 13.04%

#### 2.4.1.4. 9-Dodecyl carbazole (DDC)

To a 250 ml round bottom flask, flushed with nitrogen and equipped with a condenser and magnetic stirrer, carbazole (8 g, 4.8 mmol) dissolved in 50 ml of DMF and dodecyl bromide (11.96 g, 4.8 mmol) were added. Then,  $\text{K}_2\text{CO}_3$  (8.29 g, 6 mmol) was added to this mixture and allowed to proceed the reaction for 15 hours at 150 °C under continuous stirring. After completion of the reaction, the mixture was cooled to room temperature followed by precipitation of the product in 500 ml of cold water. The precipitate was filtered and washed with a dilute solution of KOH and water. Finally product was dried over anhydrous magnesium sulphate and it was purified by column chromatography using 1:9 ethyl acetate/hexane as the eluent.<sup>47</sup>

Yield 71%, m.p. 68 °C.

FTIR (KBr): 1261, 1446, 2845, 2911, 3021  $\text{cm}^{-1}$ ;

$^1\text{H}$  NMR (400 MHz,  $\text{CDCl}_3$ )  $\delta$  (ppm): 0.93-2.87 (dodecyl protons), 7.06-7.81 (Ar-H)

Elemental analysis: Cal: C, 85.97%, H, 9.85%, N, 4.17%

Found: C, 85.34%, H, 10.17%, N, 4.38%

#### 2.4.1.5. 1,1'-bis-2-naphthol (BINOL)

In a 500 ml three necked round bottom flask, provided with a dropping funnel, a sealed stirrer and a reflux condenser, 3 g (0.02 mol) of 2-naphthol was taken in 200 ml of water and heated to the boiling point. To the boiling liquid containing liquid 2-naphthol, 15 ml aqueous solution of 4.5 g of  $\text{FeCl}_3$  (0.02 mol) was added slowly. Soon the oily drops of 2-naphthol disappeared and the product separated out in flakes. The mixture is boiled for 1 hour and hot suspension was filtered and washed with hot water. The product was dried in vacuum and recrystallised from toluene.<sup>48</sup>

Yield 89%, m.p. 218°C.

FTIR (KBr):  $\nu = 3426, 2935 \text{ cm}^{-1}$ ;

$^1\text{H NMR}$ (400 MHz,  $\text{CDCl}_3$ )  $\delta$  (ppm): 5.03, 7.38, 7.86-7.96

Elemental analysis: Cal: C, 82.81%, H, 5.38%, O, 12.82%.

Found: C, 82.67%, H, 5.43%, O, 12.80%.

#### 2.4.2. Synthesis of polymers

##### 2.4.2.1. Poly [N,N'-bis -(2-thienylmethylene)-o-dianisidine] (PBTB)

The polymer was synthesized by following the standard procedure,  $\text{FeCl}_3$  oxidative coupling method.<sup>49</sup> In a 100 ml round bottom flask equipped with a condenser, and a nitrogen gas inlet, 2 g (4.62 mmol) of monomer (BTB) and 10 ml chloroform were introduced. 3.25 g (20 mmol) of anhydrous  $\text{FeCl}_3$  was added in small proportions over a period of 1 hour. The reaction was carried out at room temperature with continuous stirring for 24 hours. The product was precipitated in methanol containing small amount of HCl followed by washing with methanol for several times. The collected polymer powder was dissolved in DMAc and reprecipitated in methanol with small amount of ammonia repeatedly to ensure its purification.

Yield 51%.

FTIR (KBr): 3364, 3089, 2959, 1621, 1212  $\text{cm}^{-1}$

$^1\text{H NMR}$  (400 MHz, DMSO)  $\delta$  (ppm): 3.80, 7.06, 7.18, 7.54-7.71, 8.81

#### 2.4.2.2. Poly [3-phenyl azomethine ethylthiophene] (PPAET)

In a 100 ml round bottom flask equipped with a condenser and a nitrogen gas inlet, 2 g (9.24 mmol) of monomer (PAET) and 10 ml chloroform were introduced. 6.5 g (40 mmol) of anhydrous  $\text{FeCl}_3$  was added in small proportions over a period of approximately 1 hour. The reaction was carried out at room temperature with continuous stirring for 24 hours. The product was precipitated in methanol containing small amount of HCl followed by washing with methanol for several times. The collected polymer powder was dissolved in DMAc and reprecipitated in methanol, repeatedly, with small amount of ammonia to ensure its purification.

Yield 59%

FTIR (KBr): 1257, 1608, 2819, 2936, 3034  $\text{cm}^{-1}$ ;

$^1\text{H-NMR}$  (400 MHz, DMSO)  $\delta$  (ppm) : 1.28-2.63, 7.1, 7.56, 7.79, 8.31

#### 2.4.2.3. Poly [3-phenyl azomethine butylthiophene] (PPABT)

Synthetic procedure of PPABT is same as used for PPAET using the monomer PABT (2 g, 5.6 mmol) and  $\text{FeCl}_3$  (4.1 g, 30 mmol).

Yield 53%.

FTIR (KBr): 1254, 1612, 2856, 2923, 3096  $\text{cm}^{-1}$ .

$^1\text{H-NMR}$  (400 MHz, DMSO)  $\delta$  (ppm): 0.96-2.75, 6.78-7.72, 8.26

#### 2.4.2.4. Poly (9-dodecyl carbazole) (PDDC)

9-dodecyl carbazole was dissolved in 50 ml of dry dichloromethane followed by the addition of anhydrous  $\text{FeCl}_3$  (4.5 g, 5 mol eq. pre-dissolved in 30 ml dry acetonitrile). The colour of the solution was changed from white to dark green. It was allowed to stir under nitrogen for 24 hours at 0-5  $^\circ\text{C}$ . The solution was poured into 100 ml of methanol, and stirred vigorously for 1 hour. The resulting precipitate was collected and washed with methanol and 30% ammonium hydroxide. The collected polymer powder was dissolved in THF and reprecipitated in methanol repeatedly to ensure its purification.<sup>50</sup>

Yield 53%

FTIR (KBr): 1456, 1576, 2855, 2934, 3047  $\text{cm}^{-1}$

$^1\text{H NMR}$  (400MHz, DMSO)  $\delta$  (ppm): 0.94-3.18(N-alkyl), 6.61 -7.09 (Ar-H)

#### 2.4.4.5. Poly(9-dodecylcarbazole)-*co*-thiophene (PDDCT)

Synthetic procedure is same as employed in the case of PDDC with the monomer composition of 50% of 9-dodecyl carbazole (2 g, 5.9 mmol) and 50% of thiophene (0.5 g, 5.9 mmol) and 9.57 g (59 mmol) of  $\text{FeCl}_3$ .

Yield 59%

FTIR (KBr): 1496, 1579, 2867, 2918, 3018, 3049  $\text{cm}^{-1}$

$^1\text{H}$  NMR (400MHz) (DMSO):  $\delta$  0.96-3.68 (N-alkyl), 7.04, 7.22 (Thiophene-H), 7.37-7.65 ppm

#### 2.4.4.6. Poly(tolyl-1,1'-binaphthyl carbamate) ( $\text{PU}_1$ )

1 g (3.4 mmol) of 1,1'-bis-2-naphthol, 0.60 g (3.4 mmol) of 2,4-toluenediisocyanate and dried THF (20 ml) were charged in a three-necked flask equipped with nitrogen inlet, reflux condenser and a dropping funnel. The reaction mixture was stirred for 6 h at 70  $^\circ\text{C}$  under nitrogen. After completion of the reaction, the polymer was precipitated by drop wise addition of the viscous reaction mixture into methanol. The collected polymer powder was dissolved in DMAc and reprecipitated in methanol repeatedly to ensure its purification<sup>51</sup>

Yield 86%.

IR (KBr):  $\nu$  = 2967, 1714, 3376, 1207  $\text{cm}^{-1}$ .

$^1\text{H}$  NMR(400 MHz, DMSO)  $\delta$  (ppm): 2.41, 7.04-7.46, 7.78, 8.0

#### 2.4.4.7. Poly(hexamethylene-1,1'-binaphthyl carbamate) ( $\text{PU}_2$ )

Another polyurethane compound ( $\text{PU}_2$ ) was prepared using hexamethylene diisocyanate (HMDI) and 1,1'-bis-2-naphthol by employing same procedure as used in preparation of  $\text{PU}_1$ .

Yield 84%.

IR (KBr):  $\nu$  = 3089, 2959, 1721, 3364, 1212  $\text{cm}^{-1}$ .

$^1\text{H}$  NMR (400 MHz, DMSO)  $\delta$  (ppm): 1.34-2.31, 7.21-7.83, 8.0

## 2.5. Results and discussion

### 2.5.1. Characterization of monomers

The monomer (BTD) containing thiophene ring and azomethine linkage within the chain with full conjugated structure has been synthesized by condensation reaction between o-dianisidine and thiophene-2-carboxyldehyde in 1:2 ratio. The reaction scheme for preparation of BTD is shown in Scheme 2.1. The monomer was obtained in good yield. The IR peak at  $1617\text{ cm}^{-1}$  indicates the formation of azomethine linkage.  $^1\text{H}$  NMR peaks (Figure 2.1) at 3.73 ppm and 8.76 ppm infer the presence of methoxy and azomethine proton in the monomer.

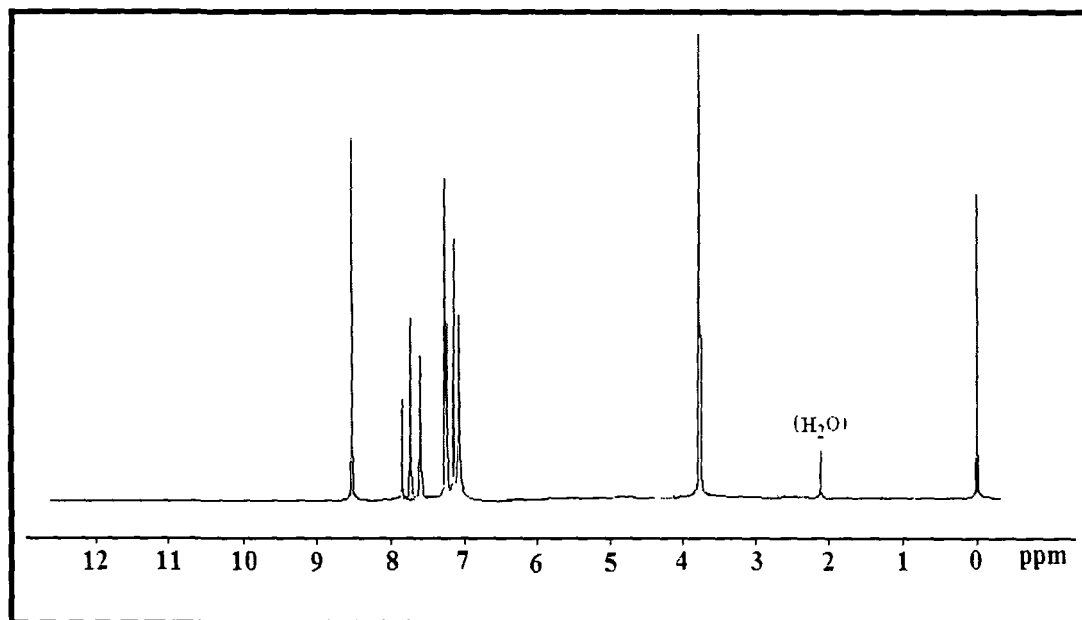


**Figure 2.1:**  $^1\text{H}$  NMR spectrum of BTD

The monomers (PAET and PABT) containing thiophene ring and azomethine linkages within the chain with full conjugated structure have been synthesized by condensation reaction between p-alkylaniline and thiophene-3-carboxyldehyde in 1:1 ratio and reaction scheme is shown in scheme 2.2. The disappearance of carbonyl vibration peak at  $1720\text{ cm}^{-1}$  and appearance of new absorption peak at  $\sim 1605\text{ cm}^{-1}$  in IR spectrum and  $^1\text{H}$  NMR singlet peak (Figure 2.2-2.3) at 8.23-8.27 ppm confirm the presence of azomethine proton. Moreover, aliphatic C-H vibrations are observed near



2950 and 2830  $\text{cm}^{-1}$  and NMR peaks in the range of 0.92-2.61 are attributed to extended alkyl chain attached to phenyl rings.<sup>24-26</sup> Elemental analyses also strongly suggest the proposed structure of monomer.

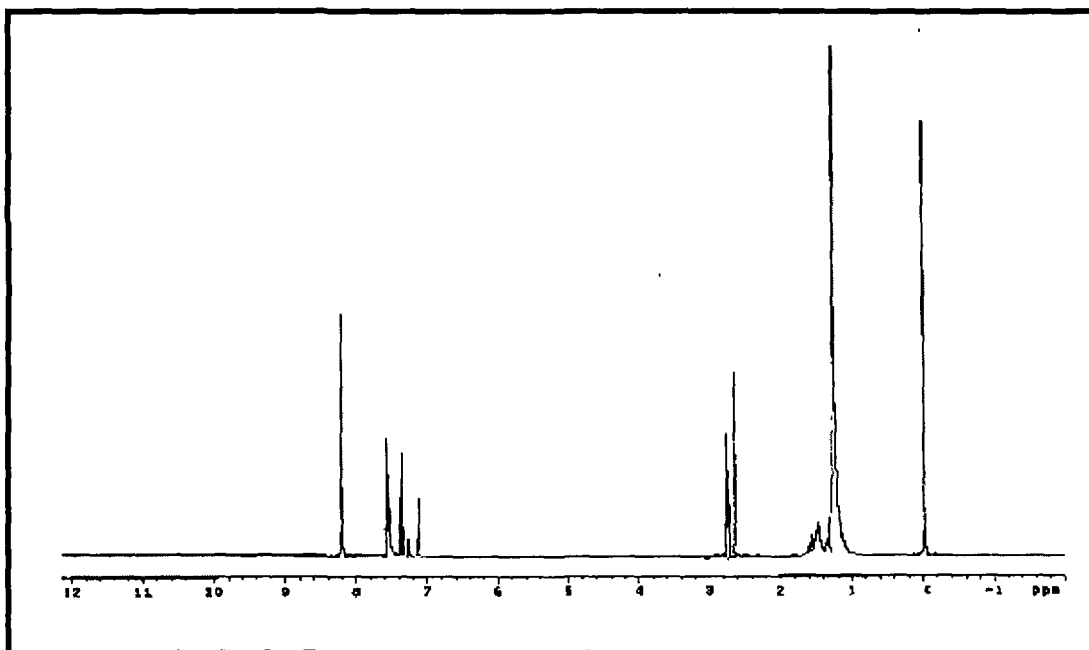


Figure 2.2: <sup>1</sup>H NMR spectrum of PAET

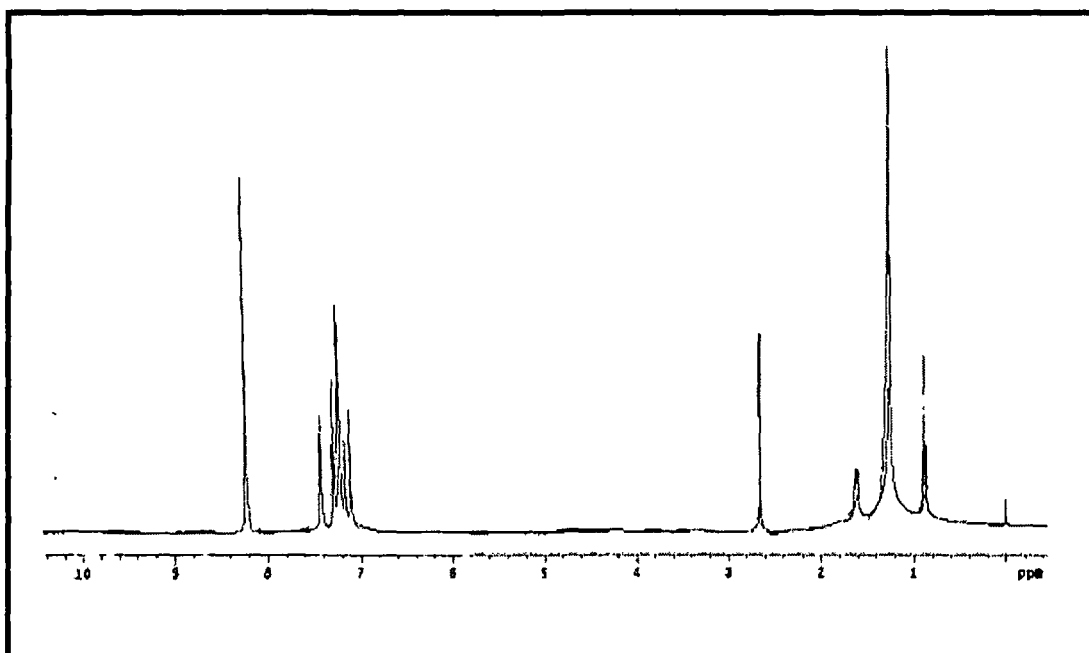
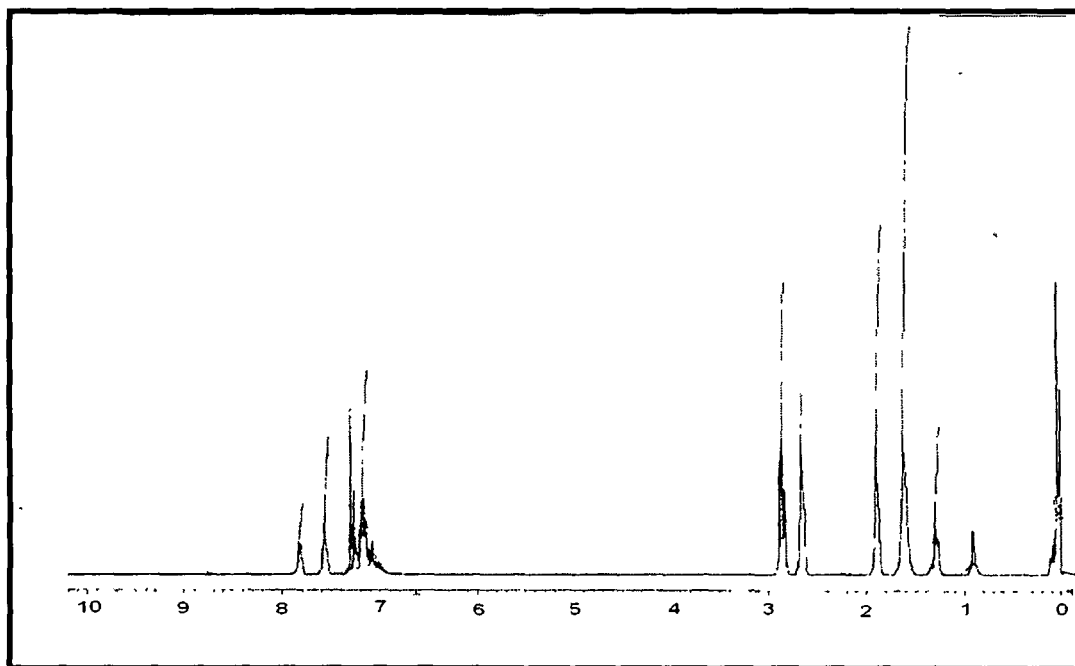


Figure 2.3: <sup>1</sup>H NMR spectrum of PABT

The monomer, 9-dodecylcarbazole (DDC) was synthesized by alkylation of carbazole in DMF solution using n-dodecylbromide in the presence of anhydrous  $K_2CO_3$ . The reaction scheme is displayed in Scheme 2.3. In FT-IR spectrum of 9-dodecylcarbazole derivative, aliphatic C-H vibrations are observed at 2911 and 2845  $cm^{-1}$ . Furthermore, characteristic N-H vibration at 3412  $cm^{-1}$  for secondary amines has disappeared due to substitution of alkyl group. Elemental analyses also suggest the proposed structures of monomers. The  $^1H$  NMR peak at 0.93 ppm is attributed to N-substituted alkyl  $-CH_3$  group and multiplet peaks in the range of 1.31–2.87 ppm indicates the  $-CH_2-$  group of long dodecyl chain<sup>27</sup> (Figure 2.4).



**Figure 2.4:**  $^1H$  NMR spectrum of DDC

The monomer (BINOL) was prepared by oxidative coupling of 2-naphthol using  $FeCl_3$  as oxidant and the reaction scheme is shown in Scheme 2.4. The characteristics hydroxyl (O-H stretching) and aromatic C-H stretching band at 3426  $cm^{-1}$  and 2935  $cm^{-1}$  are observed for 1,1'-bis-2-naphthol in FTIR spectra.  $^1H$  NMR spectra (Figure 2.5) also elucidate the structure with the chemical shift ( $\delta$ ) value at 5.03 ppm with a strong peak for two hydroxyl (O-H) protons along with the other aromatic C-H protons within 7-8 ppm of  $\delta$ -value.<sup>28</sup>

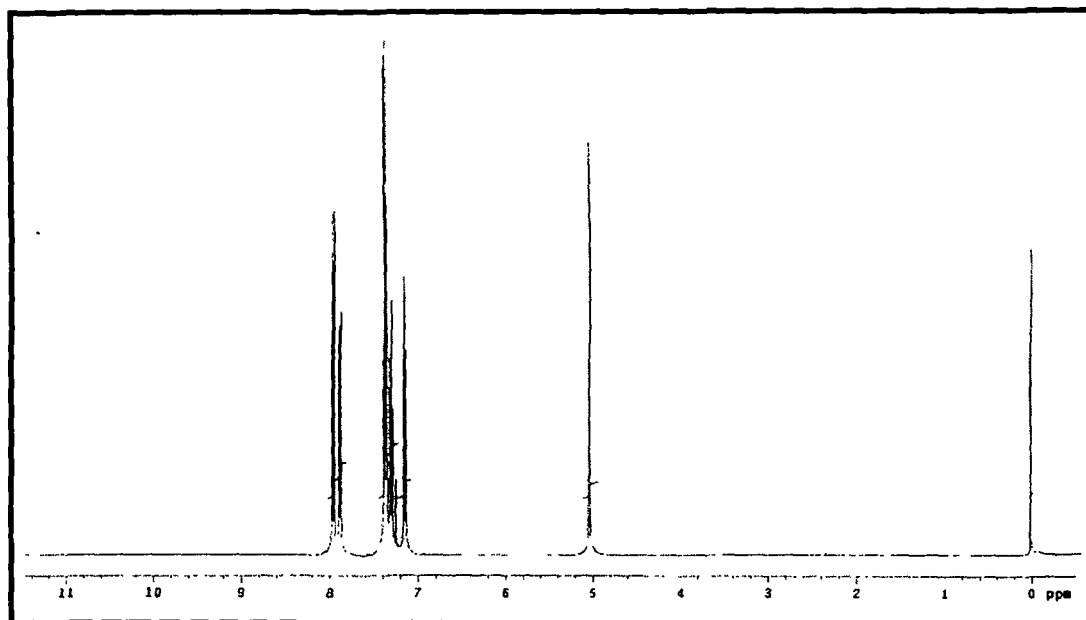
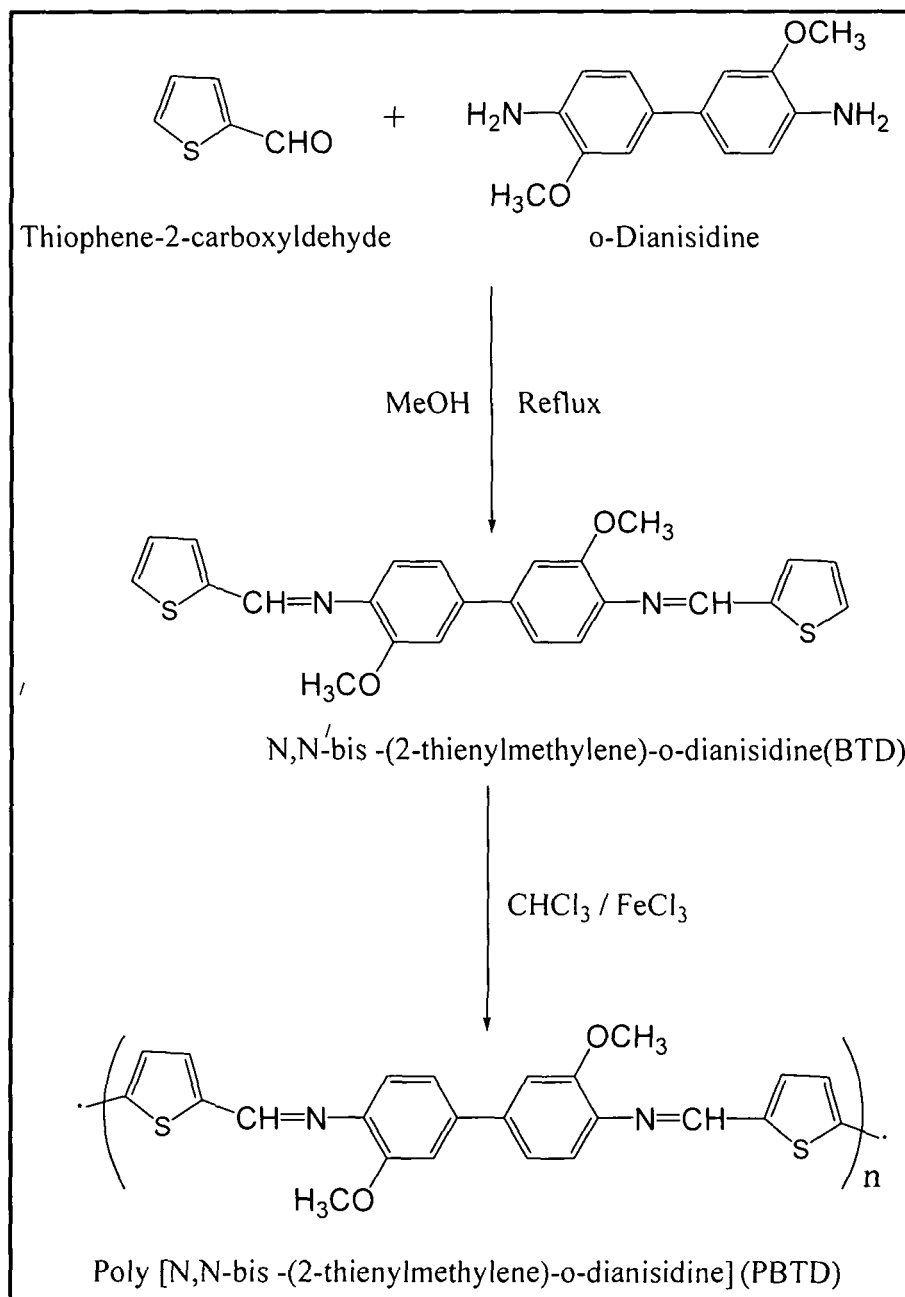


**Figure 2.5:** <sup>1</sup>H NMR spectrum of BINOL

### 2.5.2. Characterization of polymers

Chemical oxidative polymerization method is employed to synthesize the polymer PBTD using anhydrous  $\text{FeCl}_3$  as oxidant. The reaction scheme for preparation of PBTD is shown in scheme 2.1. The IR spectrum of the polymer gives important information as strong absorption peak at  $1621\text{ cm}^{-1}$  can be assigned to the  $-\text{CH}=\text{N}-$  stretching. Moreover, the intensity of the peak at  $727\text{ cm}^{-1}$  got diminished in the polymer spectrum due to the disappearance of 2-thiophene substituted ring and appearance of the 2,5-disubstituted thiophene rings. The <sup>1</sup>H NMR spectra (Figure 2.6) of the polymer, PBTD distinctly shows a singlet at 8.81 ppm attributed to the azomethine proton. The NMR singlet at 3.8 ppm and multiple peaks in the range of 7.0-8.0 ppm indicates the presence of methoxy and aromatic protons.<sup>49</sup>



**Scheme 2.1:** Reaction scheme for synthesis of BTD and PBTD

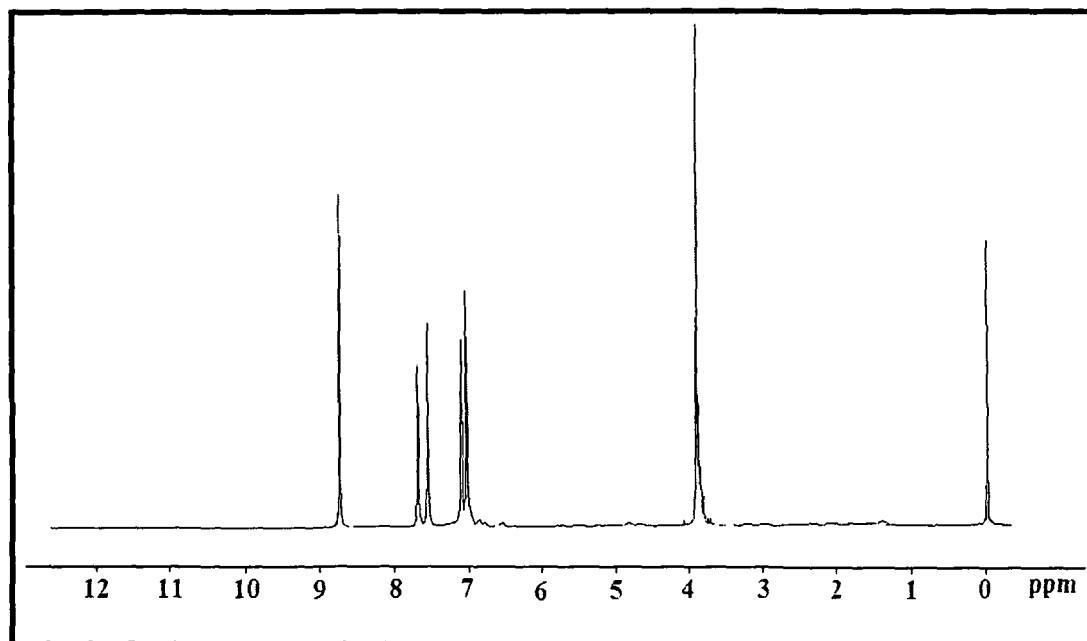
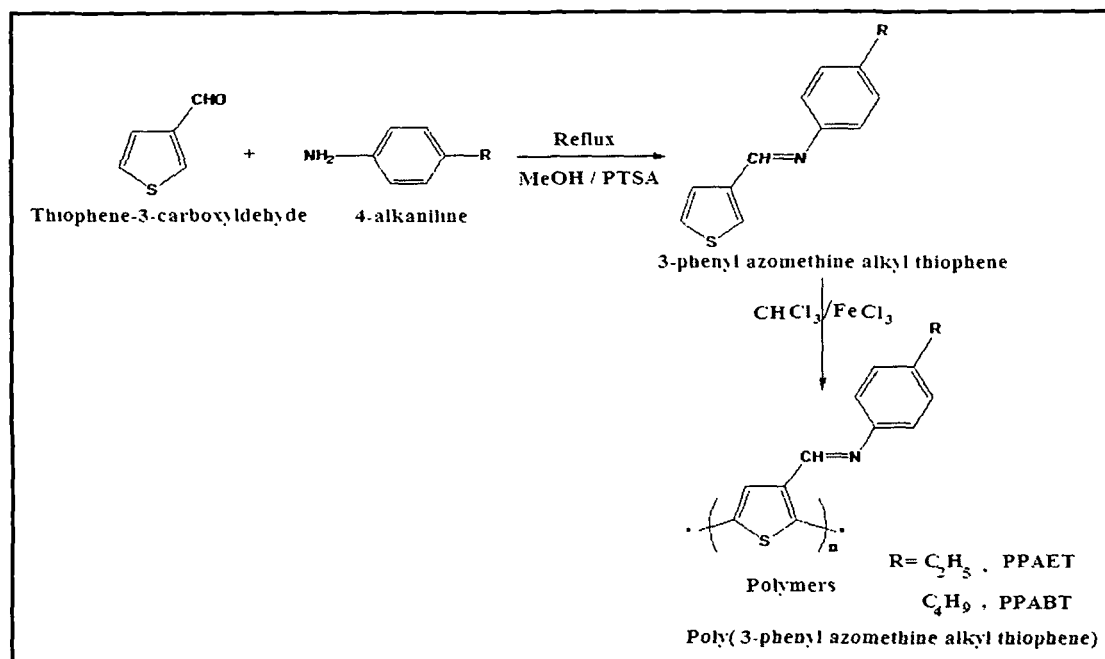


**Figure 2.6:** <sup>1</sup>H NMR spectrum of PBTD

The polymers, PPAET and PPABT are also synthesized by chemical oxidative polymerization. The reaction scheme for synthesis of PAET, PABT and PPAET, PPABT is shown in Scheme 2.2. A strong absorption peak at 1608-1612  $\text{cm}^{-1}$  observed in FTIR spectrum can be assigned to the  $-\text{CH}=\text{N}-$  stretching. Moreover, the intensity of stretching frequency as seen in the case of PBTD at 723-728  $\text{cm}^{-1}$  got diminished in the polymer spectrum due to the disappearance of 2-thiophene substituted ring and appearance of the 2,5-disubstituted thiophene rings. The <sup>1</sup>H NMR spectra of the polymers (Figure 2.7-2.8) distinctly show a singlet at 8.26-8.31 ppm attributed to the azomethine proton. The NMR multiplet peaks in the range of 6.7-8.0 ppm indicates the presence of aromatic protons. The side chain alkyl protons attached to the phenyl rings also give NMR peaks in the range of 0.92-2.75. Broadening and slight shifting of the NMR peaks compared to monomers indicates successful polymerization of the monomers.<sup>52</sup>



**Scheme 2.2:** Reaction scheme for synthesis of PAET, PABT and PPAET, PPABT

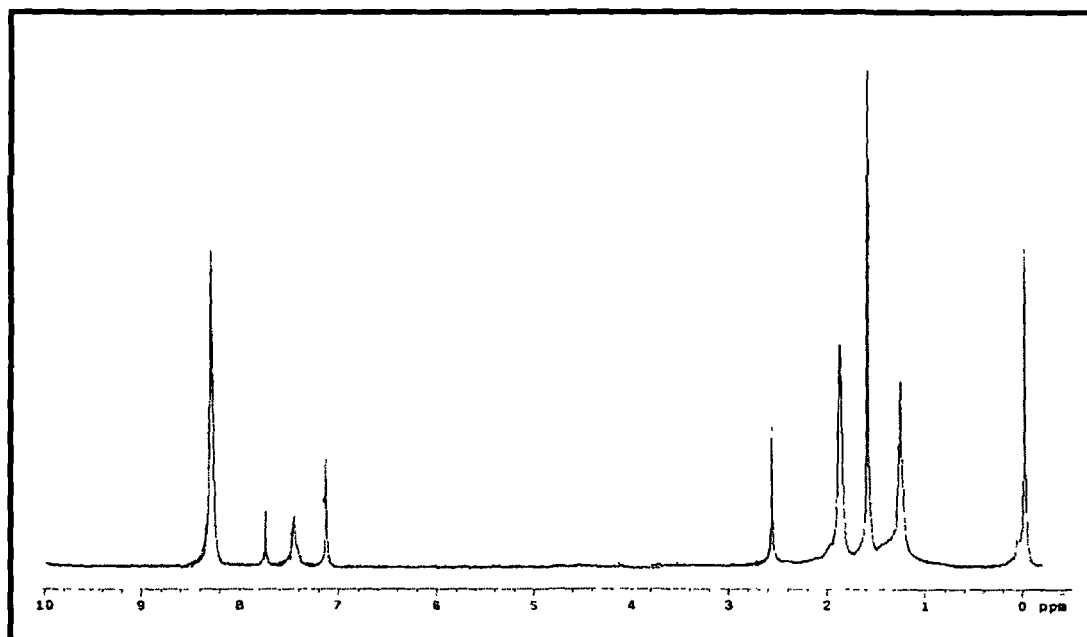


**Figure 2.7:** <sup>1</sup>H NMR spectrum of PPAET

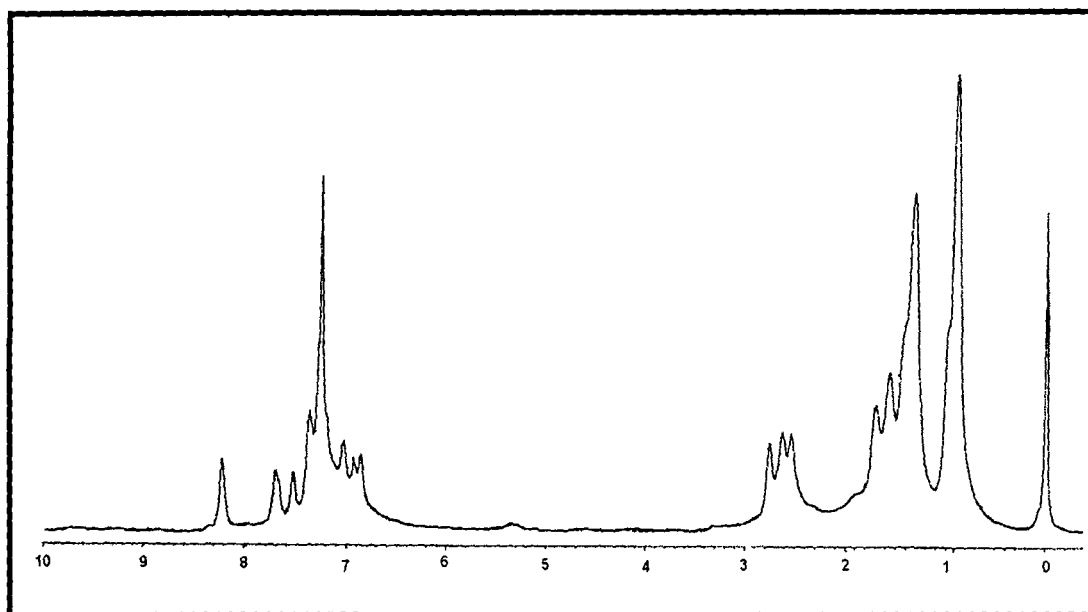
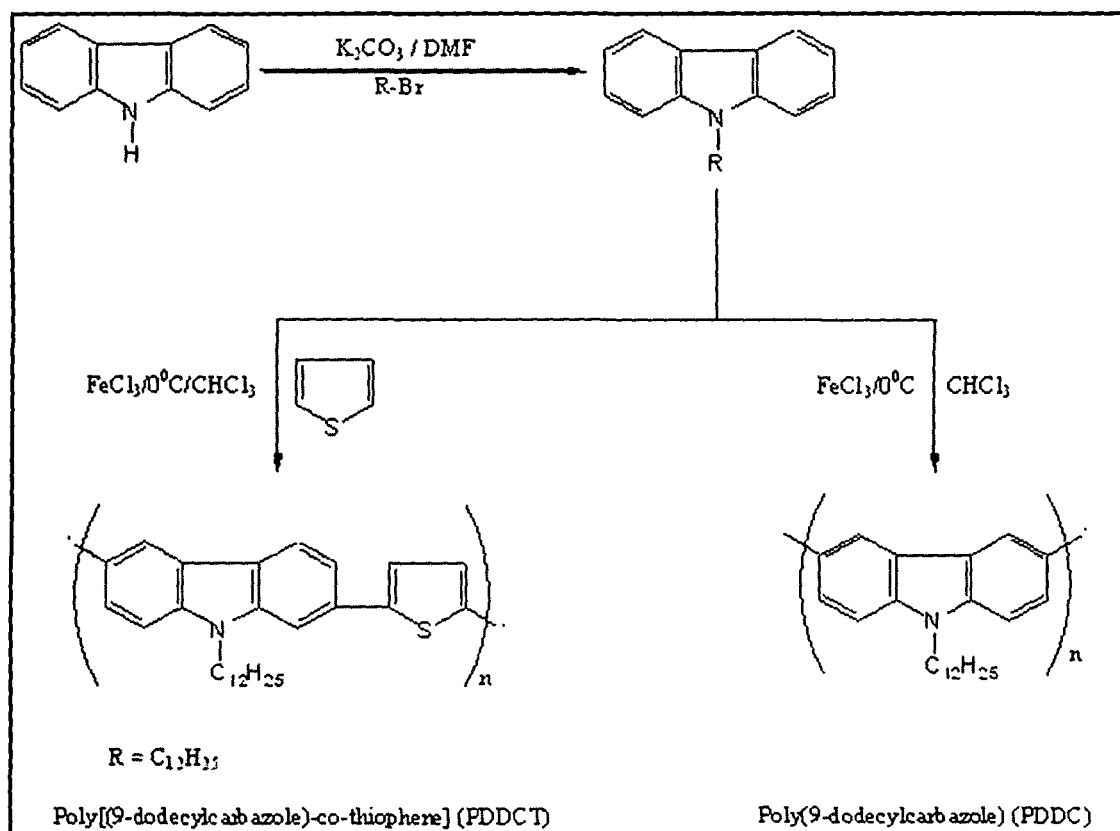


**Figure 2.8:** <sup>1</sup>H NMR spectrum of PPABT

Scheme 2.3 shows the synthetic procedure of DDC and PDDC as well as PDDCT. The IR spectrum of the polymers (PDDC and PDDCT) gives important information regarding structure of the polymers. The intensity of the absorption peak at  $725\text{ cm}^{-1}$  like other polymers, got diminished in the polymer spectrum due to the disappearance of 3,6-positions of carbazole in case of poly(9-dodecylcarbazole) and poly(9-dodecylcarbazole)-co-thiophene. The <sup>1</sup>H NMR peaks (Figure 2.9-2.10) at 7.18 ppm and 7.24 ppm can be attributed to aromatic protons of 3,4-positions of thiophene in the poly(9-dodecylcarbazole)-co-thiophene copolymer. NMR peaks ranging from 0.94-3.65 ppm are attributed to alkyl proton in PDDC and PDDCT. Moreover, slight shifting and broadening of all the <sup>1</sup>H NMR peaks compared to that of monomer implies polymer formation.<sup>52</sup> The copolymer composition in PDDCT has been determined from the integration height in <sup>1</sup>H NMR spectrum and it is found that % molar compositions of thiophene and 9-dodcylcarbazole are 55% and 45%, respectively.<sup>24</sup>



Scheme 2.3: Reaction scheme for synthesis of DDC and polymers PDDC, PDDCT



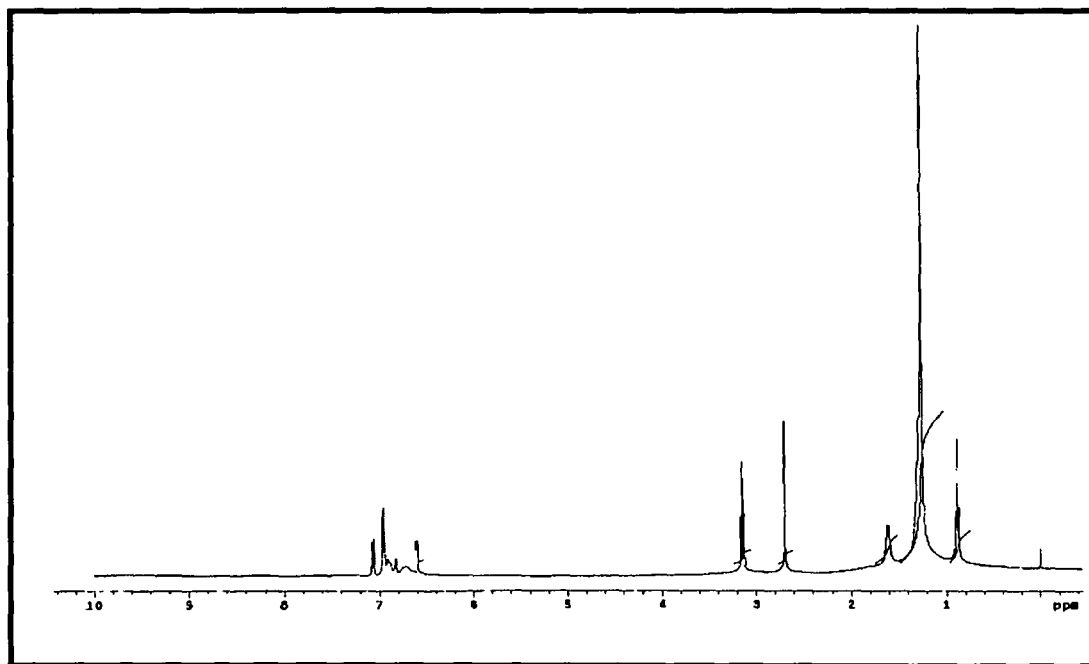


Figure 2.9: <sup>1</sup>H NMR spectrum of PDDC

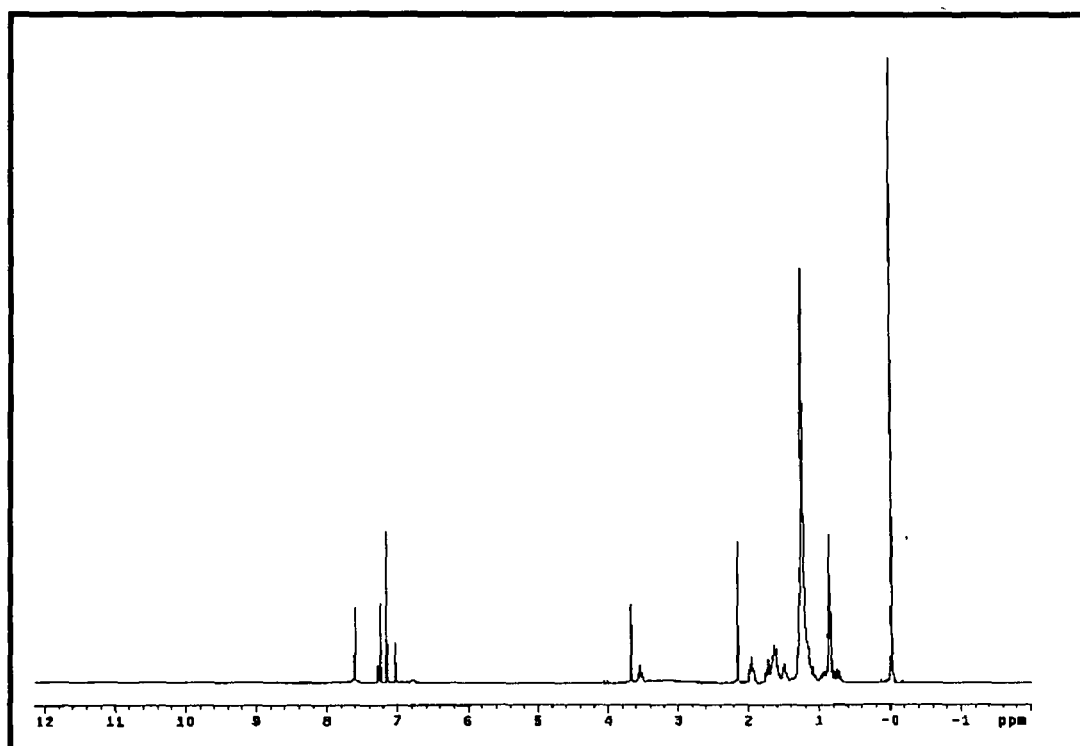
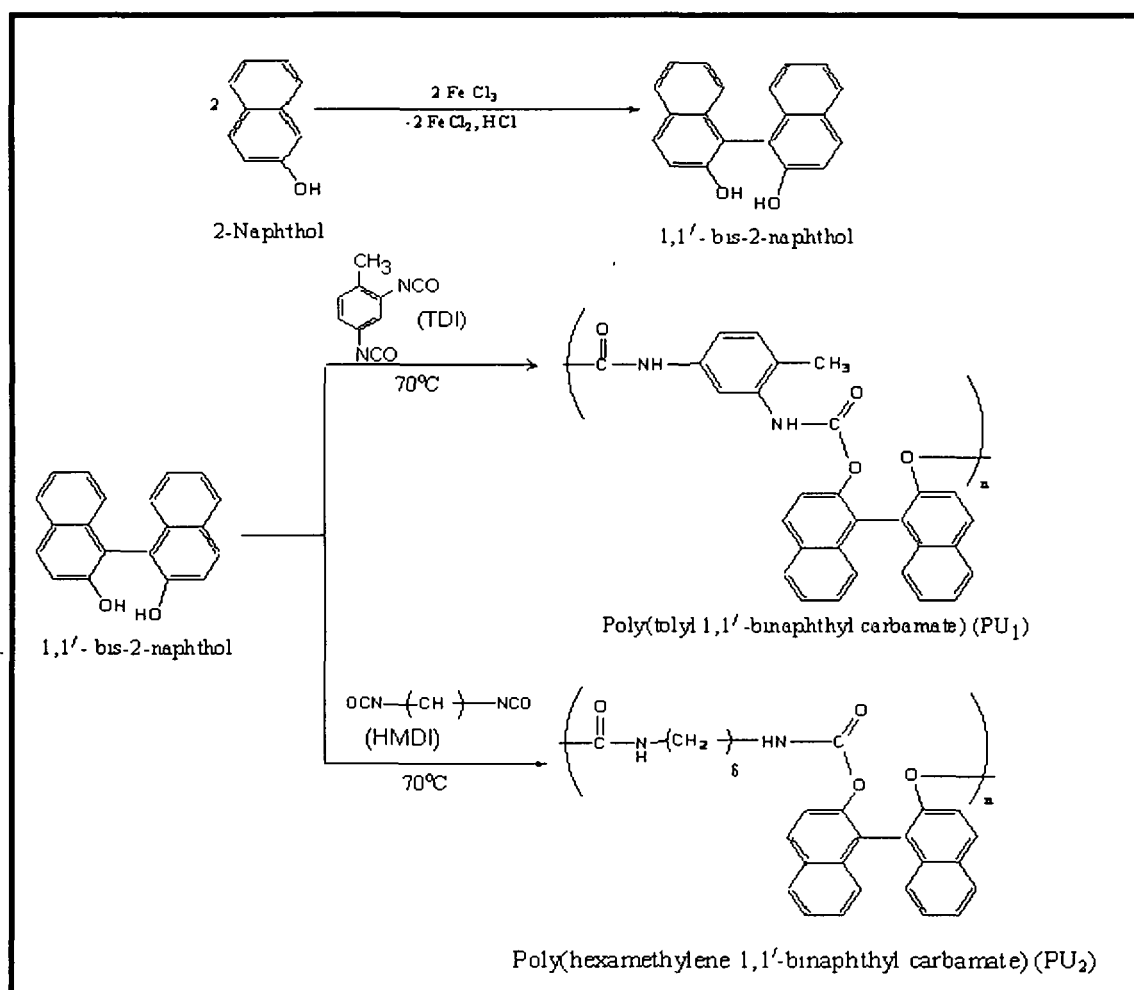


Figure 2.10: <sup>1</sup>H NMR spectrum of PDDCT

The incorporation of binaphthol into the polar polyurethane was achieved by condensation of the corresponding monomer with commercially available TDI and HMDI in dried THF to give PU<sub>1</sub> and PU<sub>2</sub>, respectively. The reaction scheme for synthesis of PU<sub>1</sub> and PU<sub>2</sub> is shown in Scheme 2.4. The formation of the polyurethanes PU<sub>1</sub> and PU<sub>2</sub> have been confirmed by the disappearance of O-H stretching frequency peaks at 3426 cm<sup>-1</sup>. Instead sharp peaks at 3376 cm<sup>-1</sup> and 3364 cm<sup>-1</sup> are observed for N-H stretching frequency in FTIR. The carbonyl frequency at 1714 cm<sup>-1</sup> and 1721 cm<sup>-1</sup> also establish the fact. In <sup>1</sup>H NMR spectra (Figure 2.11-2.12), no characteristic peaks around  $\delta$  5.0 are seen which indicate the reaction of -OH groups in the formation of polyurethanes. Further, Peaks at  $\delta$  8.0 for secondary -NH of the polymers confirmed the polyurethane formation.<sup>46</sup>



**Scheme 2.4:** Reaction scheme for synthesis of BINOL and PU<sub>1</sub>, PU<sub>2</sub>

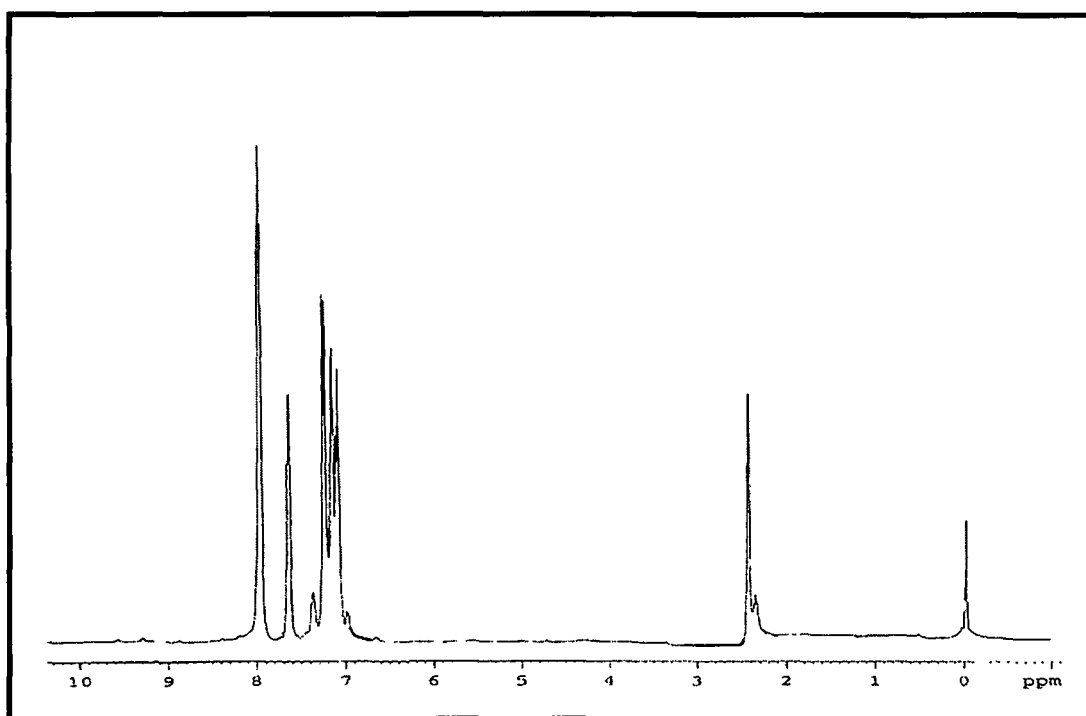


Figure 2.11:  $^1\text{H}$  NMR spectrum of PU<sub>1</sub>

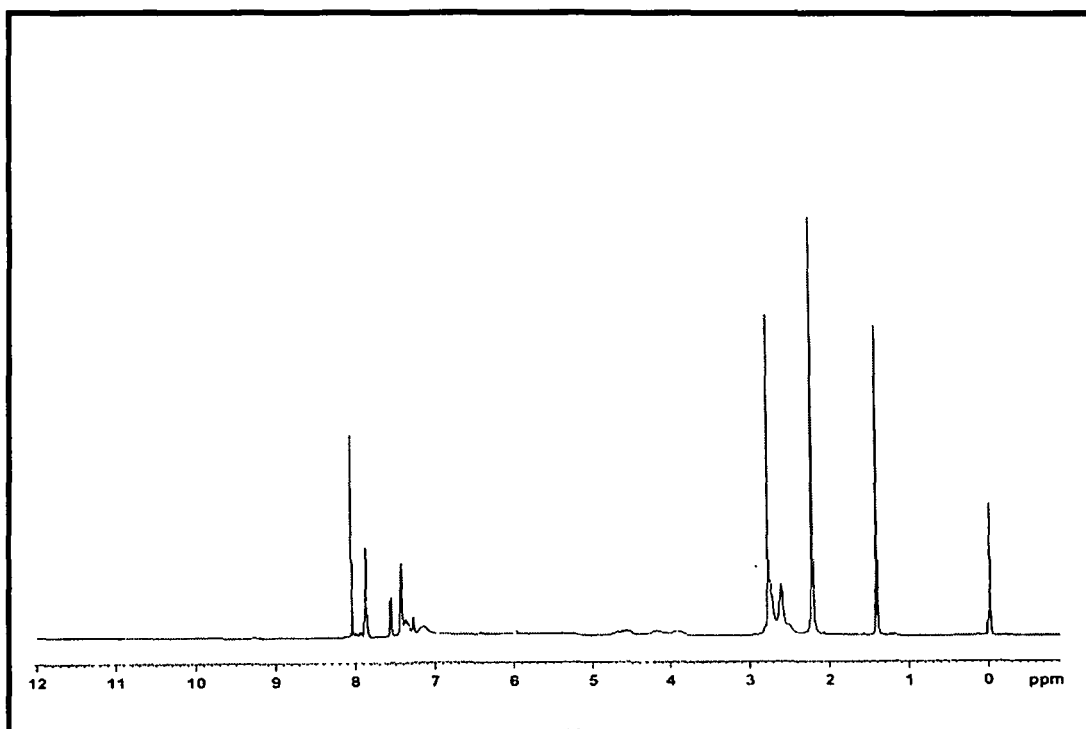


Figure 2.12:  $^1\text{H}$  NMR spectrum of PU<sub>2</sub>

Unlike other conventional conjugated polymers, the interesting feature of all the synthesized polymers is their good solubility in some organic solvents like DMF, DMAc, DMSO, THF and NMP. The presence of alkyl or alkoxy groups as the side chain in the polymer or incorporation of non-conjugated groups in the main chain as seen in case of PU<sub>1</sub> and PU<sub>2</sub> have contributed in imparting solubility to them.<sup>4,14,16,45</sup> The inherent viscosities of the polymers (Table 2.1) are also measured using suspended level Ubbelohde viscometer and found to have in the range of 0.18-0.27. Low values of inherent viscosities indicate oligomeric nature of the synthesized polymers.

**Table 2.1:** Physical properties of polymers

Polymers	Yield (%)	$\eta_{inh}$ (dLg <sup>-1</sup> )
PBTD	51	0.21
PPAET	54	0.19
PPABT	57	0.23
PDDC	53	0.18
PDDCT	59	0.22
PU <sub>1</sub>	86	0.24
PU <sub>2</sub>	84	0.26

### 2.5.3. Molecular weight of polymers

Molecular weight of polymers has been measured by gel permeation chromatography (GPC) in THF solution using polystyrene standard. Molecular weights of the polymers in THF are shown in Table 2.2. The number-average molecular weights of the resulting polymers are in the range of 3829–17,647 g/mol with polydispersity indexes (PDI) in the range of 1.05–2.14. Except PU<sub>1</sub> and PU<sub>2</sub>, the other synthesized polymers exhibit low molecular weight indicating their oligomeric nature. The weight average molecular weights of polymers have been found in the range 4307-37,891 g/mol. Degree of polymerization of the polymers were also calculated which gives information of effective conjugation length and delocalization of electrons. The polymers synthesized using oxidating coupling methods (i.e. PBTD, PPAET, PPABT, PDDC and PDDCT), show narrow molecular weight distributions (PDI ranging from 1.05-1.40). This might be

resulted from controlled reactions using slow addition of  $\text{FeCl}_3$  to the reaction mixture from time to time. However, PDDC and PDDCT show comparatively higher PDI and molecular weights to other oxidative coupled polymers which could be attributed to the poor radical stability after oxidation of the carbazole derivatives causing coupling of the species more feasible.<sup>53</sup> On the other hand, condensation polymerization of highly reactive diol (BINOL) and diisocyanates (TDI or HMDI) gives  $\text{PU}_1$  and  $\text{PU}_2$  with higher PDI. Random intermolecular reaction between molecules in a bifunctional system would lead to linear chain polymers whose chain lengths show wide variation.<sup>51</sup>

**Table 2.2:** Molecular weights and degree of polymerization of polymers

Polymers	$M_n$ (g/mol)	$M_w$ (g/mol)	$M_w/M_n$ (PDI)	Degree of polymerization (DP)
PBTD	3857	4307	1.12	9
PPAET	4256	4591	1.10	20
PPABT	4821	5074	1.05	20
PDDC	4193	5846	1.40	12
PDDCT	3829	6413	1.67	9
$\text{PU}_1$	14,563	32,798	2.25	33
$\text{PU}_2$	17,647	37,891	2.14	39

#### 2.5.4. Thermal behaviour of polymers

##### 2.5.4.1 Thermogravimetric analysis (TGA)

The thermal properties of polymers were investigated by thermogravimetric analysis under nitrogen atmosphere at the heating rate of 10 °C per minute. All the polymers showed 2-7% weight loss at the temperature range of 80-120°C which corresponds to loss of moisture and volatilization of solvent. The onset degradation temperatures of the polymers are found to be in the range of 234-305 °C.

The polymer, PBTD is found to be thermally stable upto 305 °C (Figure 2.13). The first 1.5 % of weight loss step in the TG analysis curves around 80-120°C corresponds to the loss of moisture and volatilization of the solvent. The second step of 66% of weight loss in the TGA curves between 305-360 °C is due to degradation of polymers. About 10% of residue was finally left when heated to 600 °C.

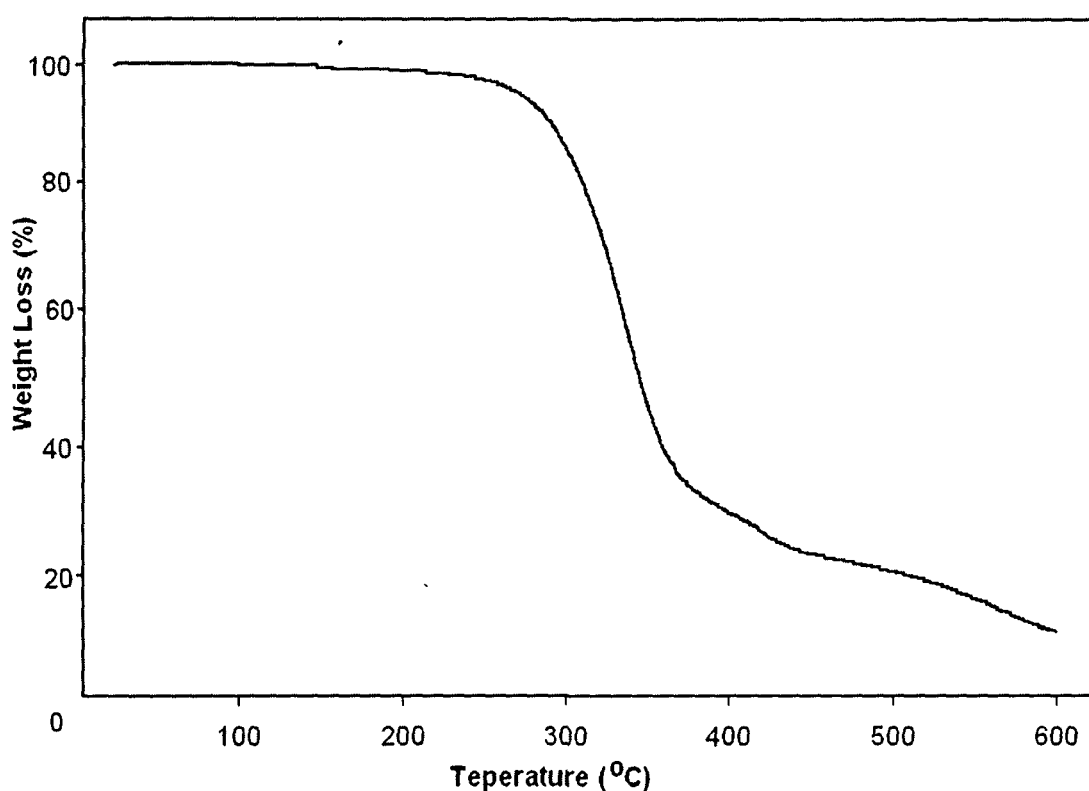


**Figure 2.13:** TGA curve of polymer PBTD

The polymers, PPAET and PPABT show gratifying thermal stability to the range of 300-380 °C (Figure 2.14). 60-70% weight loss in the TGA curves between 300-450 °C is attributed to degradation of polymers. The onset degradation temperature of PPAET ( $T_d$ , 305 °C) is found to be higher in comparison to that of PPABT ( $T_d$ , 285°C) due to variation in alkyl chain length as the side group.<sup>25</sup> Nearly, 25% of residue was left when the polymers are heated to 600 °C.

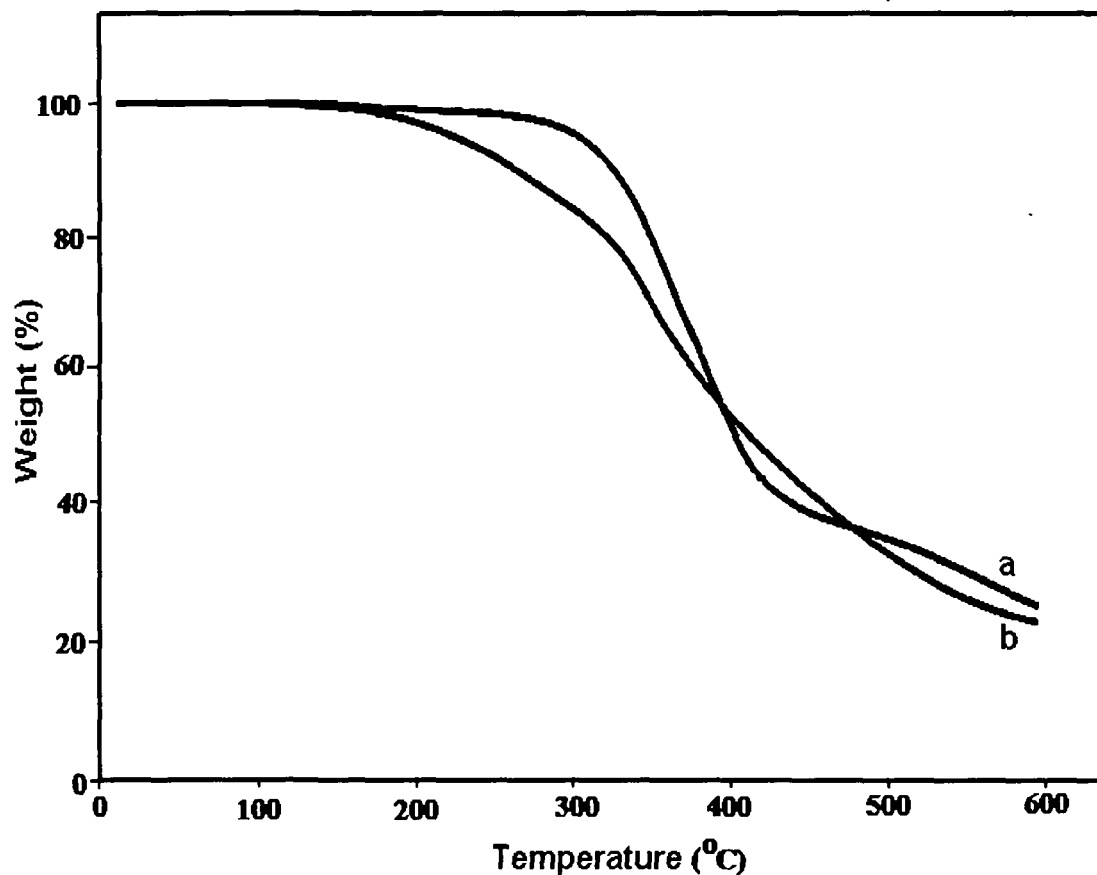


**Figure 2.14:** TGA curves of (a) PPAET (b) PPABT

The polymers, PDDC and PDDCT are found to have thermal stability upto 350<sup>0</sup>C (Figure 2.15). The first weight loss step i.e. 5% weight loss in the TGA curves around 80-120<sup>0</sup>C corresponds to the loss of moisture and volatilization of the solvent. The second step in the TGA curves by loss of 40-50% weight loss between 350-450<sup>0</sup>C is due to degradation of polymers. The onset decomposition temperature of PDDCT is found a little higher (ca.300<sup>0</sup>C) than that of PDDC which may be attributed to the attached rigid thiophene ring along the main chain.

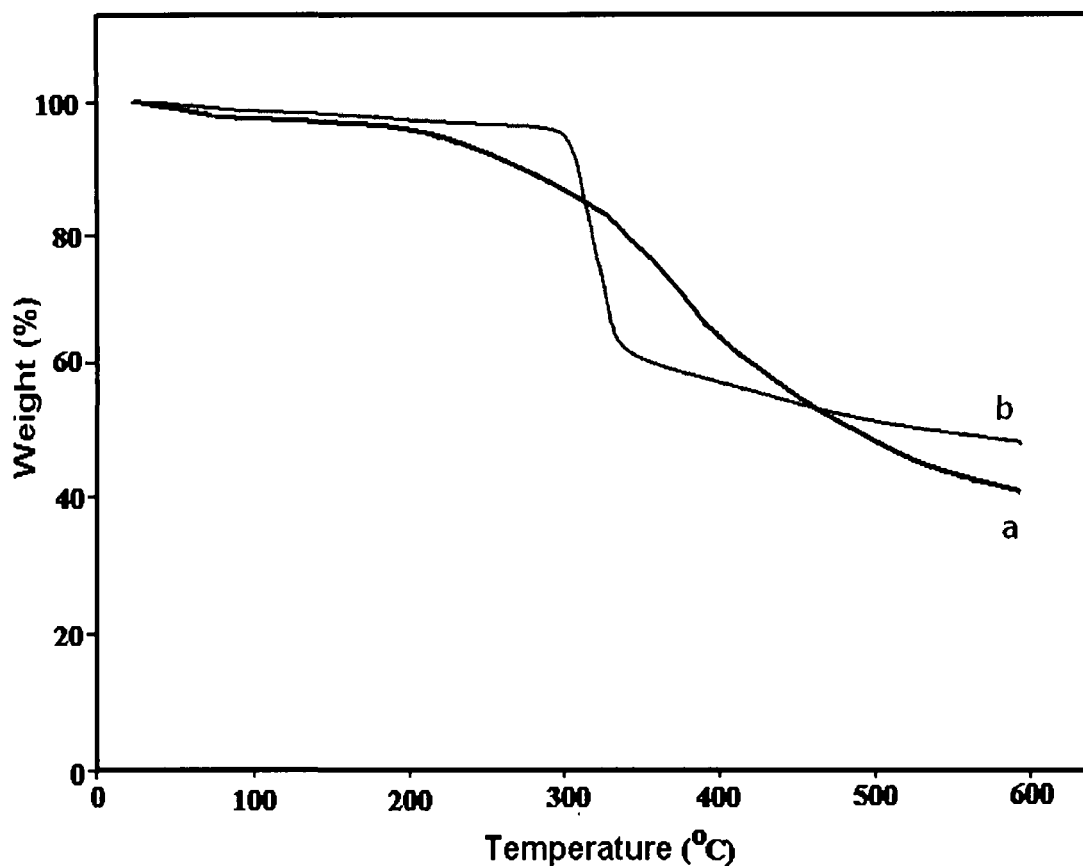
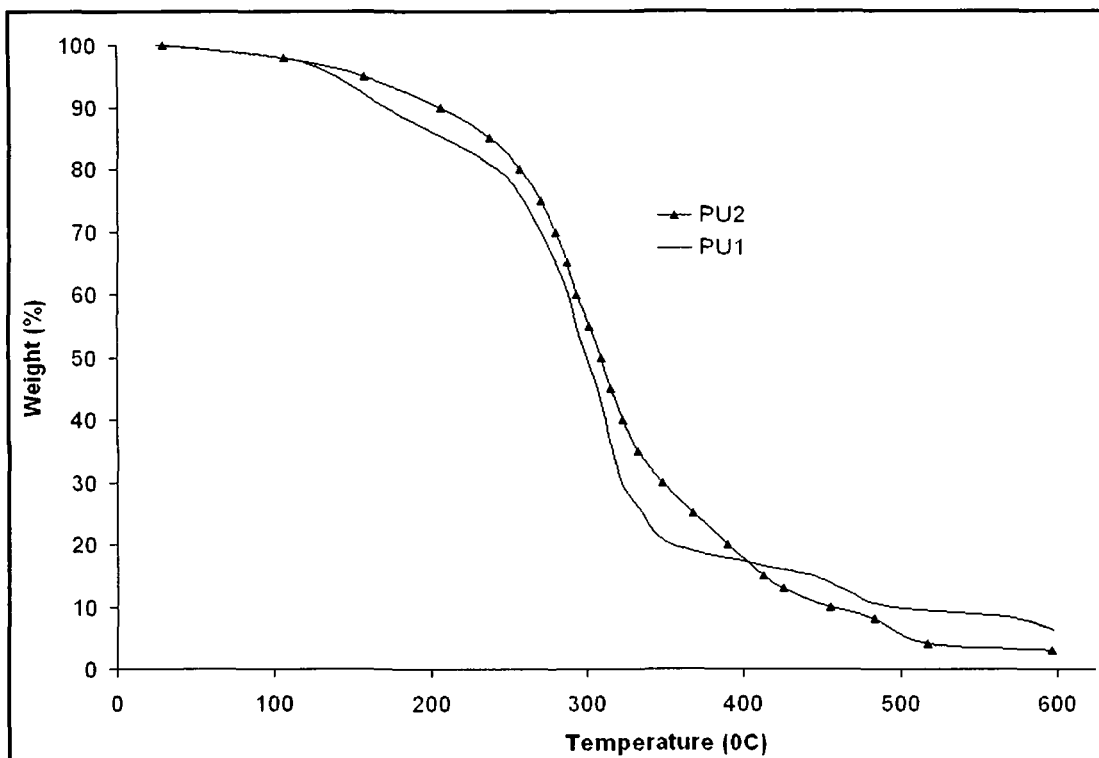


Figure 2.15: TGA curves of (a) PDDC (b) PDDCT

Both the conjugated-nonconjugated chain containing polymers,  $PU_1$  and  $PU_2$  shows similar thermal decomposition pattern (Figure 2.16). These polymers are found to have thermal stability upto 250 °C. The degradation of polymers are found in the temperature range of 250-420 °C. Hexamethylene group present in  $PU_2$  results in lowering the degradation temperature in comparison to  $PU_1$ . Summary of thermal behavior of all the polymers is given in Table 2.3.





**Figure 2.16:** TGA curves of PU<sub>1</sub> and PU<sub>2</sub>

Generally, PU<sub>1</sub>, PU<sub>2</sub> and long side chain alkyl group containing polymers i.e. PDDC and PPABT have shown comparatively lower onset degradation temperature. Whereas, PDDCT copolymer have shown improved thermal stability due to annexed thiophene unit with 9-dodecyl carbazole unit. The degradation range of the polymers witnessed from TG analyses was found within 230-355 °C attributed to final degradation of products by evaluation of CO<sub>2</sub> and nitrogenous gases.

#### 2.5.4.2. Differential scanning calorimetry (DSC) analysis

Differential scanning calorimetry (DSC) analyses of polymers have been carried under nitrogen atmosphere at the heating rate of 10 °C/min. All the thermal data of the polymers are listed in Table 2.3. DSC curves (Figure 2.17-2.20 ) of polymers reveal that the glass transition temperature ( $T_g$ ) of the polymers are in the range of 51-84 °C. PBTD exhibits the highest  $T_g$  compared to others attributed fully conjugated structure with methoxy group side chain on anisidine unit only. The presence of long dodecyl group in the polycarbazole derivatives, PDDC and PDDCT results low  $T_g$ .  $T_g$  of polymers

synthesized by oxidative coupling reactions is in order of PDDC < PDDCT < PU<sub>2</sub> < PPABT < PPAET. Long flexible alkyl groups in the polymer side chain serve as internal plasticizer which lowers T<sub>g</sub> of polymers. The response in the thermogram due to glass transition of polymers is quite low as these polymers are of low molecular weight.

The broad endothermic peaks at 160-170°C and 145-152 °C for PDDC and PDDCT, respectively, are assigned to the melting of the polymers. On the other hand, a *broad endothermic peak in the range of 140-165 °C indicates the melting range for PU<sub>2</sub>*. No distinct melting region was observed for PBT, PPAET, PPABT and PU<sub>1</sub>. It is observed that T<sub>g</sub> of the polymers and melting range decreases with increase in side chain length.<sup>25,54,55</sup> The thermal stability of the polymers are found to be sufficient for photovoltaic device performance since nonradiative decay i.e. heat dissipation during undesired exciton recombination may lead to produce high heat during the device function.

**Table 2.3:** Thermal characteristics of the polymers

Polymer	Degradation onset (T <sub>d</sub> <sup>onset</sup> ) (°C)	Weight residue (%) (at 600°C)	Glass transition temperature (T <sub>g</sub> ) (°C)	Melting temperature
PBT	285	14	84	-
PPAET	305	25	78	-
PPABT	280	22	72	-
PDDC	273	37	51	150
PDDCT	300	45	59	168
PU <sub>1</sub>	210	9	-	148
PU <sub>2</sub>	214	5	66	-

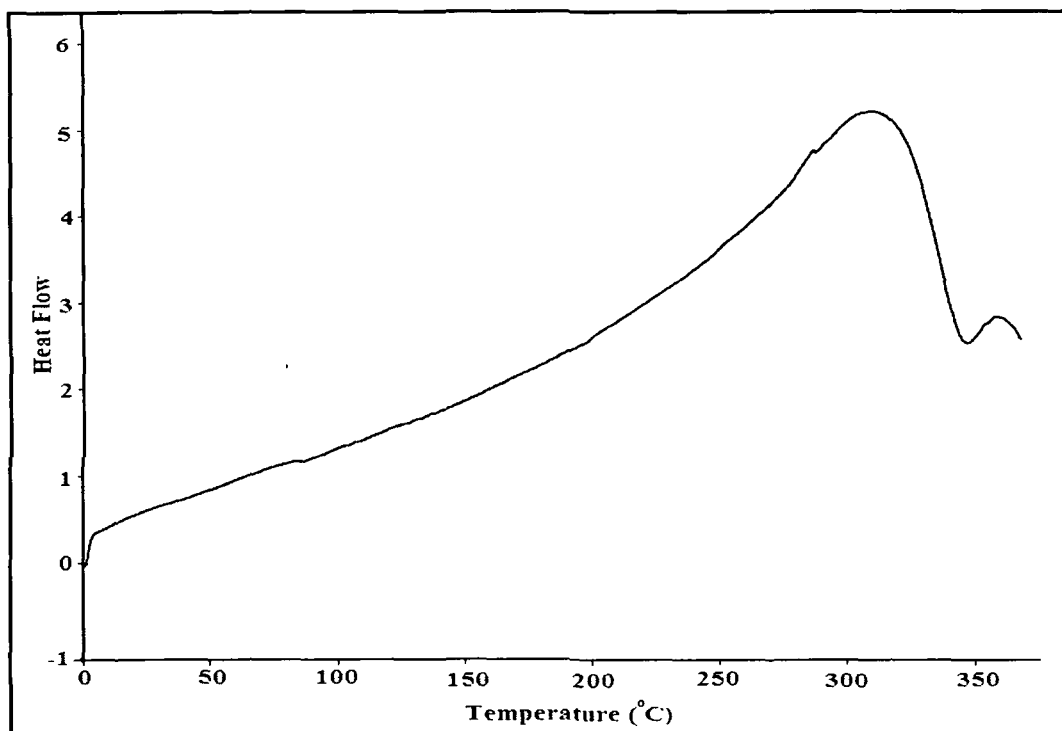


Figure 2.17: DSC thermogram of PBTD

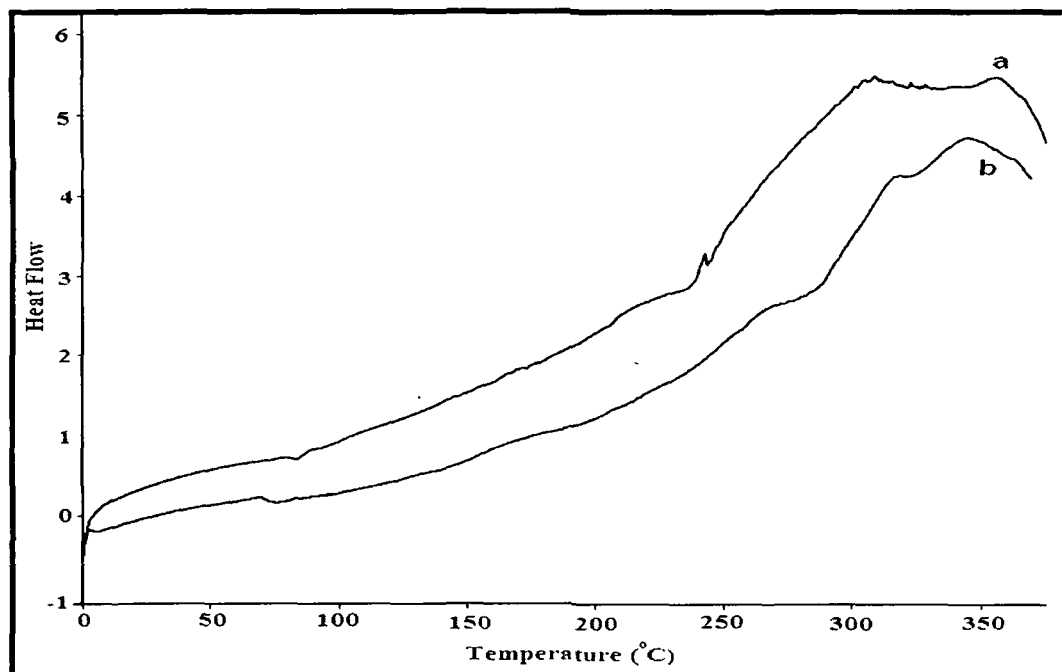


Figure 2.18: DSC thermograms of (a) PPAET (b) PPABT

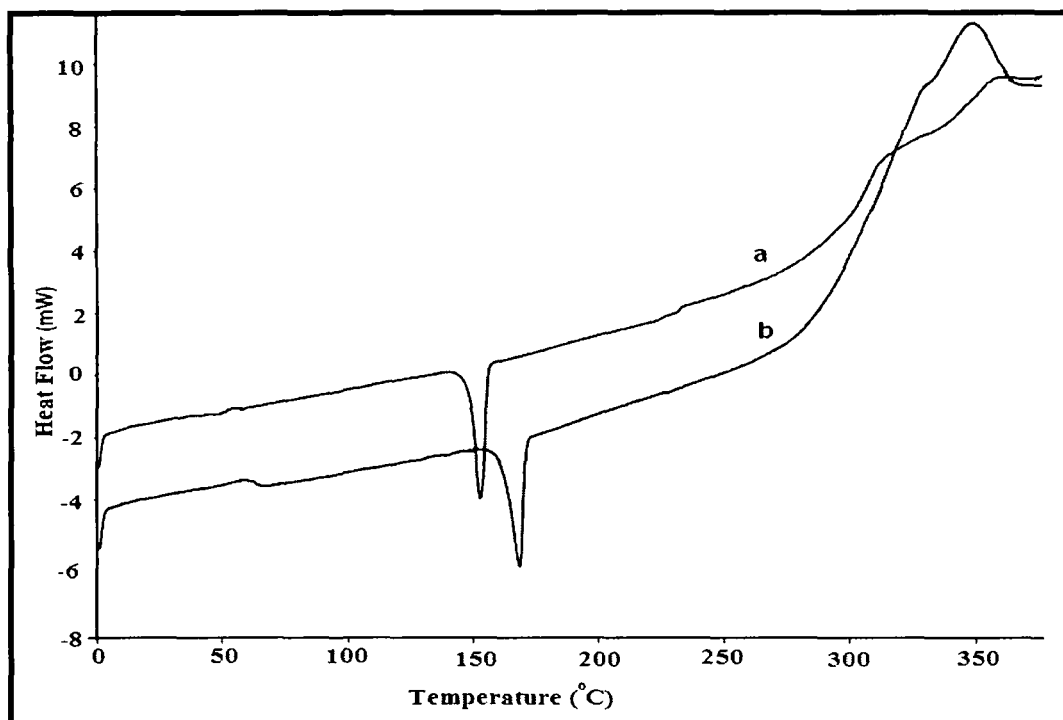


Figure 2.19: DSC thermogram of (a) PDDC (b) PDDCT

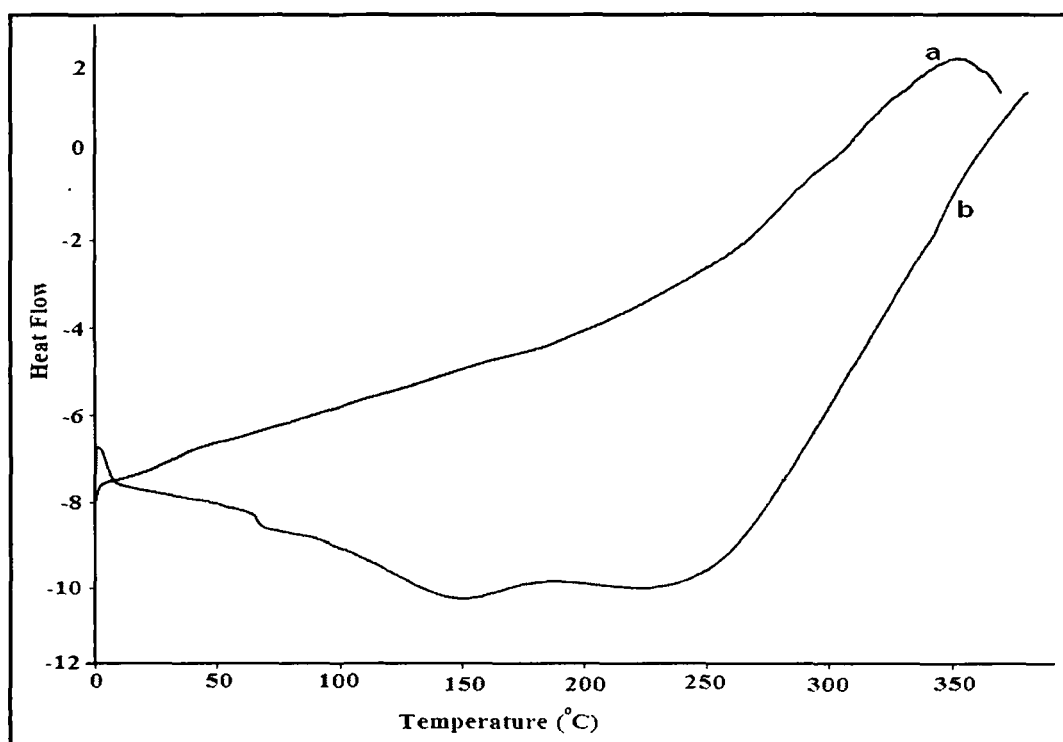


Figure 2.20: DSC thermogram of (a) PU<sub>1</sub> (b) PU<sub>2</sub>

## 2.6. Conclusion

- A series of azomethinic, N-alkyl substituted carbazole derivatives and diol monomers have been synthesised with the yield ranging from 71% to 89%. The formation of monomers was confirmed by FTIR and  $^1\text{H}$  NMR spectroscopy, and CHN analyses.
- The polymers have been prepared by oxidative polymerization using  $\text{FeCl}_3$  and polyurethanes,  $\text{PU}_1$  and  $\text{PU}_2$  have been prepared by condensation reaction. The polymerization process is slow for oxidative coupling reactions and yields are 51-59%.
- The polymers, PBTD, PPAET, PPABT, PDDC and PDDCT show good solubility in THF, DMF, DMAc, DMSO and NMP due to the presence of alkyl and alkoxy groups as side chain. The reason of good solubility for  $\text{PU}_1$  and  $\text{PU}_2$  is presence of non-conjugated spacer between the binaphthyl chromophoric groups in the polymer chain.
- The number average molecular weights of polymers are in the range of 3857 to 17647 g /mol. This indicate the prepared polymers are oligomeric in nature.
- Polymers possess good thermal stability with the onset decomposition temperature around 240-305  $^\circ\text{C}$  under nitrogen atmosphere, 30-68% weight loss at the temperature of 300-380  $^\circ\text{C}$ .
- The polymers exhibit a glass transition temperature ( $T_g$ ) in the range of 51-84 $^\circ\text{C}$ .  $T_g$  of the polymers is established to be side chain dependent. All the polymers possess the suitable thermal properties to receive its applications in photovoltaic devices.

## References

1. Nalwa, H.S.; Rohwer, L.S. (Eds), *Handbook of Luminescence, Display materials and Devices* (American Scientific Publisher, Stevenson Ranch, CA, 2003)
2. Burroughs, J.H.; Bradley, D.D.C.; Brown, A.R.; Marks, R.N.; Mackay, K.; Friend, R.H.; Burn P.L.; Holmes, A.B. Light emitting diodes based on conjugated polymers, *Nature* **347**, 539-541 (1990)
3. Grimsdale, A.C.; Chan, K.L.; Martin, R.E.; Jokisz, P.W.; Holmes, A.B. Synthesis of light emitting conjugated polymers for applications in electroluminescent devices, *Chem. Rev.* **109**, 897-1091 (2009)
4. Akcelrud L. Electroluminescent polymers, *Prog. Polym. Sci.* **28**, 875-962 (2003)
5. Zhang Y. *et al* Polymer light emitting diodes based on a bipolar transporting luminescent polymer, *J. Mater. Chem.* **13**, 773-777 (2003)
6. Bao, Z.; Lovinger, A.J. Soluble regioregular polythiophene derivative as semiconducting materials for field-effect transistors, *Chem. Mater.* **11**, 2607-2612 (1999)
7. Zou, Y.; Sang, G.; Wu, w.; Liu, Y.; Li, Y. A polythiophene derivative with octyloxyl triphenylamine-vinylene conjugated side chain: synthesis and its applications in field-effect transistor and polymer solar cell, *Synthetic Metals* **159**, 182-187 (2009)
8. Salleo, A.; Chabinyc, M.L.; Yang, M.S.; Street, R.A. Polymer thin-film transistors with chemically modified dielectric interfaces, *Appl. Phys. Lett.* **81**, 4383-4385 (2002)
9. Lee, J. *et al* Ion gel gated polymer thin-film transistors, *J. Am. Chem. Soc.* **129**, 4532-4533 (2007)
10. Dai, L.; Soundarrajan, P.; Kim, T. Sensors and sensor arrays based on conjugated polymers and carbon nanotubes, *Pure Appl. Chem.* **74**, 1753-1772 (2002)
11. Maiti, J.; Pokhrel, B.; Baruah, R.; Dolui, S.K. Polythiophene based fluorescence sensors for acids and metal ions, *Sensors and Actuators B* **141**, 447-451 (2009)
12. Rahman, A.; Kumar, P.; Park, D.-S.; Shim, Y.-B. Electrochemical sensors based on organic conjugated polymers, *Sensors* **8**, 118-141 (2008)

13. McQuade, D.T.; Pullen, A.E.; Swager, T.M. Conjugated polymer-based chemical sensor, *Chem. Rev.* **100**, 2537-2574 (2000)
14. Coakley, K.M.; McGehee, M.D. Conjugated polymer photovoltaic cells, *Chem. Mater.* **16**, 4533-4542 (2004)
15. Bundgaard, E.; Krebs, F.C. Low band gap polymers for organic photovoltaics, *Sol. Energy Mater. Sol. Cells* **91**, 954-985 (2007)
16. Cheng, Y.J.; Yang, S.H.; Hsu, C.S. Synthesis of conjugated polymer for organic solar cell applications, *Chem. Rev.* **109**, 5868-5923 (2009)
17. Helgesen, M.; Søndergaard, R.; Krebs, F.C. Advanced materials and processes for polymer solar cell devices. *J Mater Chem.* **20**, 36-60 (2010)
18. Gunes, S.; Neugebauer, H.; Sariciftci, N.S. Conjugated polymer-based organic solar cells. *Chem. Rev.* **107**, 1324-1338 (2007)
19. Dennler, G.; Scharber, M.C.; Brabec, C.J. Polymer-fullerene bulk-heterojunction solar cells. *Adv. Mater.* **21**, 1323-1338 (2009)
20. Nelson, J. Organic photovoltaic films. *Curr. Opin. Solid State Mater. Sci.* **6**, 87-95 (2002)
21. Baran, D. et al Processable multipurpose conjugated polymer for electrochromic and photovoltaic applications, *Chem. Mater.* **22**, 2978-2987 (2010)
22. Beaujuge, P.M; Reynolds, J.R. Colour control in  $\pi$ -conjugated organic polymers for use in electrochromic devices. *Chem. Rev.* **110**, 268-320 (2010)
23. Meng, H. *et al* An unusual electrochromic device based on a new low-bandgap conjugated Polymer. *Adv. Mater.* **15**, 146-149 (2003)
24. Skotheim, T.A.; Elsenbaumer, R.L.; Reynolds, J.R. *Handbook of conducting polymers* (Marcel Dekker, Inc., New York, 1998)
25. Hu, X.; Xu, L. Structure and properties of 3-alkoxy substituted polythiophene synthesized at low temperature. *Polymer* **41**, 9147-9154 (2000)
26. Ogawa, K.; Stafford, J.A.; Rothstein, S.D.; Tallman, D.E.; Rasmussen, S.C. Nitrogen-functionalized polythiophenes: Potential routes to new low band gap materials. *Synth. Met.*, **152**, 137-140 (2005)

27. Levent, A.; Toparre, L.; Cianga, I.; Yagci, Y. Synthesis and characterization of conducting copolymers of (S)-2-methylbutyl-2-(3-thienyl) acetate with pyrrole and thiophene. *Macromol. Chem. Phys.* **204**, 1118–1122 (2003)
28. Yamamoto, T. Conjugated polymers with electronic and optical functionalities: Preparation by organometallic polycondensation, properties, and applications, *Macromol. Rapid Commun.* **23**, 583-606 (2002)
29. McCullough, R.D. The chemistry of conducting polythiophenes, *Adv. Mater.* **10**, 1-23 (1998)
30. Loewe, R.S.; Ewbank, P.C.; Liu, J.; Zhai, L.; McCullough, R.D. Regioregular, head-to-tail coupled poly(3-alkylthiophenes) made easy by the GRIM method: Investigation of the reaction and the origin of regioselectivity, *Macromolecules* **34**, 4324-4333 (2001)
31. Chen, T.A.; Reike, R.D. The first regioregular head-to-tail poly(3-hexylthiophene-2,5-diyl) and a regiorandom isopolymer: nickel versus palladium catalysis of 2(5)-bromo-5(2)-(bromozincio)-3-hexylthiophene polymerization, *J. Am. Chem. Soc.* **114**, 10087-10088 (1992)
32. Rehahn, M.; Schluter, A.D.; Wegner, G.; Feast, W.J. Soluble poly(*para*-phenylene)s. 2. Improved synthesis of poly(*para*-2,5-di-n-hexylphenylene) via Pd-catalysed coupling of 4-bromo-2,5-di-n-hexylbenzeneboronic acid, *Polymer* **30**, 1060-1062 (1989)
33. Bao, Z.; Chan, W.; Lu, L. Synthesis of conjugated polymer by the Stille Coupling Reaction, *Chem. Mater.* **5**, 2-3 (1993)
34. Goncalves, V.C.; Balogh, D.T. Synthesis and characterization of a dye-functionalized polythiophene with different chromic properties. *Eur. Polym. J.* **42** 3303-3310 (2006)
35. Yamamoto, T.; Hayashi, H.  $\pi$ -Conjugated soluble and fluorescent poly(thiophene-2,5-diyl)s with phenolic, hindered phenolic and *p*-C<sub>6</sub>H<sub>4</sub>OCH<sub>3</sub> substituents: Preparation, optical properties, and redox reaction. *J. Polym. Sci. Part A: Polym. Chem.* **35**, 463 (1997)



36. Svensson, M.; Theander, M.; Inganas, O.; Andersson, M.R. Synthesis and properties of new polythiophenes with high photoluminescence efficiency *Synth. Met.* **119**, 113-114 (2001)
37. Catellani, M. *et al* Donor-acceptor polythiophene copolymers with tunable acceptor content for photoelectric conversion devices. *J. Mater. Chem.* **14**, 67-74 (2004)
38. Liu, Y.; Xu, Y.; Zhu, D. Synthesis and characterization of poly(3-alkylthiophene)s for light-emitting diodes. *Macromol. Chem. Phys.* **202**, 1010-1015 (2001)
39. Anderson, M.R.; Beggren, M.; Inganas, O.; Gustafsson, G. Electroluminescence from substituted poly(thiophenes)-from blue to nearinfrared, *Macromolecules*, **28**, 7525-7529 (1995)
40. Chittibabu, K.G.; Li, L.; Kamath, M.; Kumar, J.; Tripathy, S K. Synthesis and properties of a novel polythiophene derivative with a side-chain NLO chromophore. *Chem. Mater.* **6**, 475-480 (1994)
41. Chen, S.A.; Tsai, C.C. Structure/properties of conjugated conductive polymers. 2. 3-Ether-substituted polythiophenes and poly(4-methylthiophenes). *Macromolecules*, **26**, 2234-2239 (1993)
42. Somanathan, N.; Radhakrishnan, S.; Thelakkat, M.; Schmidt, H.W. Studies on 3-(2-ethylhexyl)thiophene polymers. *Macromol. Mater. Eng.* **287**, 236-240 (2002)
43. Tsai, F.-C.; Chang, C.C.; Liu, C. L.; Chen, W.C.; Jenekhe, S.A. New thiophene-linked conjugated poly(azomethine)s: theoretical electronic structure, synthesis, and properties. *Macromolecules* **38** 1958-1966 (2005)
44. Krebs, F.C.; Jorgensen, M. The effect of fluorination in semiconducting polymers of the polyphenyleneimine type. *Synth. Met.* **142**, 181-185 (2004)
45. Pokhrel, B.; Dolui, S.K. Synthesis and characterization of 1,1'-bis-2-naphthol chromophore containing polyurethanes and their electrochemical and photoluminescence properties. *J. Polym. Mater.* **26**, 417-426 (2009)
46. Kuo, C.H. *et al* High-performance hole-transport polyurethanes for light-emitting diodes applications. *Chem. Mater.* **18**, 4121-4129 (2006)

47. Zhang, Z.-B.; Fujiki, M.; Tang, H.-Z.; Motonaga, M.; Torimistu, K. The first high molecular weight poly(*N*-alkyl-3,6-carbazole)s. *Macromolecules* **35**, 1988-1990 (2002)
48. Furniss, B.S.; Hannaford, A.J.; Smith, P.W.G.; Tatehell, A.R.(Revised) *Vogel's textbook of practical organic chemistry* (Fifth edition, Longman Group LTd, UK, 1996)
49. Grigoras, M; Catanescu, C.O.; Colotin, G. Poly(Schiff base)s containing 1,1'-binaphthyl moieties: Synthesis and characterization. *Macromol. Chem. Phys.* **202**, 2262-2266 (2001)
50. Campos, L.M. *et al* Extended photocurrent spectrum of a low band gap polymer in a bulk heterojunction solar cell. *Chem. Mater.* **17**, 4031-4033 (2005)
51. Sandler, S.R.; Karo, W. *Polymer syntheses* (Academic Press, New York, 1992)
52. Koyuncu, S.; Kaya, I.; Koyuncu, F.B.; Ozdemir, E. Electrochemical, optical and electrochromic properties of imine polymers containing thiophene and carbazole units. *Synth. Met.* **159**, 1034-1042 (2009)
53. Lin, H.-Y.; Liou, G.-S. Poly(triphenylamine)s derived from oxidative coupling reaction: substituent effects on the polymerization, electrochemical, and electro-optical properties. *J. Polym. Sci. Part A: Polym. Chem.* **47**, 285-294 (2009)
54. Qiao, X.; Wang, X.; Mo, Z. The effects of different alkyl substitution on the structures and properties of poly(3-alkylthiophenes). *Synth. Met.* **118**, 89-95 (2001)
55. Bolgnesi, A.; Porzio, W.; Zhou, T.; Ezquerra, T. The thermal behaviour of poly(3-octylthienylene) synthesized by an Ni-based catalyst: DSC, optical microscopy and XRD analyses. *Eur. Polym. J.* **32**, 1097-1103 (1996)



## Chapter 3

Study of  
electrochemical and  
optical properties of  
conjugated polymers

### 3.1. Introduction

Polymers have long been thought of and applied as insulators. The emergence of electronically conducting polymers has resulted a paradigmatic shift in our thinking and has opened up new vistas in chemistry and physics.<sup>1</sup> This story began in the 1970s, when, somewhat surprisingly, a new class of polymers possessing high electronic conductivity in the partially oxidized (or, less frequently, in the reduced) state was discovered. Three collaborating scientists, Alan J. Heeger, Alan G. MacDiarmid and Hideki Shirakawa, played a major role in this breakthrough, and they received the Nobel Prize in Chemistry in 2000 “for the discovery and development of electronically conductive polymers”.<sup>2-8</sup> Electrochemistry has played a significant role in the preparation and characterization of these novel materials. Electrochemical techniques are especially well-suited to the controlled synthesis of these compounds and for the tuning of a well-defined oxidation state. The preparation, characterization and application of electrochemically active, electronically conducting polymeric systems are still at the foreground of research activity in electrochemistry.<sup>9</sup> After 30 years of research in the field, the fundamental nature of charge propagation is now in general understood; i.e., the transport of electrons can be assumed to occur via an electron exchange reaction (electron hopping) between neighboring redox sites in redox polymers, and by the movement of delocalized electrons through conjugated systems. Many excellent monographs and reviews of the knowledge accumulated regarding the development of conducting polymers, polymer film electrodes and their applications have been published.<sup>10-37</sup>

Cyclic voltammetry provides basic information on the oxidation potential of the monomers, on film growth, on the redox behavior of the polymer, and on the surface concentration (charge consumed by the polymer). Conclusions can also be drawn from the cyclic voltammograms regarding the rate of charge transfer, charge transport processes and the interactions that occur within the polymer segments at specific sites between the polymer and the ions and solvent molecules. The reduction and oxidation processes consist of several simultaneous and consecutive chemical and physical processes like swelling of the polymer, charge transfer between the electrode and the polymer, insertion of compensating ions into the bulk of the polymer, conformational

changes of the polymer chain and change of conductivity.<sup>23</sup> The introduction of side groups will change several properties of the polymer and it may be difficult to confirm that oxidation and reduction potentials are entirely the result of one certain functionality. Nevertheless, some trends can be extracted that may be helpful for design and application of new materials. In addition, the energy position of HOMO and LUMO of conjugated polymers can be determined by cyclic voltammetric method.<sup>38-43</sup> The relevance and generality of electrochemical characterization of conjugated polymers can be estimated by comparison to other methods. This is frequently done by calculating the electrochemical band gap and comparing it with optical band gap.<sup>42-45</sup>

Subsequently, optical properties concomitant to conjugated polymers are important as it gives ample idea regarding feasibility of the polymers to be used in electronic devices. The studies of absorption and emission characteristics provide the information of the band gap, range of emissive colours, interaction with the acceptor etc. The optical properties of conjugated polymers generally studied in solid, solution and thin film forms. The polymer conformation in dilute solutions of conjugated polymers is extended so that interconjugation segment interactions are minimized. Generally, a broad unstructured absorption is accompanied by vibronically structured fluorescence in case of dilute solutions of conjugated polymers. The lack of structure in the absorption is originated due to the effects of torsional motion of the aromatic rings on the conjugation length and is primarily a dynamical effect. While, photoluminescence (PL) is structured because of efficient energy transfer, probably via Forster mechanism, allows the fluorescence to emanate from a small subset of the chromophores that have the lowest energy. This correspond to the most highly planarized geometries with the largest conjugation length and lowest HOMO-LUMO gaps.<sup>46</sup>

This chapter reports the electrochemical and the optical properties of synthesized polymers. The oxidation and reduction potential of polymers were assessed by cyclic voltammetry method. Furthermore, band gap of polymers was measured by electrochemically and compared with optical method. The relative PL quantum yield of polymers with respect to Rhodamine B dye was measured. The PL quenching of the polymers in presence of TiO<sub>2</sub> nanoparticles in solution with 1:1 and 1:2 have also been

observed. This explains the suitability of TiO<sub>2</sub> nanoparticles as electron acceptor in hybrid photovoltaic devices indicating ultrafast electron transfer from donor polymer to acceptor.

## **3.2. Experimental**

### **3.2.1. Materials**

LiClO<sub>4</sub> (Aldrich), (6,6)-phenyl C<sub>61</sub>-butyric acid methyl ester (PCBM) (Aldrich), TiO<sub>2</sub> nanoparticles (Aldrich), Rhodamine B (Aldrich), ITO coated glass (Vin Karola, USA) were used as received. All the solvents used were purified and distilled according to the standard procedure. The synthesized polymers reported in Chapter 2 were used for electrochemical analyses.

### **3.2.2. Instrumentations**

#### **3.2.2.1. Cyclic voltammetry**

Cyclic voltammetry is a dynamic electrochemical method in which the potential applied to an electrochemical cell is scanned and the resulting change in cell current are monitored to yield a cyclic voltammogram of the redox properties of the material under study. The cyclic voltammograms reported here were recorded with a computer controlled Sycopel AEW2-10 potentiostat/galvanostat at a scan rate of 50 mV/S. Measurements were performed with a standard one compartment three-electrode configuration cell (Figure 3.1) with the polymer films deposited on ITO coated glass electrode as the working electrode, platinum as the counter electrode, and an Ag/Ag<sup>+</sup> electrode as the reference electrode. Acetonitrile containing LiClO<sub>4</sub> (0.1M) was used as the electrolytic medium. The measurements were calibrated using ferrocene as the standard. Electrochemical oxidation and reduction processes take place when potential is applied in the working electrode with respect to the reference electrode and this process is equivalent to controlling the energy of the electrons within the working electrode.

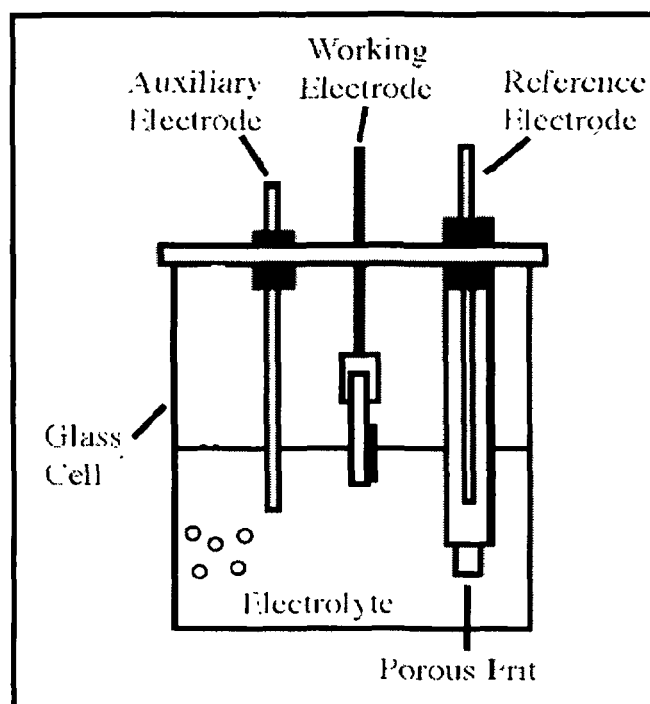


**Figure 3.1:** Standard three electrode electrochemical cell

### 3.2.2.2. UV- Visible spectrophotometer

UV-Visible (UV-Vis) spectrophotometer provides information about structure and stability of the materials in solution. Various kinds of electronic excitation may occur in organic molecules by absorbing the energies available in the UV-Vis region. The spectrophotometer records the wavelengths at which absorption occurs, together with the degree of absorption at each wavelength. The resulting spectrum is presented as a graph of absorbance versus wavelength. The intensity of the absorption is proportional to the number, type and location of colour absorbing structures (chromophores) in the molecule. UV-Visible spectra were recorded on a Shimadzu UV-2550 UV-VIS Spectrophotometer using THF solvent.

### 3.2.2.3. Photoluminescence spectroscopy

Photoluminescence spectra were recorded using a Hitachi F-2500 FL spectrophotometer, by excitation of the polymer at maximum absorption wavelength. The fluorescence spectrum of polymer at different concentration in THF solvent was recorded.

### 3.3. Results and discussion

#### 3.3.1. Estimation of energy level and band gap of the polymer

The energy levels of HOMO and LUMO provide guidelines in selecting the electrode materials when constructing a photovoltaic device based on these polymers. The highest occupied molecular orbital (HOMO) and lowest unoccupied molecular orbital (LUMO) energy levels are estimated from the onset oxidation potentials ( $\phi_{ox}$ ) and the onset reduction potentials ( $\phi_{red}$ ) of the polymers. Energy levels and electrochemical band gap ( $E_g^{ec}$ ) in turn are calculated using the following empirical equations 3.1-3.3.

$$\text{HOMO} = -(\phi_{ox} + 4.71) \text{ (eV)}; \quad (3.1)$$

$$\text{LUMO} = -(\phi_{red} + 4.71) \text{ (eV)}; \quad (3.2)$$

$$E_g^{ec} = (\phi_{ox} - \phi_{red}) \text{ (eV)} \quad (3.3)$$

All the redox potentials are measured against Ag/Ag<sup>+</sup> reference electrode and the energy level calculations are based on ferrocene / ferrocenium (Fc/Fc<sup>+</sup>) redox standard in CH<sub>3</sub>CN. The HOMO and LUMO levels are calculated from the onset potentials of oxidation and reduction and by assuming the energy level of ferrocene/ ferrocenium (Fc/Fc<sup>+</sup>) to be 4.8 eV below the vacuum level. The formal potential of Fc/Fc<sup>+</sup> was measured as 0.09 V against Ag/Ag<sup>+</sup>.<sup>38,47</sup> Hence, the equations (3.1), (3.2) and (3.3) are valid for the calculations of HOMO and LUMO energy levels and electrochemical band gap.

The charging of the polymer during the doping process is associated with conformational reorganisation and modification of the energy levels of the polymer. From this point of view only onset potential probes injection of charges to neutral polymers in the ground state. Onset is also advantageous when two or more red / ox peaks are not fully resolved. The onset has been evaluated by drawing two tangents for each peak and is assumed to be where the two tangents cross as indicated by dashed line for  $E_{pa}^{ox}$  in Figure 3.2.



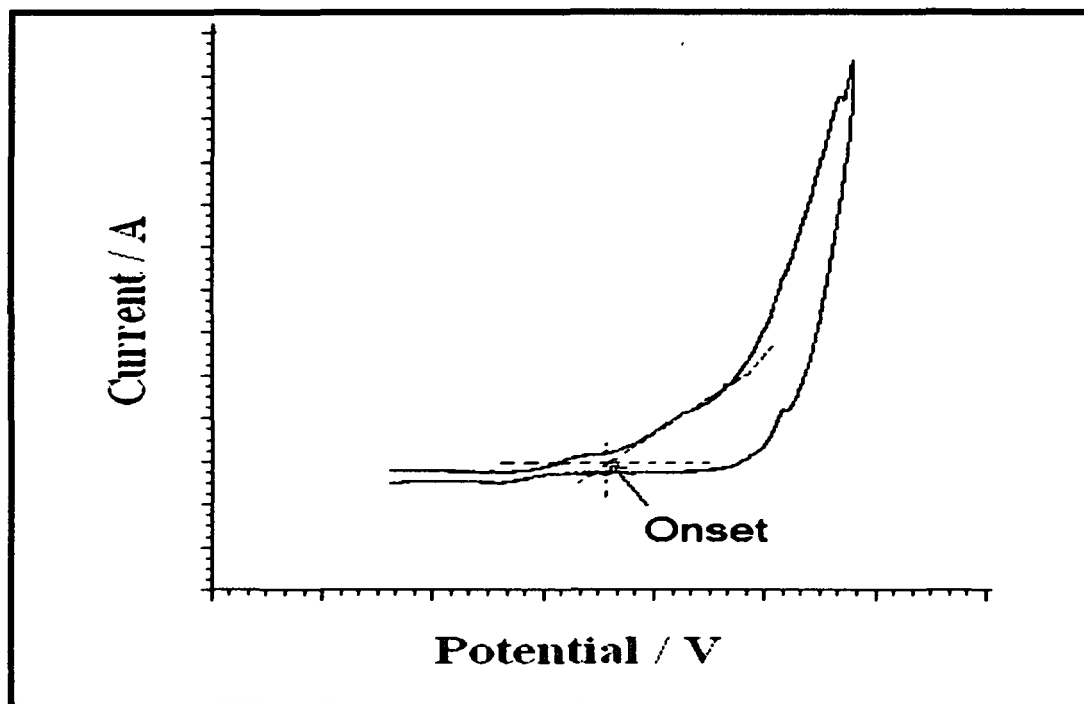
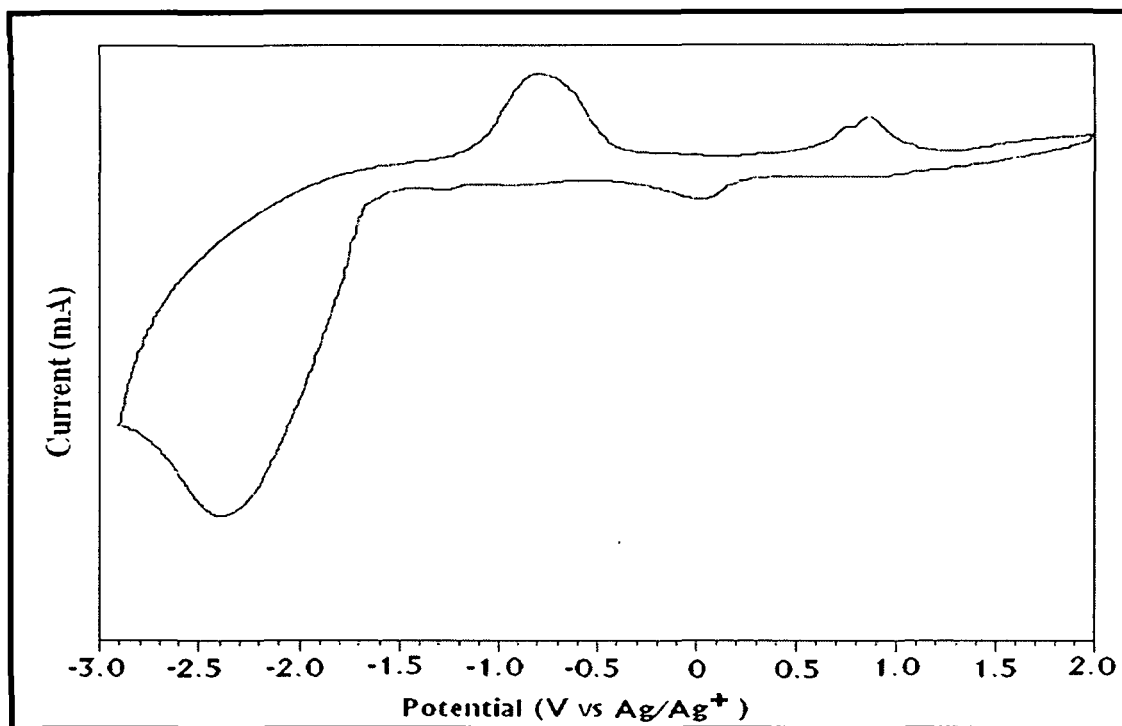


Figure 3.2: Measurement of onset in CV

### 3.3.3. Redox properties of polymers and electrochemical band gap calculation

All the synthesized polymers viz PBTD, PPAET, PPABT, PDDC, PDDCT, PU<sub>1</sub> and PU<sub>2</sub> were used for the electrochemical analyses. The detailed study and findings are discussed below. As the synthesized polymers bear different structural units, hence the electrochemical behaviors of the polymers are compared among the same type of polymers. All the electrochemical parameters are listed in Table 3.1.

Redox behavior and band gap estimation were studied from recorded cyclic voltammogram of the synthesized polymer films in 0.1 M LiClO<sub>4</sub> acetonitrile solution. The peaks in positive potentials are for oxidation whereas the peaks for negative potentials are assigned for reduction of polymer. The voltammogram (Figure 3.3) showed the irreversible oxidation and reduction pattern of the polymer, PBTD. Low oxidation potential value (0.81 V) compared to that of reduction potential (-2.3 V) of the polymer clearly indicates the electron donor nature of the polymer. The onset of oxidation potential and the onset of reduction potential measured for PBTD are 0.46 V and -1.64 V respectively.



**Figure 3.3:** Cyclic Voltammogram of PBTD film on ITO coated glass at a scanning rate of 50 mV/S

The cyclic voltammogram (Figure 3.4) for PPAET and PPABT showed single irreversible oxidation and reduction peaks. The turn-on potential for the p-doping (onset oxidation potential) for the polymers PPAET and PPABT are very low compared to the turn-on potential of the n-doping (onset reduction potentials) which in turn indicates that the polymers possess very good donor nature. The electrochemical band gaps for the polymers are 2.19 and 2.14 eV, respectively, for PPAET and PPABT. Thus it can be concluded that PPABT possesses higher effective conjugation length compared to PPAET.

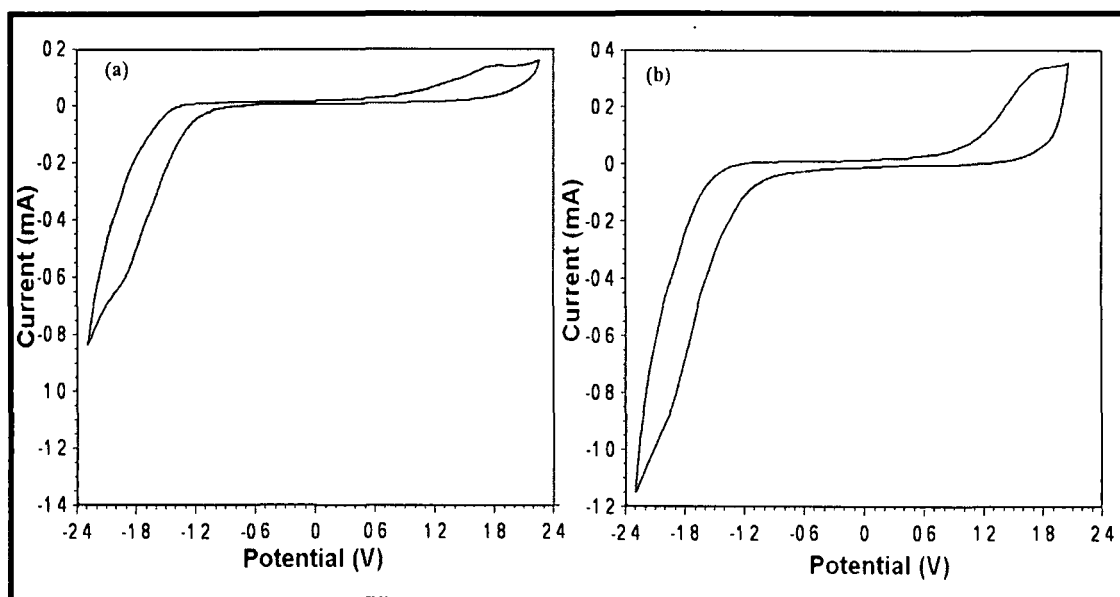


**Figure 3.4:** Cyclic Voltammogram of (a) PPAET and (b) PPABT films on ITO coated glass at a scanning rate of 50 mV/S.

Cyclic voltammograms of PDDC and PDDCT (Figure 3.5) also reveal useful information regarding electrochemical behavior of the polymers. During anodic scan region of PDDCT, two irreversible oxidation waves are observed. The first oxidation peak at +0.84 V can be attributed to thiophene oxidation, and the second one at +1.96 V can be attributed to carbazole oxidation. On the other hand, PDDC shows single anodic peak at +1.92 V for carbazole oxidation. The reduction potentials observed from the CV curve for PDDC and PDDCT are 1.89 V and 1.95 V respectively. The lower onset oxidation potential for the polymers PDDC and PDDCT indicates that the polymers possess good donor nature. The electrochemical band gaps for the polymers are 2.21 and 1.91 eV, respectively, for PDDC and PDDCT. The thiophene moiety attached to carbazole moiety has the key role in reducing oxidation potential as well as band gap in case of PDDCT.<sup>48</sup>

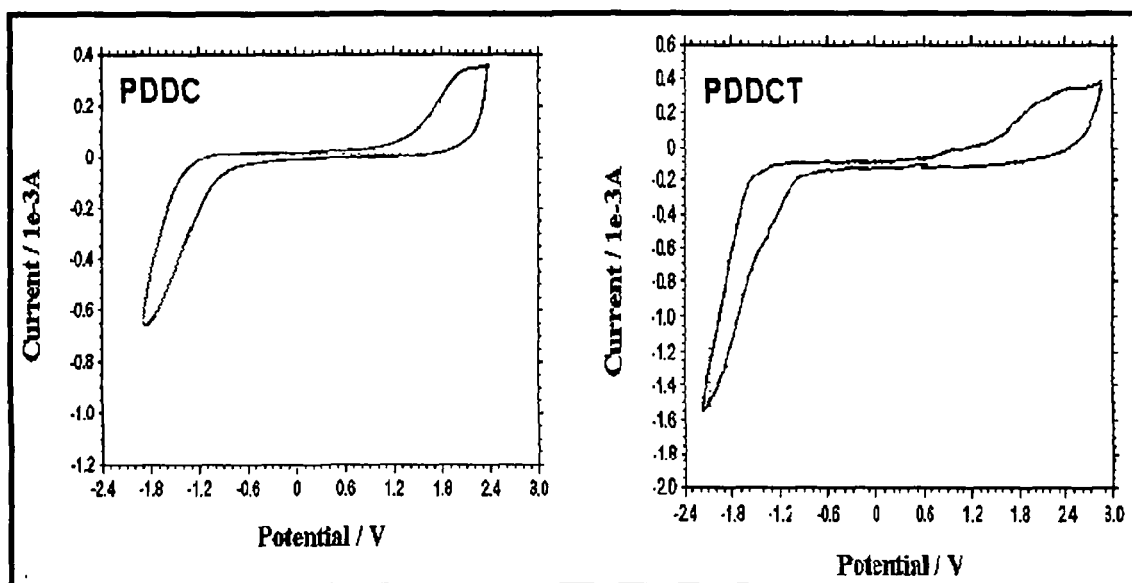
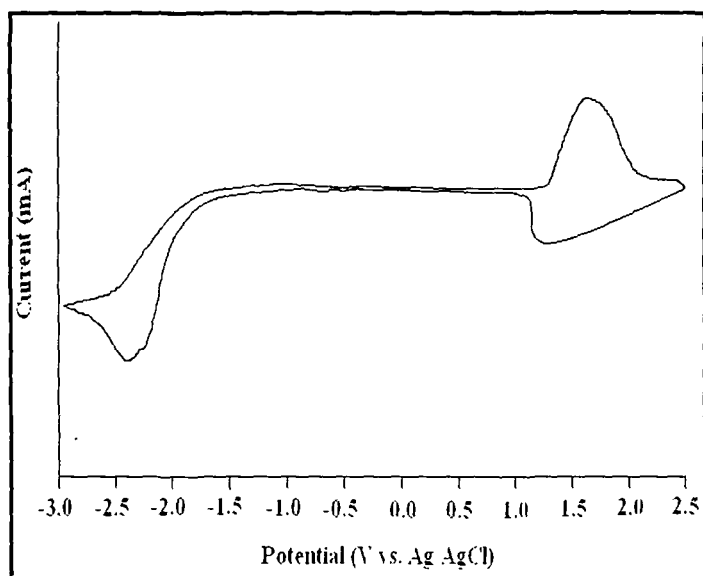
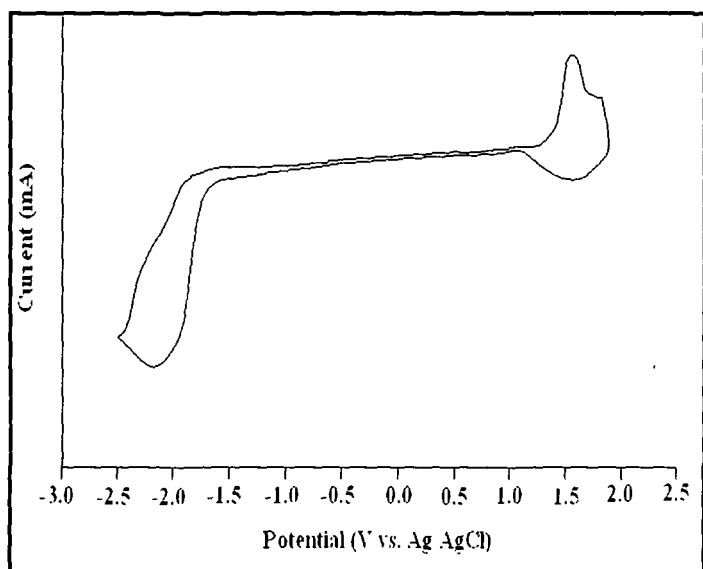


**Figure 3.5:** Cyclic Voltammogram of PDDC and PDDCT films on ITO coated glass at a scanning rate of 50 mV/S

The cyclic voltammograms of  $PU_1$  and  $PU_2$  are shown in Figure 3.6. The difference in energy for HOMO and LUMO energy levels that of  $PU_1$  and  $PU_2$  are the result of different spacers incorporated into them affecting their redox behaviour. The nearly similar onset oxidation potential and band gap observed for  $PU_1$  and  $PU_2$  are resulted due to presence of same binaphthyl chromophore with similar donor ability. The oxidation and reduction potentials measured for  $PU_1$  are 1.51 V and -2.4 V whereas those of  $PU_2$  are 1.52 V and -2.3 V, respectively. The electrochemical band gap for  $PU_1$  and  $PU_2$  found to be 3.19 eV and 3.17 eV.



(a)



(b)

**Figure 3.6:** Cyclic voltammograms of polymers (a) PU<sub>1</sub> and (b) PU<sub>2</sub> films on an ITO-coated glass in CH<sub>3</sub>CN containing 0.1M LiClO<sub>4</sub> as supporting electrolyte

**Table 3.1:** Electrochemical parameters and energy levels of the polymers

Polymers	Oxidation Potential/ Reduction Potential (V)	$\Phi_{ox}$ (V vs Ag/Ag <sup>+</sup> )/ $E_{HOMO}$ (eV) <sup>a</sup>	$\Phi_{red}$ (V vs Ag/Ag <sup>+</sup> )/ $E_{LUMO}$ (eV) <sup>a</sup>	$E_g^{ec}$ (eV)
PBTD	0.81/-2.3	0.46/-5.17	-1.64/-3.07	2.10
PPAET	1.66/-1.92	0.98/-5.69	-1.21/-3.50	2.19
PPABT	1.59/-1.94	0.91/-5.62	-1.23/-3.48	2.14
PDDC	1.92/-1.76	1.18/-5.89	-1.03/-3.68	2.21
PDDCT	0.84, 1.96/-1.95	0.84/-5.55	-1.07/-3.64	1.91
PU <sub>1</sub>	1.51/-2.4	1.31/-6.02	-1.88/-2.83	3.19
PU <sub>2</sub>	1.52/-2.3	1.41/-6.12	-1.76/-2.95	3.17

From Table 3.1, it is observed that heterocyclic ring (thiophene and carbazole) containing polymers possess lower values of oxidation potential. Moreover, azomethine linkage along the main chain or side chain has also great influence on the redox potentials. PBTD, with azomethine linkage along the main chain has the lowest value of oxidation potential and comparatively matching value of HOMO energy value to inject hole to anode in photovoltaic cells. However, the presence of non-conjugated spacer in case of PU<sub>1</sub> and PU<sub>2</sub> has resulted higher values of oxidation potential which in turn is not suitable for easy exciton formation upon irradiation of light onto it.

### 3.3.4. Scan rate dependencies on peak current

Another important characteristic concomitant to cyclic voltammograms of semiconducting polymer films is the dependence of the peak current ( $i_p$ ) on the scan rate ( $\nu$ ). In our study, the plots of anodic peak current ( $i_{pa}$ ) vs scan rate ( $\nu$ ) at the rate of 25, 50, 75 and 100 mV/S for polymer films of PBTD, PPAET, PPABT, PDDC and PDDCT are drawn and found straight lines passing through the origin. According to the well established electrochemical treatments,  $i_p$  is proportional to  $\nu^{1/2}$  for diffusion effect dominated behavior i.e. in solution state. On the other hand, for a material localized on a electrode surface,  $i_p$  is proportional to  $\nu$  thus indicating the behavior of surface-localized

electroactive surface. The curves showing relation between anodic peak current with scan rate are shown in Figure 3.7-3.9. Anodic peak currents ( $i_p$ ) observed for the polymers synthesized via oxidative coupling reactions, reveal a linear relationship as a function of scan rate ( $\nu$ ) for p-doping as shown in figures, which indicates that the electrochemical processes are not diffusion limited but surface localized.<sup>26,49</sup> However, no such characteristic is observed in case of PU<sub>1</sub> and PU<sub>2</sub>. Due to viscous nature of the PUs, relatively thick films are formed onto ITO coated glass. Hence large and sluggish dopant ions with high diffusion coefficients are required to exhibit this surface-localized electroactive behaviour.<sup>26</sup>

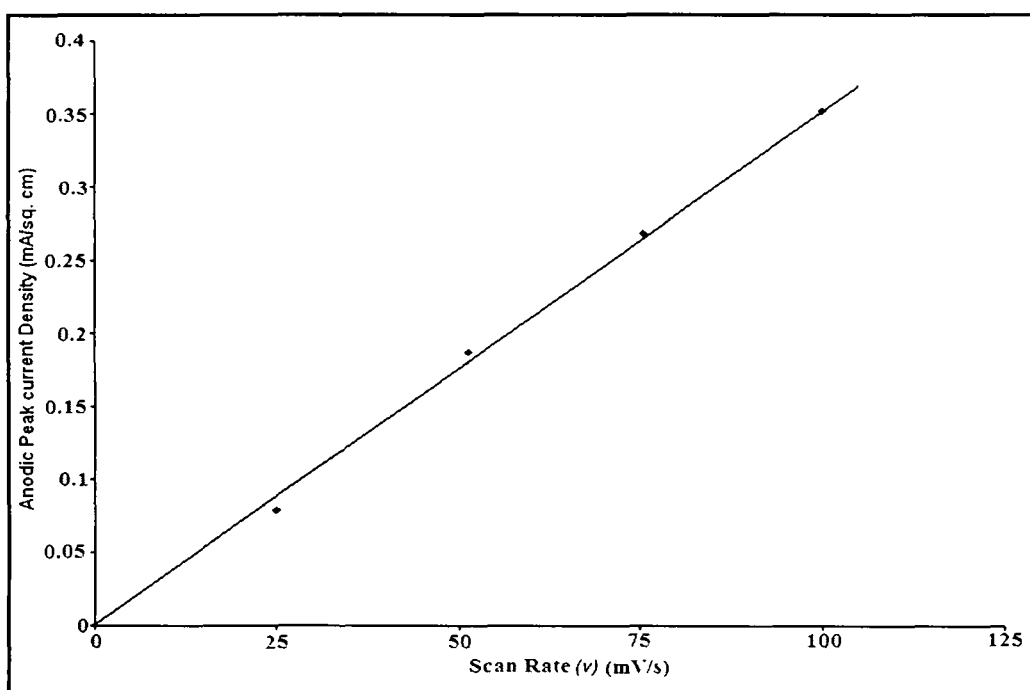


**Figure 3.7:** Anodic peak current density vs. scan rate plot of PBTD

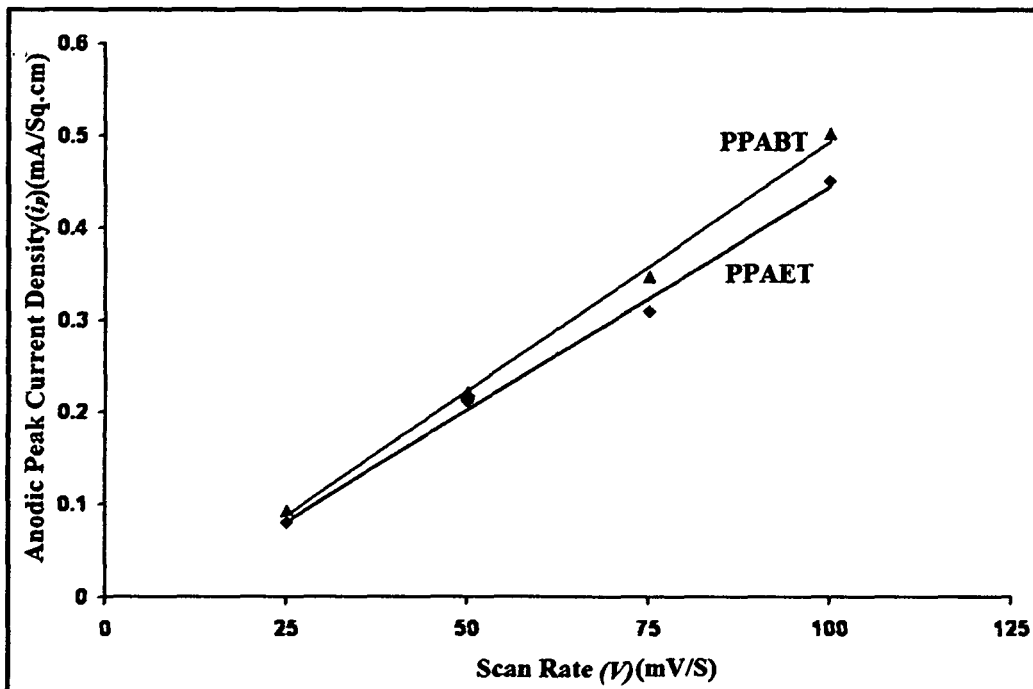


Figure 3.8: Anodic peak current density vs. scan rate plots of PPAET and PPABT

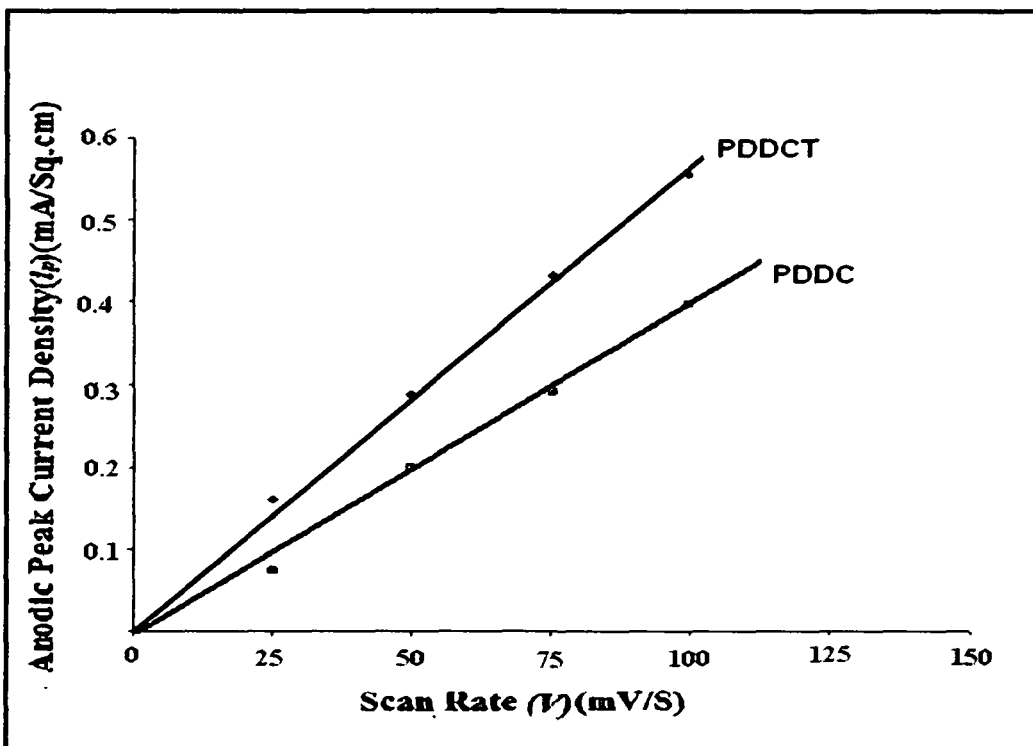


Figure 3.9: Anodic peak current density vs. scan rate plots of PDDC and PDDCT



### 3.3.5. Optical properties of polymers

#### 3.3.5.1. UV –Vis spectra of polymers

Conjugated polymers possess intensive and broad absorption bands in the UV-visible region, indicating an extensive  $\pi$ - conjugation in the polymer backbone. The  $\lambda_{\max}$  depends on the effective  $\pi$ - conjugation of the polymer chain and the aggregation state of the polymer. With increase in  $\pi$ - conjugation length, a red shift to  $\lambda_{\max}$  is observed.

Absorption spectra of the polymers also enable to provide important information regarding its optical band gap. Optical absorption in conjugated polymers which are mostly amorphous or semicrystalline may be due to the transition of charge carriers, through a forbidden energy gap, called optical band gap. Attempts have been made to determine the optical band gap using the equation 3.4.<sup>50</sup>

$$E_g^{\text{opt}} (\text{eV}) = 1240 / \lambda_{\text{edge}} (\text{nm}) \quad (3.4)$$

Where  $E_g^{\text{opt}}$  is the optical band gap of polymers and  $\lambda_{\text{edge}}$  is the absorption edge. The optical characteristic exhibited in UV-visible absorption spectra by all the polymers are summarized in Table 3.2.

The UV-vis absorption spectra of the 0.05% PBDT solution in THF is shown in the Figure 3.10. The absorption spectrum shows a broad absorption over the wavelength range of 400-600 nm with the maximum absorption peak at 467 nm ( $\lambda_{\max}$ ). This might be the result of the electronic transition throughout the whole conjugated molecule including both aromatic rings and central azomethine (-CH=N-) linkage i.e.  $\pi$ -  $\pi^*$  and n-  $\pi^*$  transition. The onset of absorption of the polymer was 587 nm which lead to the optical band gap of 2.11 eV.

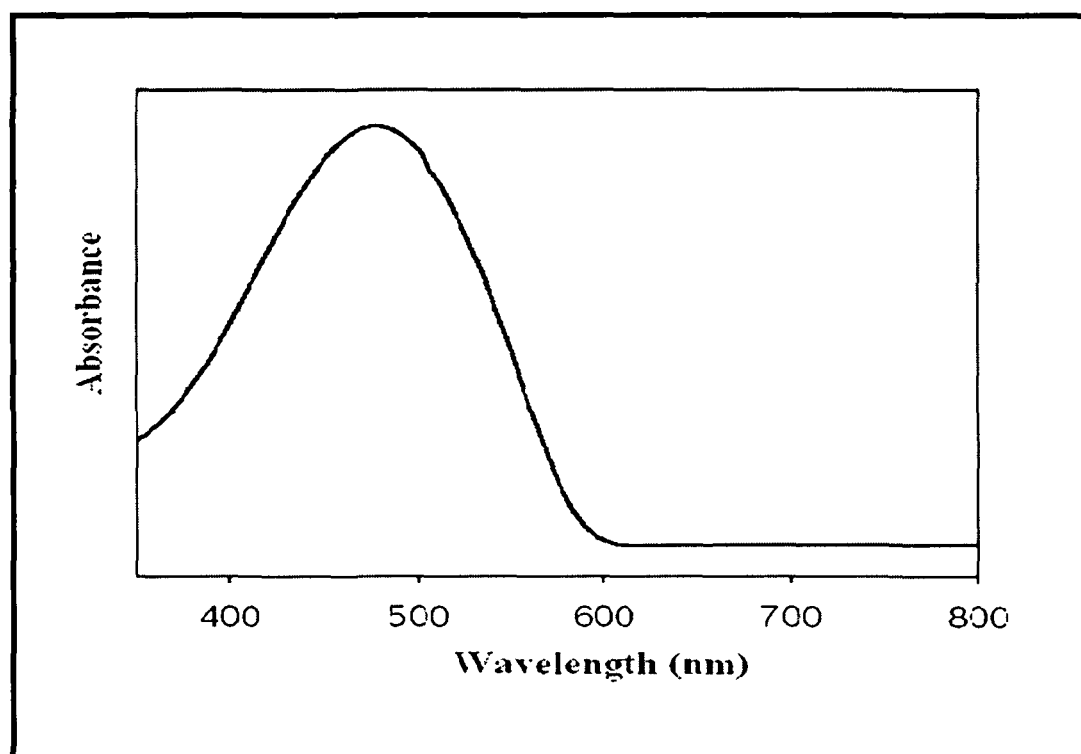


**Figure 3.10:** UV-visible absorption spectrum of 0.05% PBTD solution in THF.

The UV-vis absorption spectra of the 0.05% of PPAET and PPABT solutions in THF are shown in the Figure 3.11. The absorption spectra display a broad absorption over the wavelength range of 370-580 nm with maximum absorption peak at 407 and 415 nm ( $\lambda_{\max}$ ), respectively, for PPAET and PPABT. This is resulted due to the electronic transition throughout the whole conjugated molecule including both aromatic rings and azomethine (-CH=N-) linkage i.e.  $\pi$ - $\pi^*$  and  $n$ - $\pi^*$  transitions. The red shift of the absorption maximum of PPABT in comparison to PPAET is due to the influence of side chain alkyl group. More bulky butyl group in PPABT compared to ethyl group in PPAET reduces the torsional strain and increases the coplanarity of the polymer chain. This may help in increase the effective conjugation length of the polymer and absorption ability as well. Therefore, optoelectronic properties of PPABT are superior to that of PPAET. The onsets of absorption of the polymers are 549 nm and 569 nm which lead to the optical band gap of 2.25 eV and 2.17 eV, respectively, for PPAET and PPABT

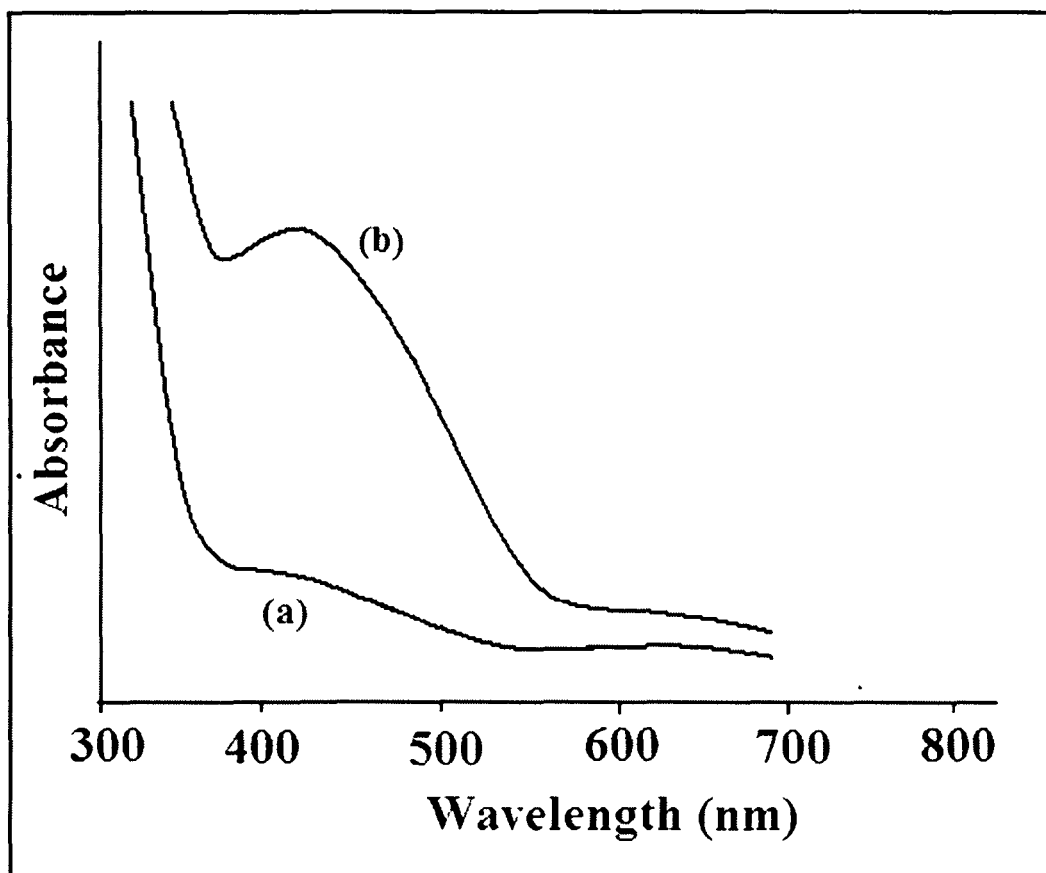


**Figure 3.11:** UV-visible absorption spectra of 0.05% of (a) PPAET and (b) PPABT solution in THF.

The UV-vis absorption spectra of the 0.05% of PDDC and PDDCT solutions in THF are shown in the Figure 3.12. The absorption spectra also show a wide absorption over the wavelength range of 350-590 nm with maximum absorption peaks at 414 and 443 nm ( $\lambda_{\max}$ ), respectively, for PDDC and PDDCT. This is the result of the electronic transition throughout the whole conjugated molecule i.e.  $\pi$ - $\pi^*$  conjugation. The presence of thiophene group along with carbazole moiety in PDDCT results in red shift compared to PDDC favoring the quinoidal structure of the polymer.<sup>48</sup> The onsets of absorption of the polymers are 532 nm and 577 nm which lead to the optical band gap of 2.33 eV and 2.15 eV respectively for PDDC and PDDCT.

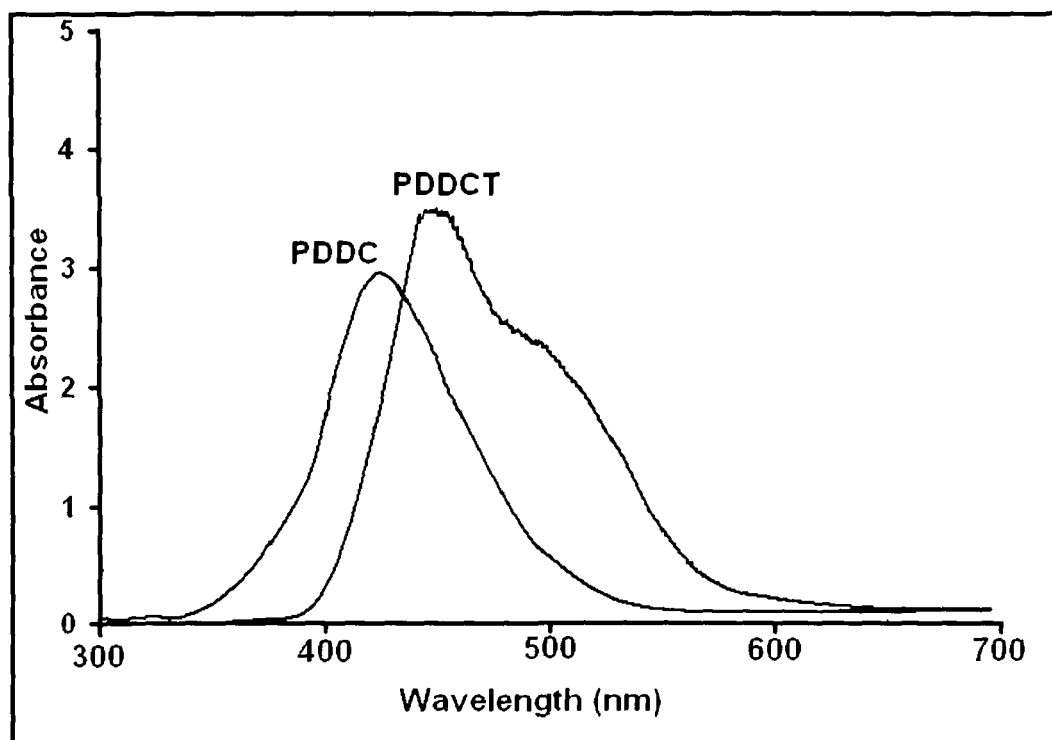


**Figure 3.12:** UV-visible absorption spectra of 0.05% of PDDC and PDDCT solutions in THF.

The UV-vis absorption spectra of the polymers, PU<sub>1</sub> and PU<sub>2</sub> for 0.5% solution in DMAc are reported in Figure 3.13. The spectra display the maximum absorption for PU<sub>1</sub> and PU<sub>2</sub> at the wavelength of 339 nm and 340 nm respectively that is due to  $\pi-\pi^*$  transition originating from the binaphthyl moieties. The absorptions of the polyurethanes with conjugated-nonconjugated system are found in near blue region. Effective conjugation length in these polymers is restricted by the presence of nonconjugated spacers and thus results decrease in absorption maximum.

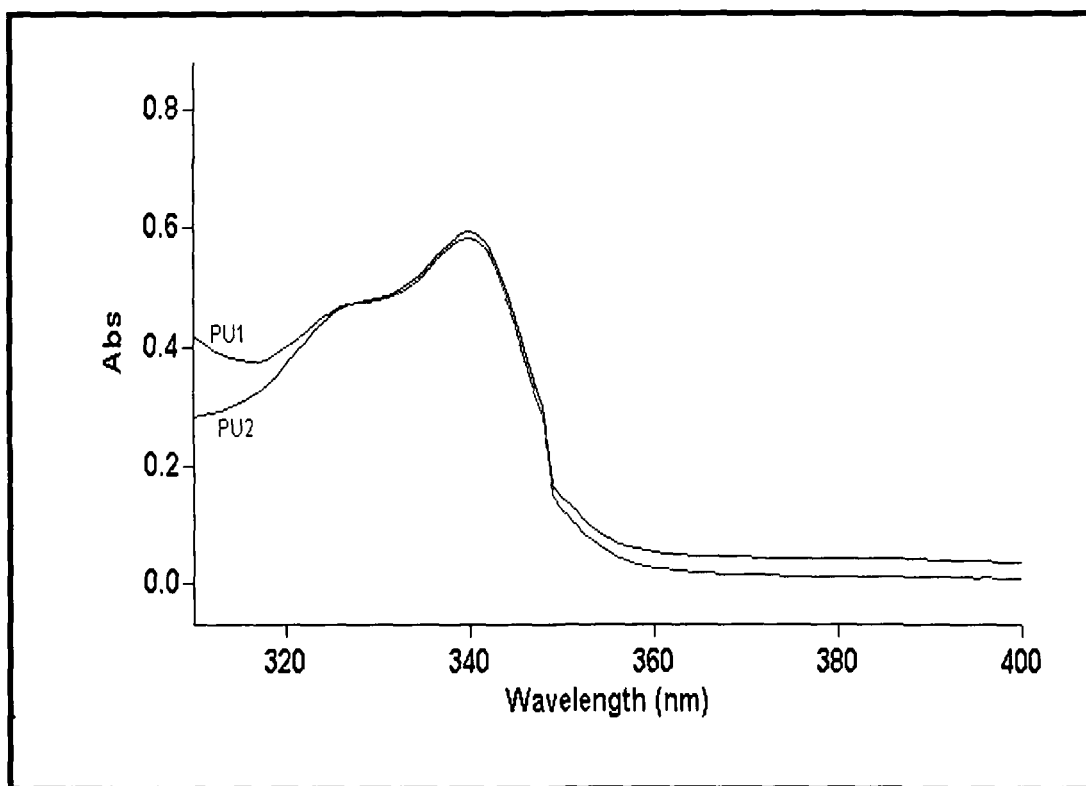


Fig.3.13: UV-visible absorption spectra of PU<sub>1</sub> and PU<sub>2</sub> in solution.

Table 3.2: Summary of the optical characteristic exhibited in UV-visible absorption spectra

Polymer	$\lambda_{\max}$ (nm)	$\lambda_{\text{edge}}$ (nm)	$E_g^{\text{opt}}$	$E_g^{\text{ec}}$
PBTD	467	587	2.11	2.10
PPAET	407	549	2.25	2.19
PPABT	415	569	2.17	2.14
PDDC	414	532	2.33	2.21
PDDCT	443	577	2.15	1.91
PU <sub>1</sub>	339	365	3.40	3.19
PU <sub>2</sub>	340	366	3.39	3.17

### 3.3.5.2. Comparison of band gap estimated from optical and electrochemical method

The band gap is an important parameter whose magnitude governs the intrinsic electronic and optical properties of conjugated polymers. The existence of a finite band gap in conjugated polymers is considered to originate principally from bond length alternation.

The electrochemical determination of band gap actually leads to the formation of charge carriers. On contrary, optical transitions do not reveal the formation of free charge carriers, as the excited state in conjugated polymers may be viewed as a bound exciton. At the same time, optical transitions cannot be directly compared to the electrochemical doping process.<sup>23</sup> But in our case, we have found nearly matching electrochemical and optical band gaps (Table 3.2) and the similar trend of variation. Only the difference in observed electrochemical and optical band gap is recorded in case of PDDC, PU<sub>1</sub> and PU<sub>2</sub>.

### 3.3.5.3. Photoluminescence and quantum yield of polymers in solution

The photoluminescence (PL) of the polymers in THF solution, excited at the maximum absorption wavelength is measured. The emission maxima ( $\lambda_{\text{max}}^{\text{PL}}$ ) of the polymers have been found in the range of 548nm for PDDC and 644 nm for PBTD (Table 3.4), indicating difference of effective conjugation length and structural changes in the relaxed excited state. Only, PU<sub>1</sub> and PU<sub>2</sub> exhibited PL in blue region i.e. 379 nm and 380 nm respectively.

A study of photoluminescence (PL) spectra of 0.05% solution of PPAET, PPABT, PDDC, PDDCT, PU<sub>1</sub> and PU<sub>2</sub> in THF with varying amounts of TiO<sub>2</sub> nanoparticles and PCBM (for PBTD) (1:1 and 1:2 ratio to polymer) has also been carried out. The PL spectra are displayed in Figure 3.14-3.18. The PL intensity of blended solutions of polymers got quenched with increasing amount of TiO<sub>2</sub> (PCBM in case of PBTD) compared to that of pristine polymer solution. The quenching of PL emission is 2-20 times for 1:1 and 1:2 ratio of polymer to TiO<sub>2</sub> (or PCBM for PBTD) than that of the pristine polymer solution. This can be attributed to strong photoinduced electronic interactions between polymers and acceptors (TiO<sub>2</sub> and PCBM) indicating efficient

exciton dissociation in the blend by ultrafast electron transfer from polymer to acceptor.<sup>49,53</sup> This study indicates the possibility of utilising PCBM and TiO<sub>2</sub> nanoparticles as acceptor along with the synthesized polymers as donor in fabrication of polymer photovoltaic devices.

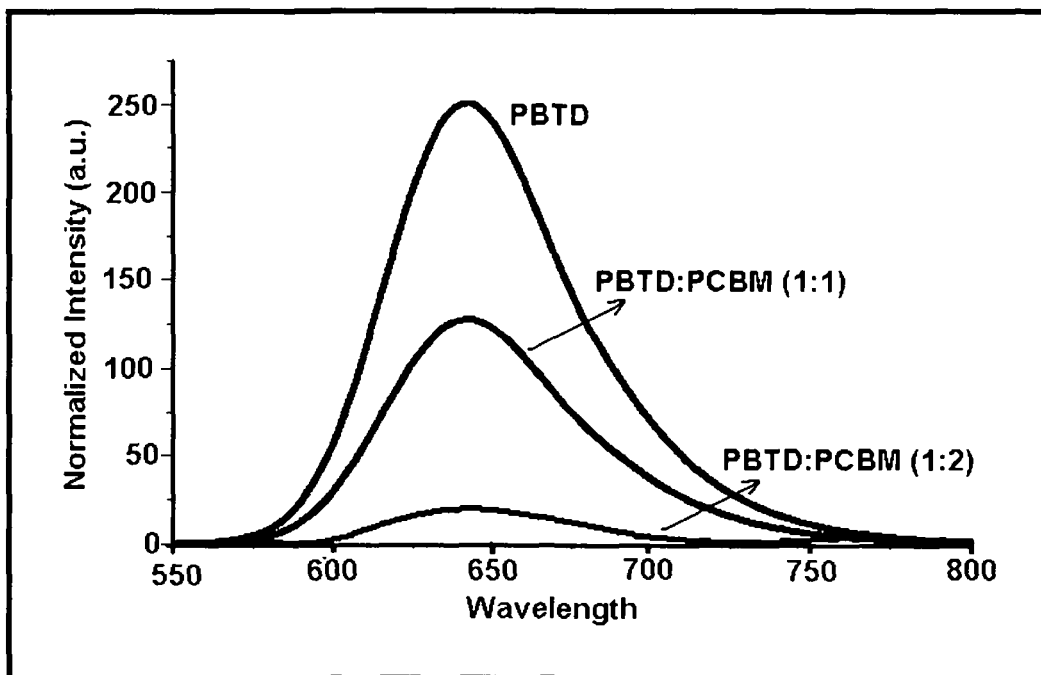


**Figure 3.14:** PL spectra of 0.05% PBDT solution and blend of PBDT and PCBM in THF

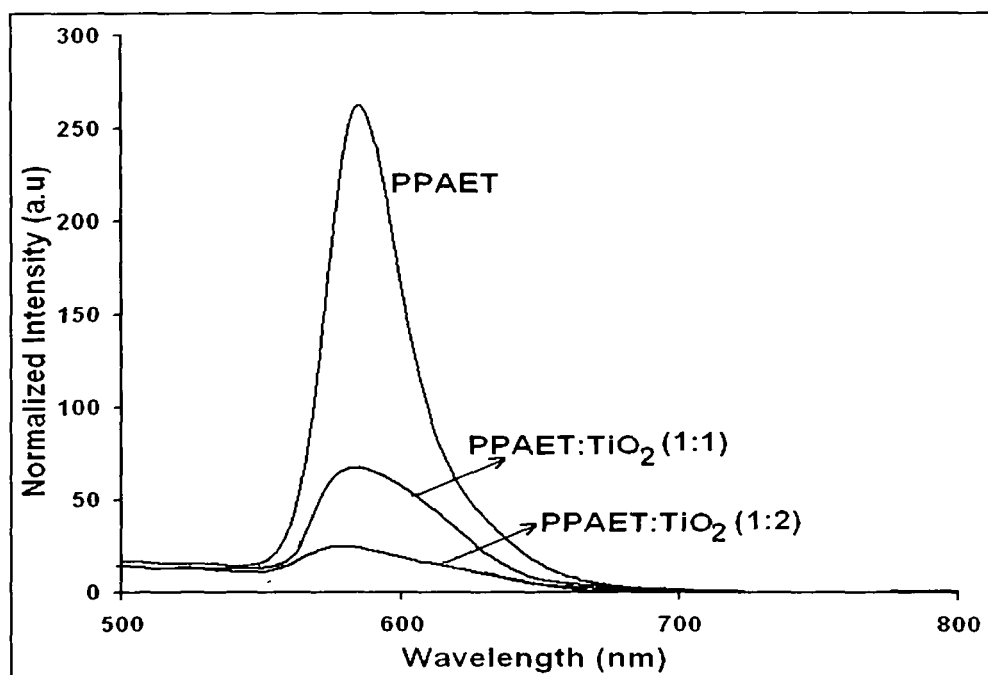


Figure 3.15: PL spectra of 0.05% PPAET solution and blend of PPAET and  $\text{TiO}_2$  in THF

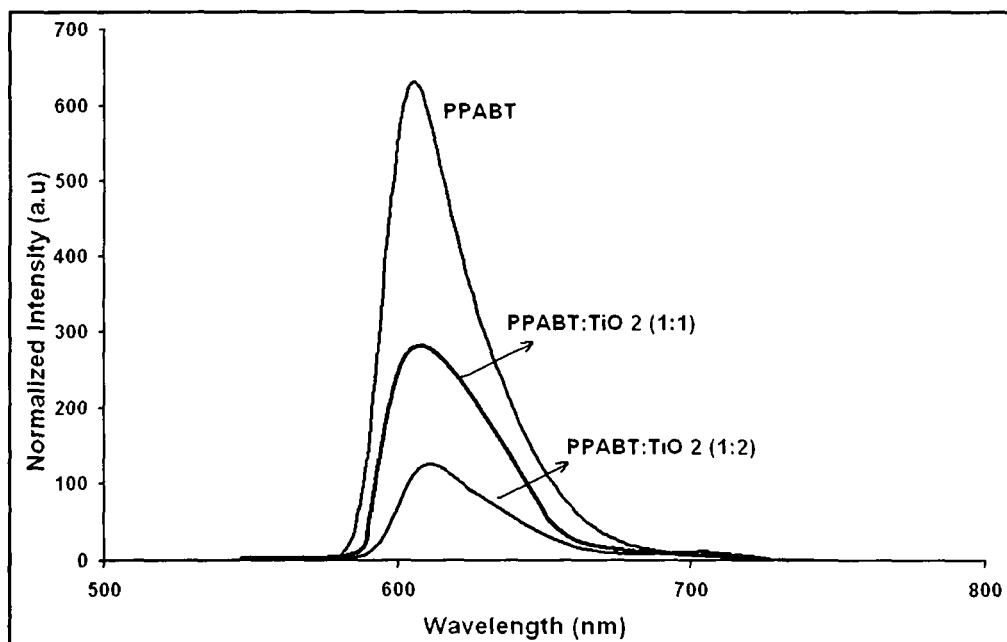


Figure 3.16: PL spectra of 0.05% PPABT solution and blend PPABT and  $\text{TiO}_2$  in THF



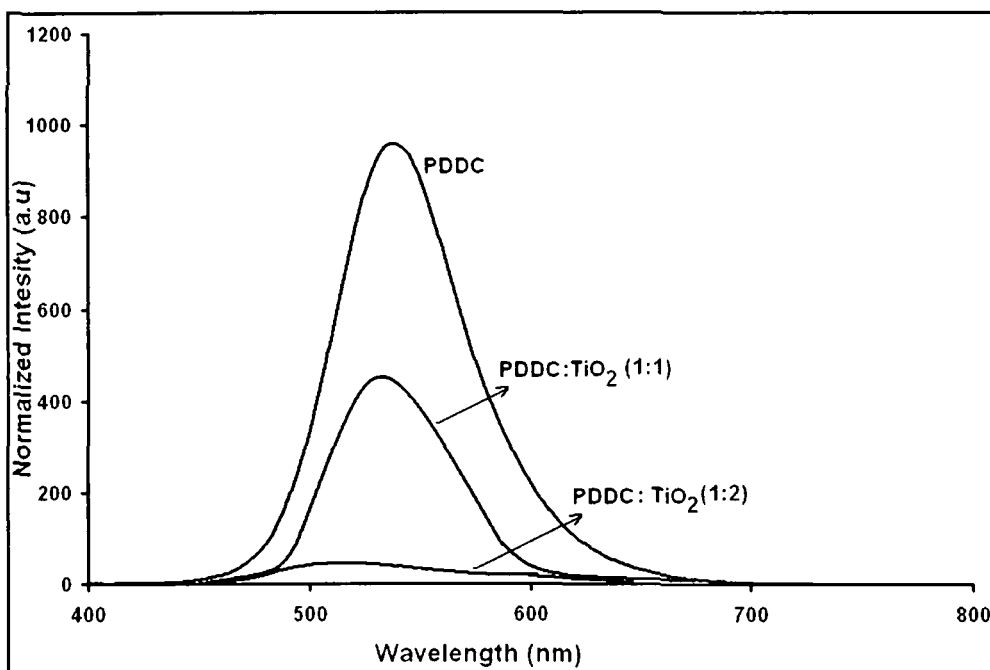


Figure 3.17: PL spectra of 0.05% PDDC solution and blend of PDDC and  $\text{TiO}_2$  in THF

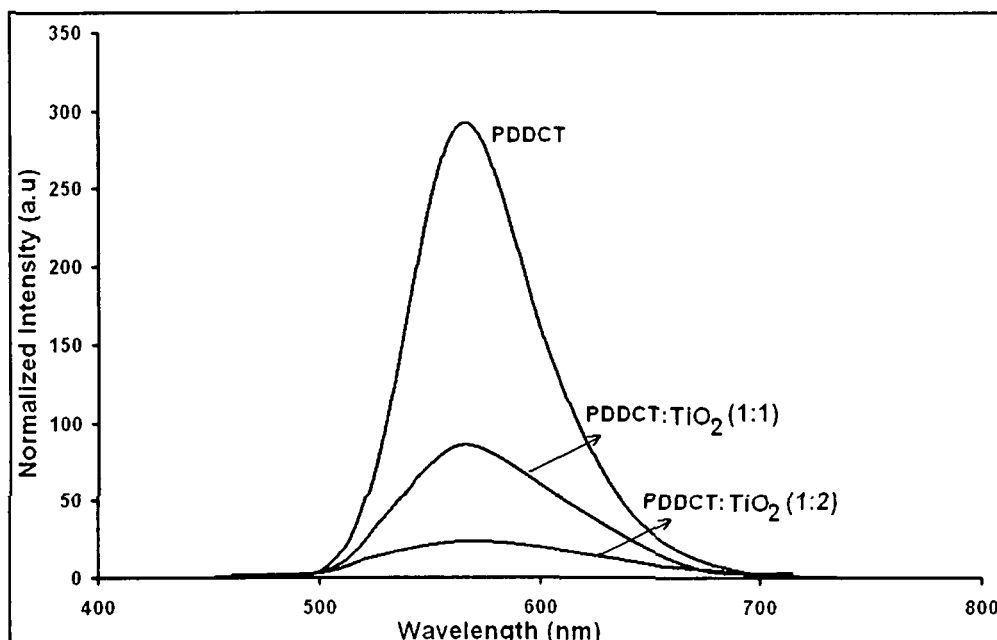


Figure 3.18: PL spectra of 0.05% PDDCT solution and blend of PDDCT and  $\text{TiO}_2$  in THF

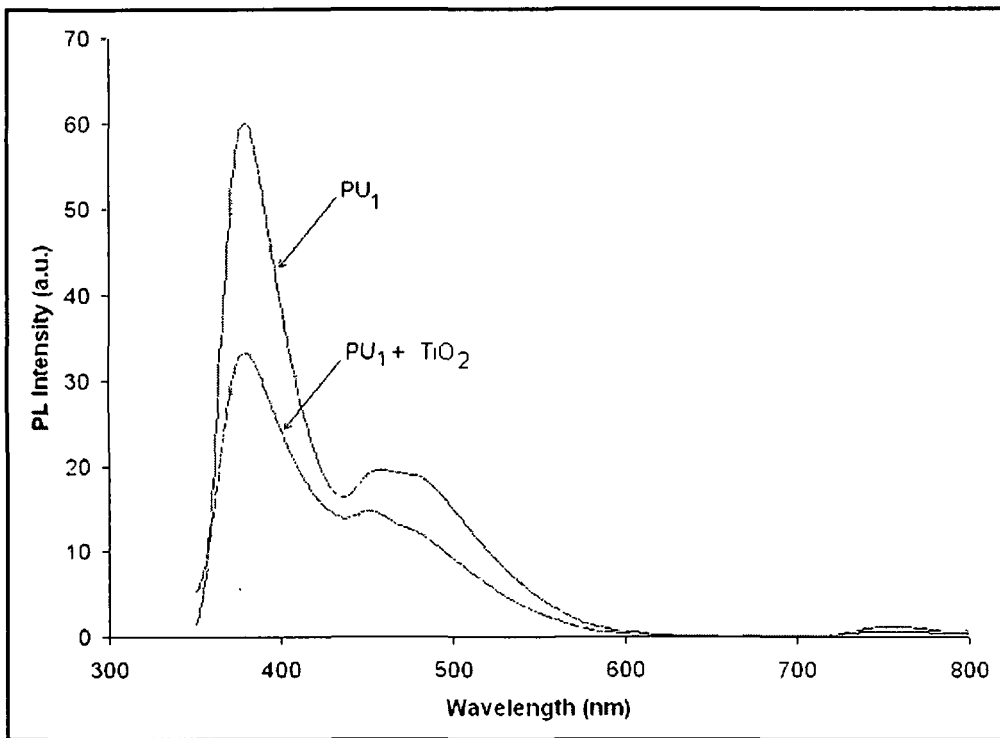


Figure 3.19: PL spectra of 0.05% PU<sub>1</sub> solution and blend of PU<sub>1</sub> and TiO<sub>2</sub> in THF

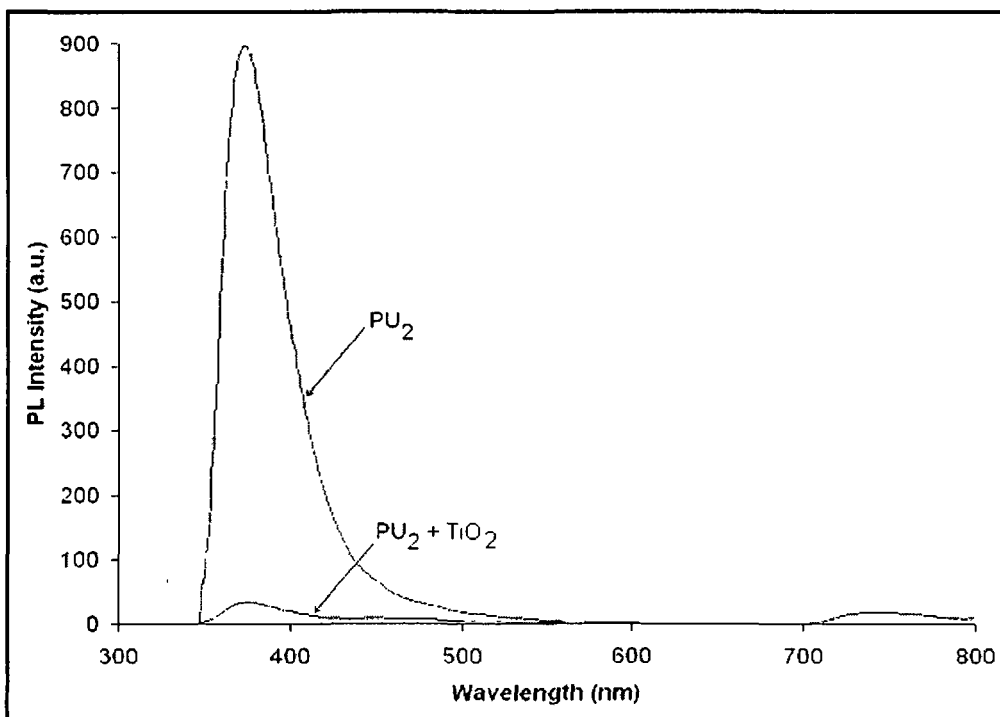


Figure 3.20: PL spectra of 0.05% PU<sub>2</sub> solution and blend of PU<sub>2</sub> and TiO<sub>2</sub> in THF

The maximum fluorescence of polymer intensity value at 0.05 wt % in THF is taken for quantum yield calculation. The standard fluorescent sample, Rhodamine B dye has been chosen because it emits in a similar region to these polymers. The fluorescence spectrum of Rhodamine B dye at 0.05 wt% in THF solvent was recorded. The quantum yield value of polymers was calculated using the standard sample Rhodamine B dye. The quantum yield of a polymer sample in solution  $\Phi_s$  relative to a reference sample of known quantum yield  $\Phi_r$  may be related by equation 3.5.<sup>54</sup>

$$\Phi_s = \Phi_r (A_r/A_s \times I_s/I_r) \quad (3.5)$$

Where  $A_s$  and  $A_r$  are the absorbance of the sample and reference solutions respectively at the excitation wavelength;  $I_r$  and  $I_s$  are the corresponding relative integrated fluorescence intensities.

The fluorescence quantum yield of polymers is measured and compared with Rhodamine B dye (Table 3.3). The relative quantum yield of polymers is found to be 0.113-0.846 with respect to Rhodamine B dye at 0.05 wt %. It is observed that heterocyclic ring containing polymers i.e. PBTD, PPAET, PPABT, PDDCT showed good fluorescent quantum yield compared to others. The effect of azomethine linkage on quantum yield is also found to be pronounced as PBTD, PPAET and PPABT exhibited comparatively higher quantum yield. The presence of non-conjugated spacers with binaphthyl chromophore in PU<sub>1</sub> and PU<sub>2</sub> might have resulted lower relative quantum yields compared to other fully conjugated polymers.

**Table 3.3:** Absorption, emission and relative quantum yield values of polymers in solution

Polymer	Absorption (nm)	Emission (nm)	Stokes shift (nm)	PL quantum yield (Relative*)
PBTD	467	644	177	0.864
PPAET	407	582	175	0.436
PPABT	415	608	193	0.769
PDDC	414	548	134	0.345
PDDCT	433	576	143	0.792
PU <sub>1</sub>	339	379	40	0.113
PU <sub>2</sub>	340	380	40	0.146

\* Relative quantum yield is measured with respect to Rhodamine

### 3.4. Conclusion

- Electrochemical properties of the synthesized polymers are studied from recorded cyclic voltammogram. The polymers bear low oxidation potential compared to reduction potential which indicates that they possess good electron donor ability. HOMO and LUMO energy levels are calculated approximately from the onset oxidation and reduction potential and difference of these level gives band gap of the polymers.

- Electrochemical band gaps of these polymers are found to be in the range of 1.93-3.2 eV. The polymers PU<sub>1</sub> and PU<sub>2</sub> with conjugated-non conjugated system exhibit comparatively higher electrochemical band gaps due to limited conjugation length in the polymer chain.

- The UV-vis absorption spectra of the 0.05% polymer solutions in THF show a broad absorption over the wavelength range of 350-590 nm with maximum absorption peak at 407 nm, 415 nm and 467 nm ( $\lambda_{\text{max}}$ ), respectively, for PPAET, PPABT and PBTD. This is resulted due to the electronic transition throughout the whole conjugated molecule including both aromatic rings and azomethine (-CH=N-) linkage i.e.  $\pi$ - $\pi^*$  and  $n$ - $\pi^*$  transition. PDDC and PDDCT also exhibit absorption maxima at 412 nm and 462 nm. Thiophene moiety attached with 9-dodecyl carbazole unit in PDDCT results in increase of absorption ability.

- The absorptions of the polyurethanes, PU<sub>1</sub> and PU<sub>2</sub> with conjugated-nonconjugated system are found in near blue region. Effective conjugation length in these polymers is restricted by the presence of nonconjugated spacers and thus results decrease in absorption maximum.

- The calculated optical band gaps from onset of absorption spectra are in the range of 2.1-3.4 eV. The polymers exhibit good photoluminescence characteristics in solution. Relative quantum yield with respect to Rhodamine B dye have been calculated and found to be in the range of 0.113-0.846. PBTD exhibited the highest quantum yield whereas PU<sub>1</sub> exhibited the lowest.

- PL characteristic depends on the type of chromophores and conjugation length in the polymers. The PL quenching of the polymers in presence of TiO<sub>2</sub> nanoparticles (or PCBM in case of PBTD) in solution with 1:1 and 1:2 have been observed. This explains the suitability of TiO<sub>2</sub> nanoparticles as electron acceptor in hybrid photovoltaic devices indicating ultrafast electron transfer from donor polymer to acceptor.

### References

1. Ingelt, G. *Conducting polymers: A new era in electrochemistry* (Springer, Germany, 2008)
2. Chiang, C.K. et al. Electrical Conductivity in Doped Polyacetylene. *Phys. Rev. Lett.* **39**, 1098-1101 (1977)
3. Chiang, C.K. et al. Synthesis of highly conducting films of derivatives of polyacetylene, (CH)<sub>x</sub>. *J. Am. Chem. Soc.* **100**, 1013-1015 (1978)
4. Shirakawa, H. The discovery of polyacetylene film: the dawning of an era of conducting polymers. *Angew. Chem. Int. Ed.* **40**, 2574-2580 (2001)
5. MacDiarmid, A.G. Synthetic metals: A novel role for organic polymers (Nobel Lecture). *Angew. Chem. Int. Ed.* **40**, 2581-2590 (2001)
6. Heeger, A.J. Semiconducting and metallic polymers: The fourth generation of polymeric materials. *J. Angew. Chem. Int. Ed.* **40**, 2591-2611 (2001)
7. Letheby, H. On the production of a blue substance by the electrolysis of sulphate of aniline. *J. Chem. Soc.* **15**, 161-163 (1862)
8. Bard, A.J. *Integrated chemical systems* (Wiley, New York, 1994)
9. Fujihira, M. *Modified electrodes. In: Fry AJ, Britton WE. Topics in organic electrochemistry* (Plenum, New York, 1986)
10. Gerard, M. Chaubey, A. Malhotra, B.D. Applications of conducting polymers to biosensors. *Biosens. Bioelectron.* **17**, 345-359 (2002)
11. Inzelt, G. *Mechanism of charge transport in polymer-modified electrodes. In: Bard AJ Electroanalytical chemistry* (Marcel Dekker, New York, 1994)
12. Kaneko, M.; Wöhrle, D. *Polymer-coated electrodes: new materials for science and industry* (Advances in polymer science, Springer, Berlin, 1988)
13. Kutner, W.; Wang, J.; L'Her, M.; Buck, R.P. Analytical aspects of chemically modified electrodes: Classification, critical evaluation and recommendations. (IUPAC Recommendations 1998) *Pure. Appl. Chem* **70**, 1301-1318 (1998)
14. Linford, R.G. *Electrochemical science and technology of polymers* (vol 1. Elsevier, London, 1987)

15. Skotheim, T.A.; Elsenbaumer, R.L.; Reynolds, J.R. *Handbook of conducting polymers* (Marcel Dekker, Inc., New York, 1998)
16. Stejkal, J.; Sapurina, I. Polyaniline: Thin films and colloidal dispersions (IUPAC Technical Report). *Pure. Appl. Chem.* **77**, 815-826 (2005)
17. Biallozor, S.; Kupniewska, A. Conducting polymers electrodeposited on active metals. *Synth. Met.* **155**, 443-449 (2005)
18. Li, X.G.; Huang, M.R.; Duan, W. Novel Multifunctional Polymers from Aromatic Diamines by Oxidative Polymerizations. *Chem. Rev.* **102**, 2925-3030 (2002)
19. Tallman, D.; Spinks, G.; Dominis, A.; Wallace, G. Electroactive conducting polymers for corrosion control part. 1. General introduction and a review of non ferrous metals. *J. Solid. State. Electrochem.* **6**, 73-84 (2002)
20. Ramanavicius, A.; Ramanaviciene, A.; Malinauskas, A. Electrochemical sensors based on conducting polymer-polypyrrole. *Electrochim. Acta.* **51**, 6025-6037 (2006)
21. Barbero, C.A. Ion exchange at the electrode/electrolyte interface studied by probe beam deflection techniques. *Phys. Chem. Chem. Phys.* **7**, 1885-1899 (2005)
22. Malev, V.V.; Konratiev, V.V. Charge Transfer Processes in Conducting Polymer Films. *Russ. Chem. Rev.* **75**, 147-160 (2006)
23. Johansson, T.; Mammo, W.; Svensson, M.; Andersson, M.R.; Inganas, O. electrochemical bandgaps of substituted polythiophenes. *J. Mater. Chem.* **13**, 1316-1323 (2003)
24. Linford, R.G. *Electrochemical science and technology of polymers* (Elsevier, London, 1987).
25. Bredas, J.L.; Silbey, R. Bourdreaux, D.S.; Chance, R.R. Chain-length dependence of electronic and electrochemical properties of conjugated systems: polyacetylene, polyphenylene, polythiophene, and polypyrrole. *J. Am. Chem. Soc.* **105**, 6555-6559 (1983)
26. Chandrasekhar, P. *Conducting polymers, fundamental and applications: A practical approach* (Kluwer Academic Publishers, London, 1999)

27. Buck, R.P.; Lindner, E.; Kutner, W.; Inzelt, G. Piezoelectric chemical sensors. *Pure. Appl. Chem.* **76**, 1139-1160 (2004)
28. Heinze, J.; Frontana-Uribe, B.A.; Ludwigs, S. Electrochemistry of conducting polymers-persistent models and new concepts. DOI- 10.1021/cr900226k (2010).
29. Roncali, J. Conjugated poly(thiophenes): synthesis, functionalization, and applications. *Chem. Rev.* **92**, 711-738 (1992)
30. Sanchez-Carrera, R.S. *et al* Electronic Properties of the 2,6-Diiododithieno[3,2-*b*:2',3'-*d*]thiophene Molecule and Crystal: A Joint Experimental and Theoretical Study. *J. Phys. Chem. B* **114**, 749-755 (2010)
31. Doblhofer, K. Thin polymer films on electrodes. In: Lipkowski J, (Ross PN Electrochemistry of novel materials, VCH, New York, 1994)
32. Nalwa, H.S. *Handbook of organic conducting molecules and polymers* (Vols 1-4, Wiley, New York, 1997-2001)
33. Romero, A.J.F.; Cascales, J.J.L.; Otero, T.F. In situ FTIR spectroscopy study of the break-in phenomenon observed for PPy/PVS films in acetonitrile. *J. Phys. Chem. B.* **109**, 21078-21085 (2005)
34. Stejkal, J.; Gilbert, R.G. Polyaniline. Preparation of a conducting polymer. (IUPAC Technical Report) *Pure. Appl. Chem.* **74**, 857-867 (2002)
35. Linford, R.G. *Electrochemical science and technology of polymers* (Vol 2, Elsevier, London, 1990)
36. Rahman, A.; Kumar, P.; Park, D.S.; Shim, Y.B. Electrochemical sensors based on organic conjugated polymers. *Sensors* **8**, 118-141 (2008)
37. Inganas, O. Hybrid electronics and electrochemistry with conjugated polymers. *Chem. Soc. Rev.* **39**, 2633-2642 (2010)
38. Sun, Q.; Wang, H.; Yang, C.; Li, Y. Synthesis and electroluminescence of novel copolymers containing crown ether spacers. *J. Mater. Chem.* **13**, 800-806, (2003)
39. Zanietz, S. *et al* Electrochemical determination of the ionization potential and electron affinity of poly.9,9-dioctylfluorene. *Appl. Phys. Lett.* **73**, 2453-2455 (1998)



40. Brédas, J. L.; Silbey, R.; Boudreaux, D.S.; Chance, R.R. Chain-Length Dependence of Electronic and Electrochemical Properties of Conjugated Systems: Polyacetylene, Polyphenylene, Polythiophene, and Polypyrrole. *J. Am. Chem. Soc.* **105**, 6555-6559, (1983)
41. Liou, G.S.; Hsiao, S.H.; Chen, W.C.; Yen, H.J. A New Class of High  $T_g$  and Organosoluble Aromatic Poly(amine-1,3,4-oxadiazole)s Containing Donor and Acceptor Moieties for Blue-Light-Emitting Materials. *Macromolecules* **39**, 6036-6045 (2006)
42. Zhou, E.; He, C.; Tan, Z.; Yang, C. Li, Y. Effect of side-chain end groups on the optical, electrochemical, and photovoltaic properties of side chain conjugated polythiophenes. *J. Polym. Sci.: Part A: Polym. Chem.* **44**, 4916-4922 (2006)
43. Koyuncu, S.; Kaya, I.; Koyuncu, F.B.; Ozdemir, E. Electrochemical, optical and electrochromic properties of imine polymers containing thiophene and carbazole units. *Synthetic Metals* **159**, 1034-1042 (2009)
44. Skompska, M.; Szkurlat, A. The influence of the structural defects and microscopic aggregation of poly(3-alkylthiophenes) on electrochemical and optical properties of the polymer films: discussion of an origin of redox peaks in the cyclic voltammograms. *Electrochim. Acta.* **46**, 4007-4015 (2001)
45. Hillman, A.R.; Efimov, I.; Skompska, M. Dynamics of regioregular conducting polymer electrodes in response to electrochemical stimuli. *Faraday Discuss.* **121**, 423-439 (2002)
46. Hadziioannou, G.; Malliaras, C.G. *Semiconducting polymers: Chemistry, physics and engineering* (Second edition, 1<sup>st</sup> Vol., Wiley-VCH, Germany, 2007)
47. Pommerehne, J.; Vestweber, H.; Guss, W.; Mahrt, R. F.; Bassler, H.; Porsch, M.; Daub, J. Efficient two layer LEDs on a polymer blend basis. *Adv. Mater.* **7**, 551-554 (1995)
48. Cheng, Y.-J.; Yang, S.-H.; Hsu, C.-S. Synthesis of conjugated polymers for organic solar cell applications. *Chem. Rev.* **109**, 5868-5923 (2009)

49. Baran, D.; Balan, A.; Celebi, S.; Esteban, B.M.; Neugebauer, H.; Sariciftci, N.S. Toppare, L. Processable multipurpose conjugated polymer for electrochromic and photovoltaic applications. *Chem. Mater.* **22**, 2978-2987 (2010)
50. Tsai, F.-C. *et al* New thiophene-linked conjugated poly(azomethine)s: Theoretical electronic structure, synthesis, and properties. *Macromolecules* **38**, 1958-1966 (2005)
51. Radhkrishnan, S.; Parthasarathy, P.; Subramanian, V.; Somanathan, N. Quantum chemical studies on polythiophenes containing heterocyclic substituents: Effect of structure on the band gap. *J. Chem. Phys.* **123**, 164905 (2005)
52. Hotta, S.; Waragai, K. Solid-state absorption spectroscopy of alkyl-substituted oligothiophenes. *J. Phys. Chem.* **97**, 7427-7434 (1993)
53. Chen, H. *et al* Novel fluorine-based conjugated copolymers with donor-acceptor structures for photovoltaic applications. *Polymer Bulletin* **60**, 581-590 (2008).
54. Chosrovian, H. *et al* Time-resolved fluorescence studies on thiophene oligomers in solution. *Synth. Met.* **60**, 23-26 (1993).



## Chapter 4

Photovoltaic property  
evaluation of  
conjugated polymers

#### 4.1. Introduction

Sustainability of our ecosystem depends on the development of renewable energy sources. The toxic and climate changing by-products of our current energy sources are doing serious damage to the planet. Healing effect to the mess that has been already done to the earth can be made by photo conversion of sunlight to electricity directly by means of solar cells or photovoltaic cells. This seems to be the viable long term strategy for a sustainable energy future. Utilization of solar energy as alternative to fossil fuel is a promising option and hence receiving impetus in research field.<sup>1,2</sup> Polymer based organic photovoltaic systems hold the promise for a cost-effective, light weight solar energy conversion platform which could benefit from simple solution processing of the active layer.<sup>3-9</sup> The function of such excitonic solar cells is based on photoinduced electron transfer from a donor to an acceptor. Significant advances in the fundamental understanding of the complex interplay between the active layer morphology and electronic properties are required if this technology is to find viable application.

Although common materials used for photovoltaic are generally inorganic, a serious attention has been made to develop conjugated polymers for polymeric solar cell during last few decades due to its easy processibility, flexibility and low cost.<sup>10-16</sup> Extended  $\pi$ -conjugation along the polymer chain is the pre-requisite condition for photovoltaic applications for such polymers, yet choice of suitable side chains also influences the properties like band gap, ionic conductivity, morphology and miscibility with other substances.<sup>10-12,15</sup> The semiconducting polymers, to be a good photovoltaic material should have effective absorption of the visible light i.e. they are preferred to be low band gap materials.<sup>11,13,17</sup> Generally, polythiophene derivatives viz. poly(3-hexylthiophene) (P3HT), poly(3-octylthiophene)(P3OT) and polyphenylene vinylene (PPV) derivatives are commonly used for this purpose.<sup>8-13,18-21</sup>

The first generation of organic solar cells includes a single organic layer sandwiched between two metal electrodes of different work functions.<sup>22,23</sup> Gradually, development of new conjugated polymers with tailor made properties opened a new path for organic solar cell application. But the single layer devices based on these polymers were showing power conversion efficiency of less than 0.1% only.<sup>24,25</sup> This shortfall of efficiency had harnessed for new device architecture which led to the development of

polymer-fullerene bilayer heterojunction and bulk heterojunction device incorporating C-60 or C-60 derivatives. C-60 and C-60 derivatives act as electron acceptor favoring ultrafast photoinduced electron transfer from optically excited conjugated polymers which provides efficient exciton splitting and improved power conversion efficiency in turn.<sup>26-31</sup>

The concept of hybrid solar cells using simultaneously organic and inorganic materials has been implemented to overcome certain drawbacks of organic semiconductors. Common conjugated polymers suffer from low charge carrier mobility and narrow absorption spectrum. Hybrid polymer-inorganic nanocomposites offer combined advantage of both the materials like solution processing of organic semiconductors and high electron mobility of inorganic semiconductors.<sup>32</sup> Moreover, strong size dependent optical properties of inorganic semiconductor nanoparticles provide the opportunity of optical band gap tuning and sensitization of conjugated polymers. Several hybrid polymer bulk heterojunction solar cells have been reported including nanoparticles of CdSe, TiO<sub>2</sub> and ZnO.<sup>11,32,33-37</sup>

The other useful approach for organic solar cells is the guest–host approach. The basic idea is to form a system composed of three components: donor component, acceptor component and the polymeric matrix. The embedding of the photoactive conjugated polymer–acceptor blend into a conventional polymer matrix i.e. guest-host approach is a sound and promising method to improve photoactive sample quality for the following reasons: less interchain interaction, possibility of ordering in the matrix, increase in the stability of the photoactive polymer, possibility of tuning of charge transfer by changing intermolecular distance or dielectric permittivity of the host matrix. In the guest-host approach the conjugated polymers are better encapsulated against environmental influences.<sup>38-40</sup>

In this chapter, we have demonstrated the photovoltaic performance of the synthesized polymers. Single layer, bulk heterojunction, hybrid organic-inorganic and host-guest approach of solar cells for the developed conjugated polymers have been reported. The polymers showed power conversion efficiency in the range 0.019-0.38% with respect to polymers and processing conditions.

## 4.2. Experimental

### 4.2.1. Materials

Poly(ethylene-dioxy-thiophene):poly(styrene sulphonate) (PEDOT:PSS) (Aldrich), (6,6)-phenyl C<sub>61</sub>-butyric acid methyl ester (PCBM) (Aldrich), ITO coated glass (Aldrich), TiO<sub>2</sub> nanoparticles (5 nm)(Aldrich) were used as received. All the solvents were properly purified before use by standard methods. The synthesized polymers reported in Chapter 2 were used for study of photovoltaic performance.

### 4.2.2. Fabrication and characterization of polymer solar cells

Solar cells were fabricated with the structure of ITO/PEDOT:PSS/Polymer:PCBM (or TiO<sub>2</sub> nanoparticles)/Al. The ITO coated glasses were pre-cleaned and a thin layer PEDOT:PSS was spin cast from a PEDOT:PSS (Aldrich) aqueous solution onto it and dried in vacuum oven at 120<sup>0</sup>C for 20 min. The thickness of PEDOT:PSS layer was ca. 60 nm. The photosensitive blend layers were composed of polymer and PCBM in tetrahydrofuran (THF) (1:2. w/w) in case of organic bulk heterojunction (BHJ) device. Polymer-inorganic hybrid solar cells involve dispersion of TiO<sub>2</sub> nanoparticles in polymer solution in THF (1:2 w/w). In both the cases, concentration of polymer is maintained at 10mg/ml for active layer film formation. The photosensitive blend layer was spin-cast on the ITO/PEDOT:PSS electrode and dried at 75<sup>0</sup>C for 30 min. The thickness of the photosensitive layer was ca. 90 nm which was spin cast at the rotating speed of 1200rpm for 60 seconds. Then the metal cathode of Al was deposited on the polymer layer by vacuum evaporation under (4X10<sup>-5</sup>Pa). The effective area of one cell is about 3 mm<sup>2</sup>. The single layer solar cell was also fabricated by the same procedure with the structure ITO/Polymer/Al. The current-voltage (*I-V*) measurements of the device were conducted on Keithley 2420 Source Measure Unit. A Xenon lamp with AM1.5 filter (Newport Oriel, USA) was used as the white light source, and the incident optical power at the sample was 100mW/cm<sup>2</sup>.

The photovoltaic cells with host-guest structures using two polyurethanes viz. PU<sub>1</sub> and PU<sub>2</sub> with Rhodamine B were fabricated with the structure of ITO/PEDOT:PSS/PU<sub>1</sub> (or PU<sub>2</sub>) + Rhodamine B:TiO<sub>2</sub> nanoparticles/Al. The

photosensitive blend layer comprising polyurethane and Rhodamine B as host-guest mixture as well as dispersed TiO<sub>2</sub> nanoparticles in tetrahydrofuran (THF) was spin-coated on the ITO/PEDOT:PSS electrode and dried at 75°C for 30 min. Polyurethane and Rhodamine B, the host-guest mixture were taken in 3:1 (w/w) ratio whereas TiO<sub>2</sub> nanoparticles was taken in 2:1 (w/w) ratio to the composite weight of host-guest mixture. This composition gives stable film when 2% (w/v) host-guest mixture in THF is spin coated onto anode.

#### 4.2.3. Test system and configuration

Figure 4.1 illustrates the measurement configuration for generating the illuminated forward bias *I-V* characteristics, using a Keithley Model 2420 and a 4-wire connection to the cell. A solar simulator provides appropriate illumination for the cell and a cooled, vacuum hold-down chuck secures the cell and provides isothermal test conditions

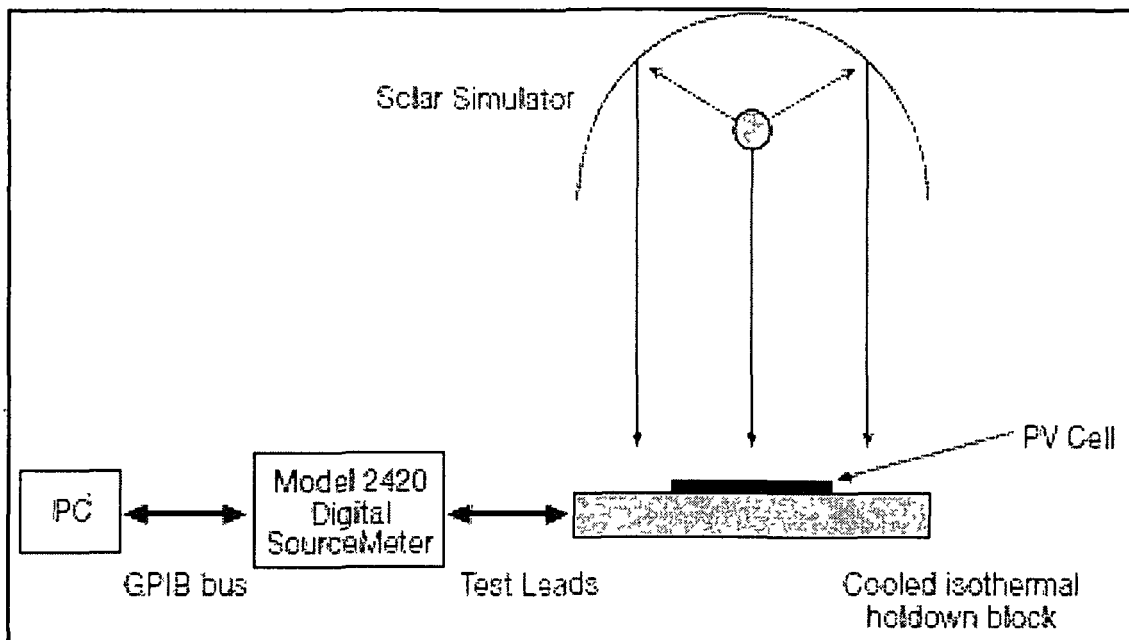
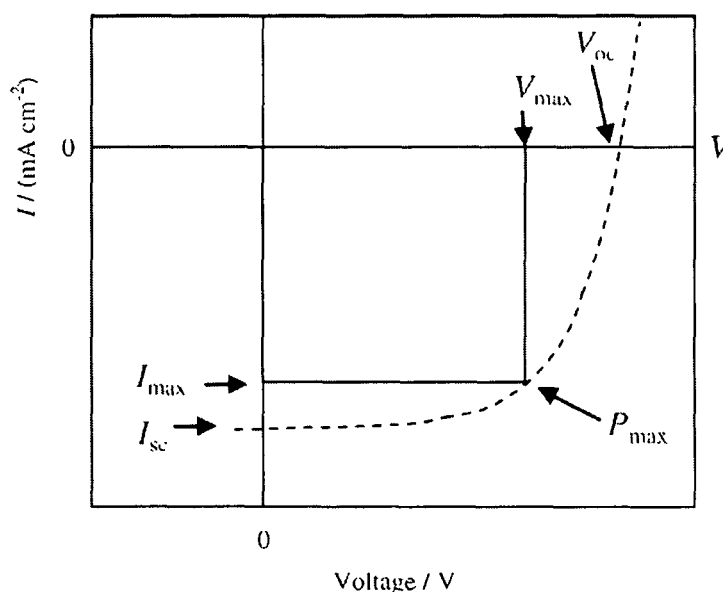


Figure 4.1; *I-V* Measurement configuration

#### 4.2.4. Evaluation of photovoltaic parameters

Photovoltaic parameters and efficiency of the cells can be evaluated from the characteristic  $I$ - $V$  curve under illumination of AM 1.5 with intensity of  $100 \text{ mW/cm}^2$ . The typical  $I$ - $V$  curve of a sample is shown in Figure 4.2 to illustrate the calculation of different parameters.



**Figure 4.2:** Typical  $I$ - $V$  curve of a photovoltaic cell

The device parameters can be calculated using the following equations:

$$FF = P_{\max} / I_{SC} \cdot V_{OC} = I_{\max} \cdot V_{\max} / I_{SC} \cdot V_{OC} \quad (4.1)$$

$$\eta_e (\%) = FF \cdot I_{SC} \cdot V_{OC} / P_{in} \times 100 \quad (4.2)$$

where  $V_{OC}$  is the open-circuit voltage,  $I_{SC}$  is the short-circuit current, FF is the fill factor,  $\eta_e$  is the power conversion efficiency,  $P_{in}$  is the intensity of the white light and  $V_{\max}$  and  $I_{\max}$  are the voltage and the current at the maximum power point of the  $I$ - $V$  curve.



### 4.3. Results and discussion

#### 4.3.1. Single layer and bulk heterojunction photovoltaic performance of PBTD

Single layer solar cells consisting of only one semiconductor material are often referred to as Schottky type devices. In such cells, a single organic layer is sandwiched between two metal electrodes of different work functions. The structure is simple but an absorption covering the entire visible range is rare using a single type of molecules. In our case, The single layer solar cell based on PBTD with the structure ITO/Polymer/ Al has power conversion efficiency ( $\eta_e$ ) of 0.019% with short circuit current  $I_{SC} = 0.86$  mA/cm<sup>2</sup> and open circuit voltage  $V_{OC} = 0.1$  V. The fill factor (FF) of the device is calculated to be 0.23. The photoactive region is very thin and since both positive and negative photoexcited charges may travel through the same path, recombination losses are generally very high.<sup>41</sup> So, Power conversion efficiency in the case of single layer polymer solar cells is low as witnessed in case of PBTD based single layer solar cell.

The increase in power conversion efficiency (PCE) to high extent is observed for the bulk heterojunction solar cell device based on the same polymer. The structure of the solar cell is ITO/PEDOT:PSS/PBTD:PCBM (1:2 w/w)/ Al where the polymer is used as electron donor, PCBM is used as the electron acceptor and PEDOT:PSS layer is used as hole injecting layer. The power conversion efficiency (PCE) for this device is 0.38% with the calculated  $V_{OC}$  and  $I_{SC}$  values of 0.37 V and 2.51 mA/cm<sup>2</sup>, respectively. *I-V* curves of single layer and bulk heterojunction devices (BHJ) are shown in Figure 4.3 and the photovoltaic parameters are listed in Table 4.1. The PCE of bulk heterojunction structured solar cell has shown increase of PCE to 20 times compared to single layer cell which is the result of efficient exciton harvesting by creating a highly folded architecture such that all excitons are formed near a heterojunction. This favours splitting as well as collection of opposite charges by the respective electrodes.<sup>26,30,31</sup> Although, the polymer possesses matching HOMO levels as shown in Figure 4.4 to inject holes to ITO through PEDOT:PSS layer, PCE of the BHJ is found to be low. This may be attributed to the comparatively high band gap of PBTD (> 2.0 eV) and inability of harvesting higher range solar spectrum thereby limiting the photocurrent.<sup>11</sup> PCE of the polymer (PBTD) based solar cell may be increased to higher level by optimization. Polymer purity, polymer to

acceptor (PCBM) ratio, use of processing additives, solvent annealing are the some of the factors which affect the efficiency ( $\eta_e$ ) of the polymeric solar cells.<sup>6,42-45</sup> Although by introducing PCBM as electron acceptor we are achieving higher conversion efficiency, the cost of the same is much higher than inorganic known acceptor,  $\text{TiO}_2$ . This encourages us to replace PCBM as acceptor for rest of our studies.

**Table 4.1:** Summary of the photovoltaic performance for the solar cells based on PBTD

Photoactive layer	$V_{oc}$ (V)	$I_{sc}$ ( $\text{mA}/\text{cm}^2$ )	FF	PCE, $\eta_e$ (%)
Single Layer	0.1	0.86	0.23	0.019
PBTD / PCBM BHJ Layer	0.37	2.51	0.41	0.38

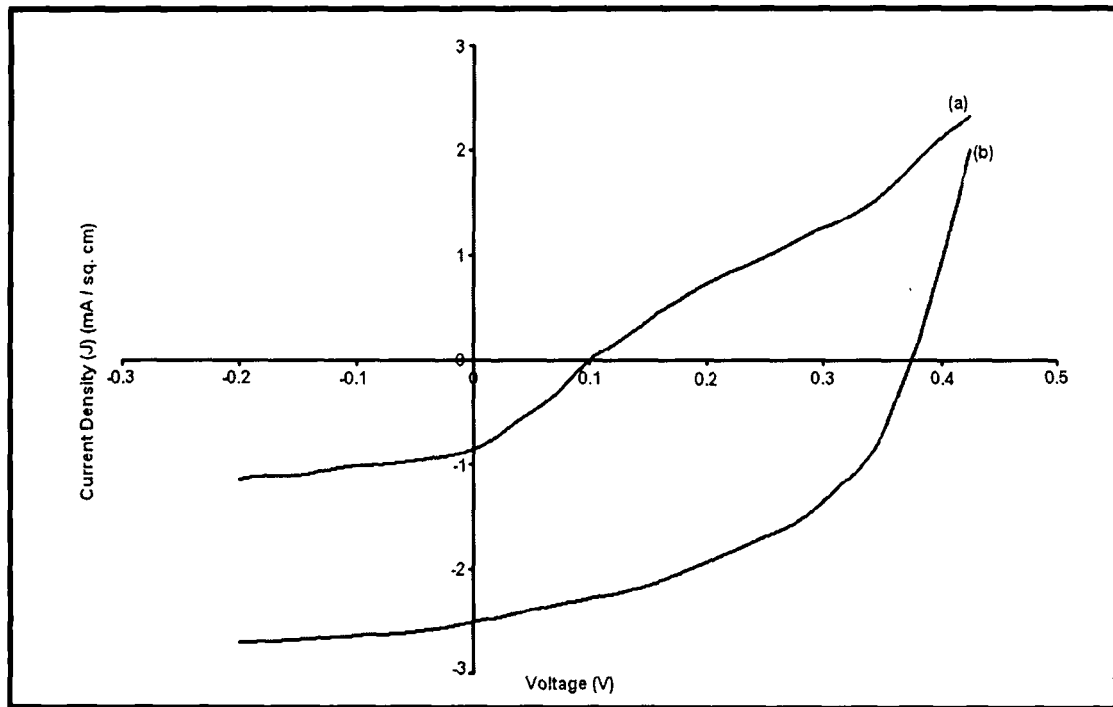


**Figure 4.3:**  $I$ - $V$  characteristics of photovoltaic devices (a) single layer structure (ITO/PBTD/Al), and (b) bulk heterojunction structure (ITO/PEDOT:PSS/PBTD:PCBM (1:2 w/w)/ Al

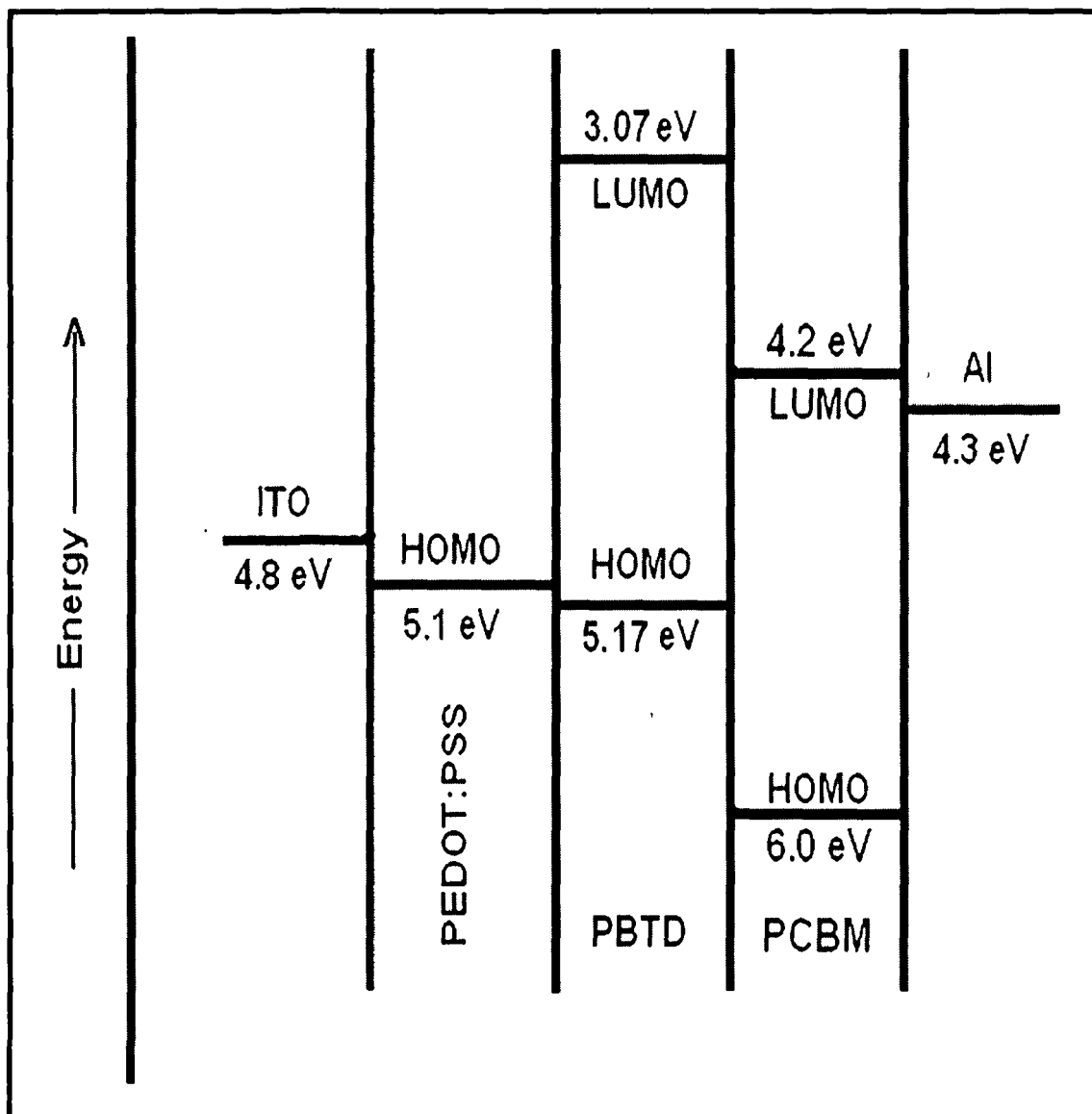


**Figure 4.4:** Schematic energy level diagram for PBTd based bulk heterojunction device, with energy levels in eV relative to vacuum.

### 4.3.2. Polymer-inorganic hybrid photovoltaic cells based on PPAET and PPABT

The concept of hybrid solar cells using simultaneously organic and inorganic materials has been implemented to overcome certain drawbacks of organic semiconductors. Hybrid polymer-inorganic nanocomposites offer the combined advantages of both the materials: solution processing of polymer semiconductors and high electron mobility of inorganic semiconductors. Moreover, strong size dependent optical properties of inorganic semiconductor nanoparticles provide the opportunity of optical band gap tuning and potentially sensitization of conjugated polymers by mixing them. Several hybrid polymer bulk heterojunction solar cells have been reported including nanoparticles of CdSe, TiO<sub>2</sub> and ZnO. Hybrid device based on zinc oxide (ZnO) nanoparticles (5 nm) and poly[2-methoxy-5-(3,7-dimethyloctyloxy)]-1,4-phenylenevinylene(MDMO-PPV) exhibited power conversion efficiency (PCE) of 1.1%.<sup>37</sup> PCE reported for hybrid solar cells based on blends of isotropic TiO<sub>2</sub> particles with poly(3-hexylthiophene) (P3HT) and elongated TiO<sub>2</sub> rods with poly[2-methoxy-5-(2'-ethyl-hexyloxy)-1,4-phenylene vinylene] (MEH-PPV) were 0.42% and 0.49%, respectively.<sup>46,47</sup> G. D. Sharma et al. reported hybrid solar cell from poly(3-phenyl azomethine thiophene) (PPHT) with ZnO and dye-sensitized PPHT with ZnO thin films. The dependence of photovoltaic parameters on the weight fraction of ZnO in PPHT: ZnO was also investigated and found that the device with 45% of ZnO in both composites exhibited the best photovoltaic performance with PCE being 0.12% and 0.52%, respectively.<sup>48</sup>

The photovoltaic properties of the side chain azomethine linkage containing polythiophene derivatives i.e. PPAET and PPABT have been studied by fabricating the device with the structure of ITO/PEDOT:PSS/Polymer:TiO<sub>2</sub> nanoparticles (1:2 w/w)/ Al where the conjugated polymers are used as electron donor and TiO<sub>2</sub> nanoparticle is used as the electron acceptor. The exciton formation upon absorption of photon is the primary process which is followed by ultrafast electron transfer from LUMO of donor to acceptor. Thus electrons are collected at Al electrode through acceptor and holes are collected at ITO via hole injecting PEDOT: PSS layer thereby causing voltage difference in two electrodes. *I-V* curve for the devices based on PPAET and PPABT is shown in Figure 4.5 and photovoltaic parameters are listed in Table 4.2.

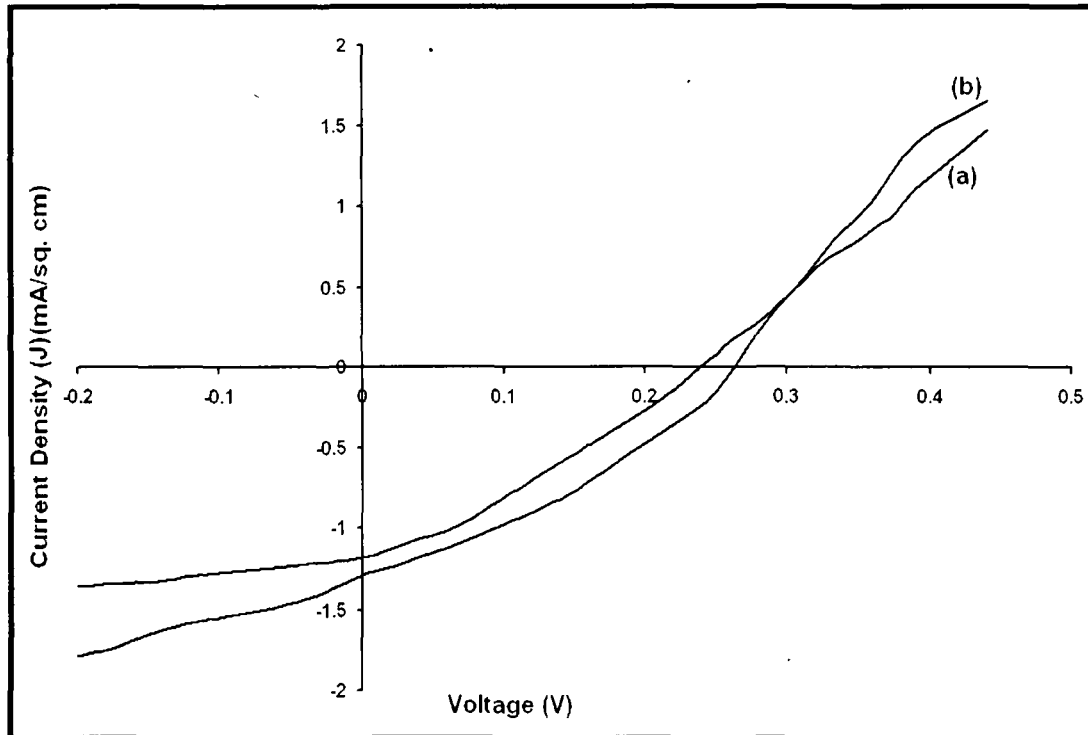


**Figure 4.5:** *I-V* characteristics of photovoltaic devices of the structures (a) (ITO/PEDOT:PSS/PPAET:TiO<sub>2</sub> nanoparticles (1:2 w/w)/ Al) and (b) (ITO/PEDOT:PSS/PPABT: TiO<sub>2</sub> nanoparticles (1:2 w/w)/ Al)

The fabricated photovoltaic devices based on the synthesized polymers, PPAET and PPABT show power conversion efficiency (PCE) ( $\eta_e$ ) of 0.102% and 0.125%, respectively.  $I_{SC}$ ,  $V_{OC}$  and FF exhibited by the device based on PPAET are 1.16 mA/cm<sup>2</sup>, 0.24 V and 0.36 while the same parameters exhibited by the device based on PPABT are 1.29 mA/cm<sup>2</sup>, 0.26 V and 0.37. PPABT based hybrid photovoltaic device shows higher PCE compared to the device based on PPAET though the devices are fabricated in similar conditions. This is attributed to higher donor ability of PPABT than that of PPAET as revealed in electrochemical study resulting easier exciton formation. Moreover, lower band gap of PPABT facilitates higher absorption of irradiated radiation thereby affecting improvement of PCE. The energy level diagram (Figure 4.6) of the devices also explain the reason of higher  $I_{SC}$  and PCE exhibited by the photovoltaic device with the donor polymer, PPABT compared to the other fabricated device with PPAET. The HOMO

energy level of PPAET is lying 0.06 eV lower to that of PPABT causing less efficient hole migration to PEDOT:PSS hole injecting layer.

**Table 4.2:** Photovoltaic properties of PPAET and PPABT based hybrid devices

Photoactive layer	$V_{OC}$ (V)	$I_{SC}$ (mA/cm <sup>2</sup> )	FF	PCE, $\eta_e$ (%)
PPAET: TiO <sub>2</sub> nanoparticles	0.24	1.16	0.36	0.102
PPABT: TiO <sub>2</sub> nanoparticles	0.26	1.29	0.37	0.125

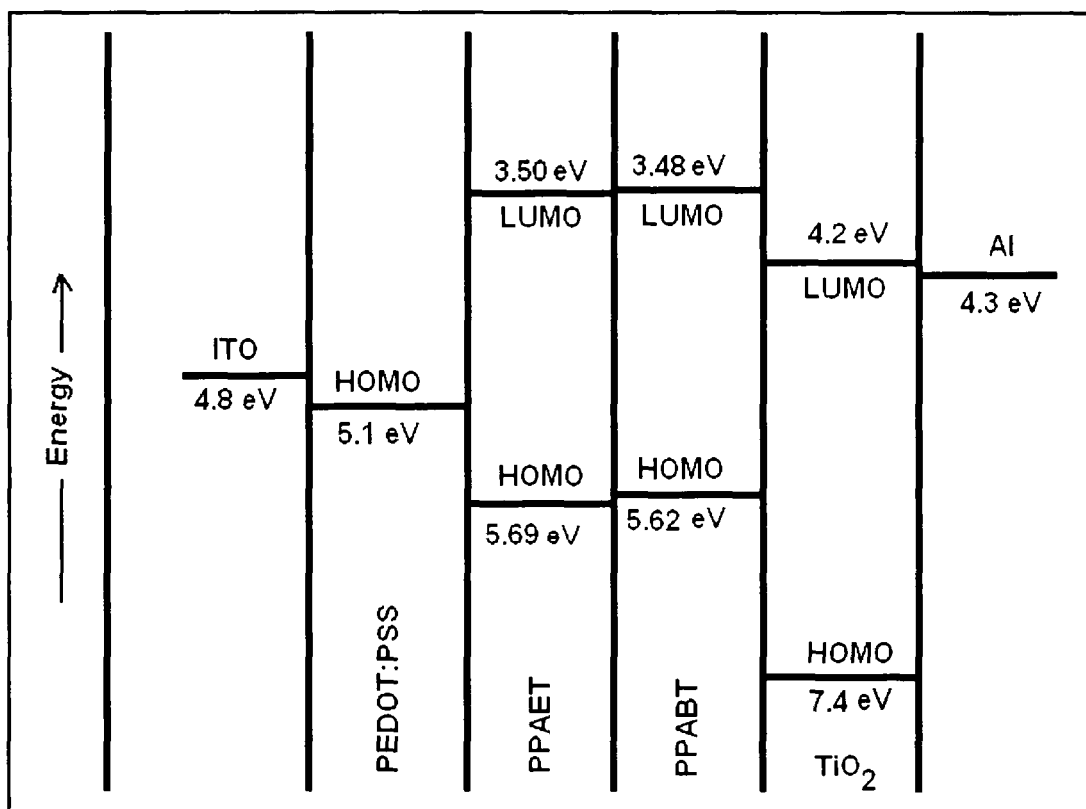


**Figure 4.6:** Schematic energy level diagram for the PPAET and PPABT based hybrid photovoltaic devices device, with energy levels in eV relative to vacuum.

### 4.3.3. Polymer-inorganic hybrid photovoltaic device for PDDC and PDDCT and effect of annealing

Among the different conjugated polymers, polycarbazole derivatives are of great importance owing to its various useful properties; such as easy formation of relatively stable radical cations (holes), high charge carrier mobility's, and high thermal and photochemical stability and hence are suitable in many optoelectronic applications.<sup>49-56</sup> A soluble and processable polycarbazole with a branched 2-decyltetradecyl substituent on nitrogen was designed and synthesized by a Ni(COD)<sub>2</sub>-mediated Yamamoto coupling polymerization by J. Li et al.<sup>54</sup> The same polymer was used to fabricate photovoltaic device with perylene diimide dye as an electron acceptor and showed a short circuit current ( $I_{sc}$ ) of 0.26 mA/cm<sup>2</sup>, an open circuit voltage ( $V_{oc}$ ) of 0.71 V, a fill factor (FF) of 37%, and a PCE value of 0.63%. Leclerc and co-workers further reported a series of poly(3,6-carbazole) derivatives using different electron-deficient moieties fabricated solar cell with the acceptor [6,6]-phenyl C<sub>61</sub>-butyric acid methyl ester (PCBM) and found power conversion efficiency in the range of 0.8-1.1% .<sup>50</sup> The power conversion efficiency of polymeric solar cells can be improved by multiparametric optimization, where annealing of active layer plays a vital role.<sup>57-59</sup> J. H.-J. Huang *et.al.* reported the effect of annealing on polymer photovoltaic devices with blends of poly[9,9'-dioctyl-fluorene-co-bithiophene] with PCBM. The highest PCE of 2.14% with  $V_{oc}$  of 0.99 V and  $J_{sc}$  of 4.24 mA/cm<sup>2</sup> was achieved by annealing of polymer films at 70 °C for 30 minutes.<sup>57</sup> Although many reports regarding study of photovoltaic characteristic of polycarbazole derivatives with organic acceptors (PCBM, perylene diimide etc.) are ubiquitous, very few reports mentioned the study of photovoltaic performance of these derivatives with inorganic acceptors like TiO<sub>2</sub>, ZnO, CdSe etc. Hence, in our approach we have attempted to study the photovoltaic performance of the photoactive layer containing TiO<sub>2</sub> nanoparticles blended with N-alkyl substituted polycarbazole derivatives.

The photovoltaic properties of PDDC and PDDCT have been studied by fabricating the device with the structure of ITO/PEDOT:PSS/Polymer:TiO<sub>2</sub> nanoparticles (1:2 w/w)/ Al where the polymers are used as electron donor and TiO<sub>2</sub> nanoparticle is used as the electron acceptor. The photovoltaic performances of these devices are evaluated before annealing and after annealing at 150 °C for 30 minutes. Figure 4.7 and

Figure 4.8 show the  $I-V$  curves of the PDDC and PDDCT based solar cells under the illumination of AM 1.5,  $100\text{mW}/\text{cm}^2$ , and photovoltaic properties obtained from the  $I-V$  curves are listed in Table 4.3.

The fabricated solar cells based on PDDC and PDDCT have power conversion efficiency ( $\eta_e$ ) of 0.11% and 0.14% for poly(9-dodecylcarbazole) (PDDC) and poly(9-dodecylcarbazole)-co-thiophene (PDDCT), respectively, before annealing. Short circuit current,  $I_{\text{SC}}$  of  $1.27\text{ mA}/\text{cm}^2$  and open circuit voltage,  $V_{\text{OC}}$  of 0.25 V are calculated for PDDC based device and the same for PDDCT based device are  $1.39\text{ mA}/\text{cm}^2$  and 0.28V. The fill factors of the photovoltaic cells are 0.35 and 0.36 for PDDC and PDDCT based polymer-inorganic devices before annealing. The photovoltaic device based on PDDCT shows higher power conversion efficiency compared to that based on PDDC even the devices were fabricated in similar environment and keeping the polymer to acceptor proportion same. This may be due to higher donor ability of PDDCT than PDDC as revealed in electrochemical study and lower band gap of PDDCT compared to PDDC facilitating more absorption of irradiated radiation. The energy level diagram for the fabricated solar cells is shown in Figure 4.9.

The solar cells based on same polymers have been evaluated after annealing the polymer films above their  $T_g$  and near melting region where maximum chain re-organization can be achieved. The spin-coated polymer: acceptor film was thermally annealed at  $150^\circ\text{C}$  to enhance the film morphology characteristic. The fabricated solar cells based on PDDC and PDDCT show power conversion efficiency ( $\eta_e$ ) of 0.18% and 0.24% for poly(9-dodecylcarbazole) (PDDC) and poly(9-dodecylcarbazole)-co-thiophene (PDDCT), respectively, with short circuit current,  $I_{\text{SC}} = 1.34\text{ mA}/\text{cm}^2$  and open circuit voltage,  $V_{\text{OC}} = 0.33\text{ V}$  for PDDC and  $I_{\text{SC}} = 1.74\text{ mA}/\text{cm}^2$  and  $V_{\text{OC}} = 0.36\text{ V}$  for PDDCT based devices. The fill factors of the solar Cells are 0.41 and 0.39 for PDDC and PDDCT donor polymer based polymer-inorganic heterojunction solar cells after annealing. The increase in power conversion efficiency of the cells in this case is the result of thermal annealing. The thermal annealing process enables spatial rearrangements of the polymer chains leading to tight stacking and a strong interchain interaction thereby increasing absorption ability of light.<sup>6,43,57,58</sup> Thus a higher extraction of photocurrent can be expected due to strong absorption of light after annealing of the polymer films.



**Table 4.3.** Photovoltaic properties of PDDC and PDDCT based photovoltaic devices before and after annealing at 150°C for 30 minutes

Processing condition	Photoactive layer	$V_{OC}$ (V)	$I_{SC}$ (mA/cm <sup>2</sup> )	Fill factor (FF)	PCE, $\eta_e$ (%)
Before annealing	PDDC: TiO <sub>2</sub>	0.25	1.27	0.35	0.11
	PDDCT: TiO <sub>2</sub>	0.28	1.39	0.36	0.14
After annealing at 150°C for 30 minutes	PDDC: TiO <sub>2</sub>	0.33	1.34	0.41	0.18
	PDDCT: TiO <sub>2</sub>	0.36	1.74	0.39	0.24

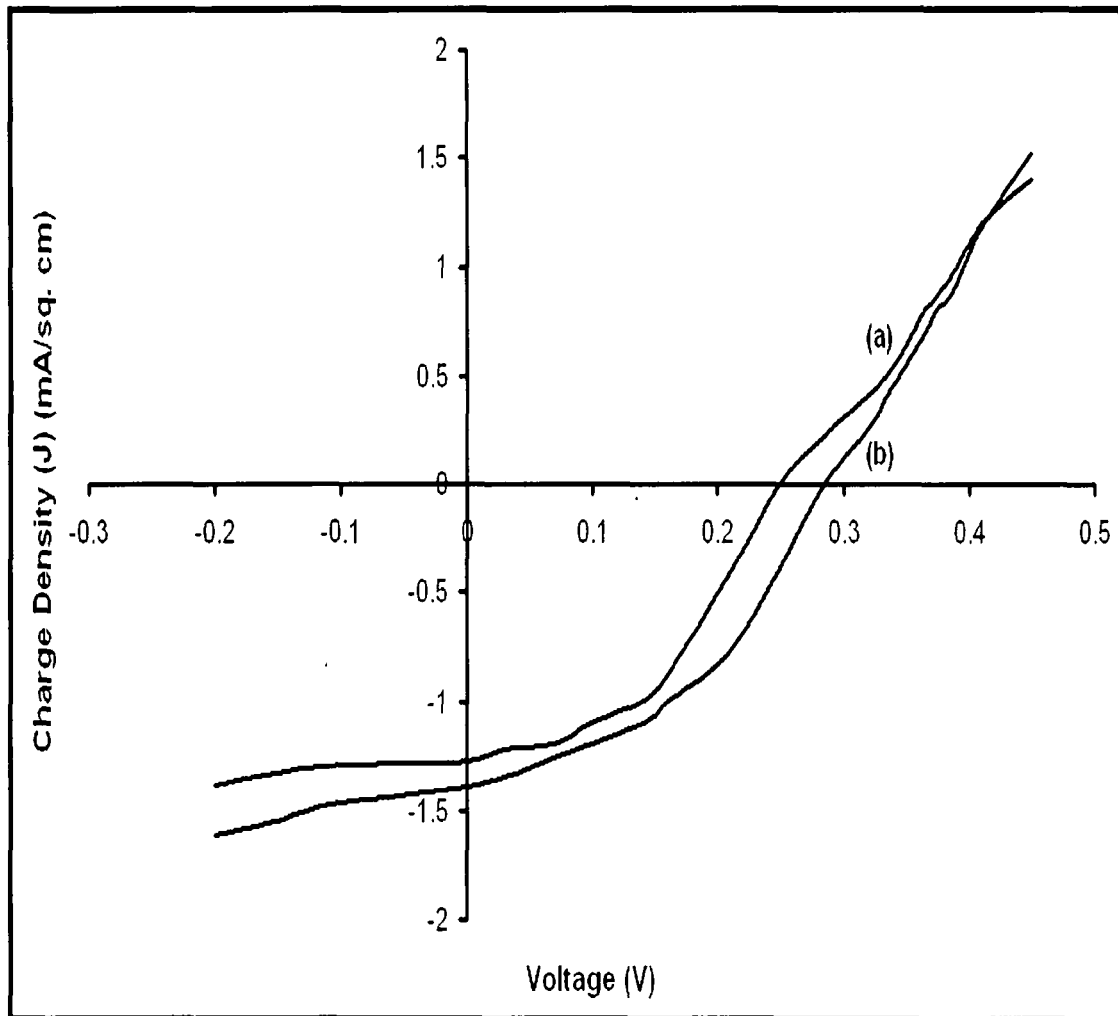


**Figure 4.7:** *I-V* characteristics before annealing of photovoltaic devices with the structures (a) (ITO/PEDOT:PSS/PDDC:TiO<sub>2</sub> nanoparticles (1:2 w/w)/ Al) and (b) (ITO/PEDOT:PSS/PDDCT: TiO<sub>2</sub> nanoparticles (1:2 w/w)/ Al)

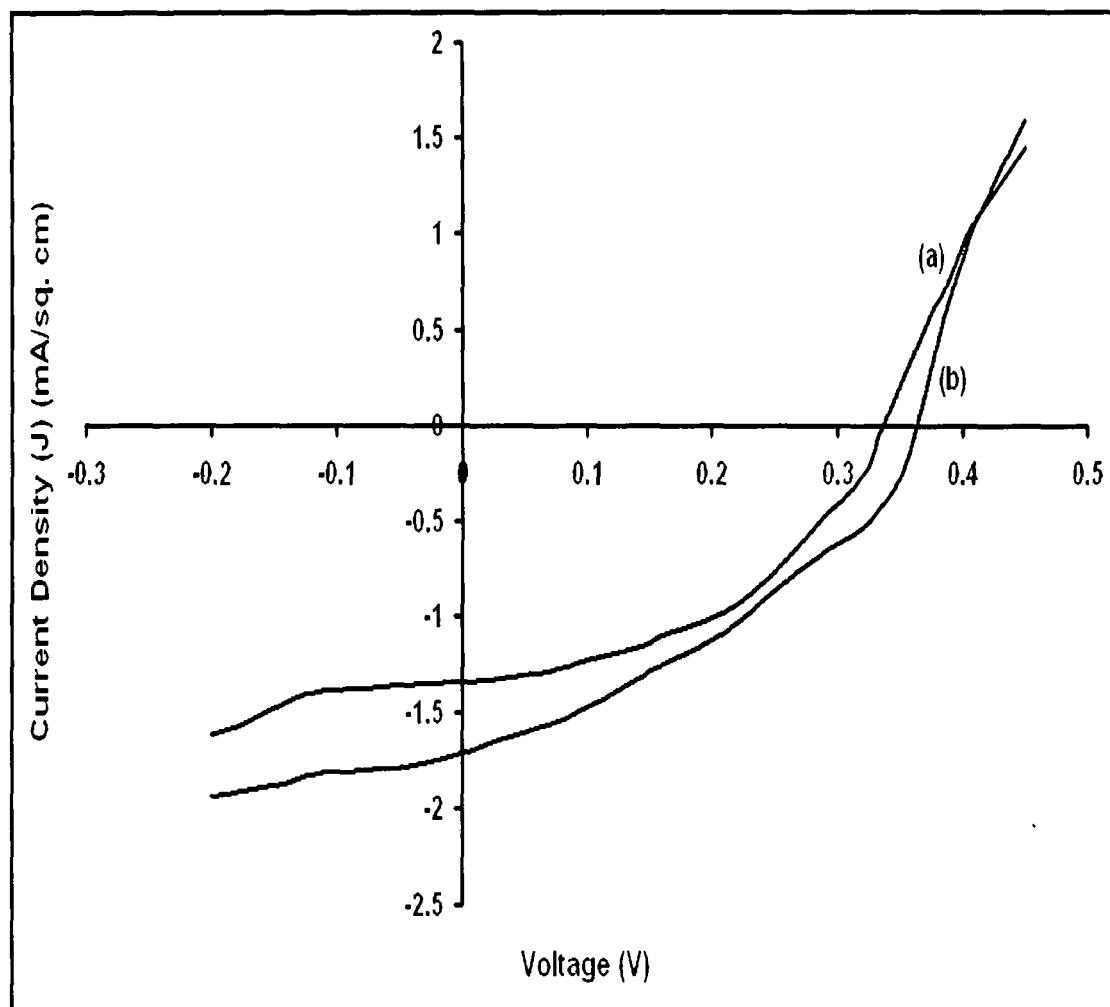


**Figure 4.8:** *I-V* characteristics after annealing to 150°C of photovoltaic devices with the structures (a) (ITO/PEDOT:PSS/PDDC:TiO<sub>2</sub> nanoparticles (1:2 w/w)/ Al) and (b) (ITO/PEDOT:PSS/PDDCT: TiO<sub>2</sub> nanoparticles (1:2 w/w)/ Al

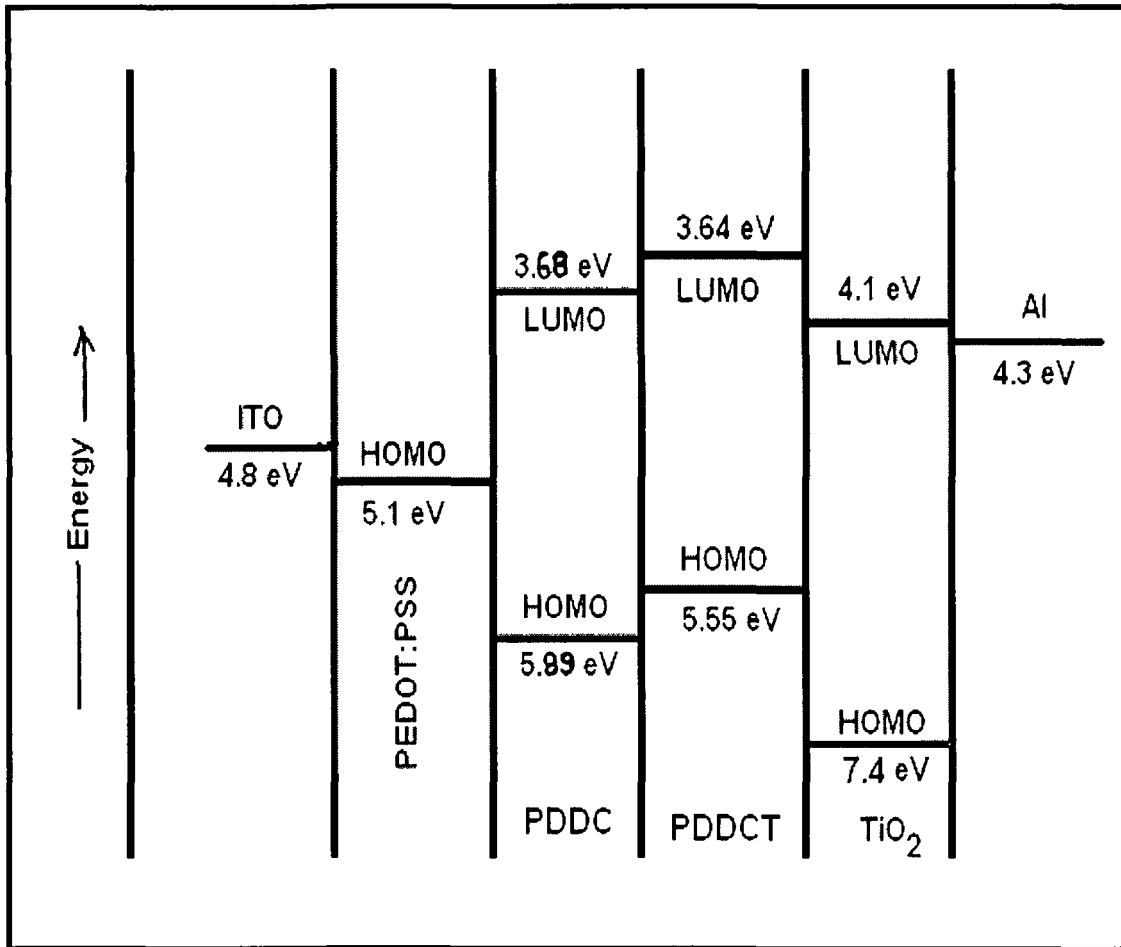


**Figure 4.9:** Schematic energy level diagram for PDDC and PDDCT based devices, with energy levels in eV relative to vacuum.

#### 4.3.4. Host-guest system based photovoltaic cells comprising optically active polyurethanes and Rhodamine B dye

The guest-host approach has been used with success for various applications for the following reasons: less interchain interaction, possibility of ordering in the matrix, increase in stability of the photoactive polymer, possibility of tuning of charge transfer by changing intermolecular distance or dielectric permittivity of the host matrix.<sup>38-40</sup> A set of systems based on conjugated polymer–methanofullerene networks in polystyrene matrix may serve as an example. Solar cell based on a soluble derivative of *p*-phenylene vinylene (MDMO-PPV), and a highly soluble methanofullerene, [6,6']-phenyl C<sub>61</sub>-butyric acid methyl ester (PCBM), embedded into a conventional polymer, polystyrene showed the power conversion efficiency (PCE) of 1.5%.<sup>38</sup> W. A. Luhman et al. reported a composite electron donor layer with host-guest approach consisting of a N,N'-bis(naphthalene-1-yl)-N,N'-bis(phenyl)-benzidine (NPD) host doped with the phosphorescent guest *fac*-tris(2-phenylpyridine)iridium [Ir(ppy)<sub>3</sub>] where the presence of phosphor allows increase in exciton diffusion length. This led to ~80% improvement in power conversion efficiency relative to devices containing an undoped donor layer.<sup>60</sup> The use of small molecules like dyes in organic solar cell is also growing rapidly although there possesses stability issue and dye molecules are one of the widely studied organic compounds in solar cells.<sup>61</sup> P. Ruankham et al. studied performance of ZnO dye sensitized solar cells (DSSC) with Eosin-Y, Rhodamine B and Crystal Violet dyes as sensitizer and showed the energy conversion efficiency of 0.42%.<sup>62</sup> Whereas Rhodamine B and Crystal Violet based DSSCs exhibited an energy conversion efficiency of 0.18% and 0.08%, respectively. But guest-host approach with optically active host materials and small molecule i.e. dye as guests are not properly addressed for solar cell applications yet. In our approach, we have demonstrated the use photoluminescent polyurethane as host material and Rhodamine B dye as guest for efficient solar cells performance so that combination of both would offer easy way of fabricating solar cell by solution processing.

The photovoltaic properties of the guest-host system have been studied by fabricating the device with the bulk heterojunction structure using polyurethane and Rhodamine B dye composite as active material and TiO<sub>2</sub> as acceptor. Figure 4.10 shows

the  $I$ - $V$  Characteristic curve of the fabricated solar cells under the illumination of AM 1.5,  $100\text{mW}/\text{cm}^2$ , and photovoltaic properties obtained from the curve are listed in Table 4.4.

The hybrid polymer-inorganic solar cell based on the guest-host system with the structure ITO/PEDOT:PSS/PU<sub>1</sub>+Rhodamine B:TiO<sub>2</sub> nanoparticles/Al exhibits power conversion efficiency ( $\eta_e$ ) of 0.043% with short circuit current  $I_{SC} = 0.81 \text{ mA}/\text{cm}^2$  and open circuit voltage  $V_{OC} = 0.19 \text{ V}$ . The fill factor (FF) of the device is calculated to be 0.28. Whereas PCE for the device structure ITO/PEDOT:PSS/PU<sub>2</sub>+Rhodamine B:TiO<sub>2</sub> nanoparticles/Al is 0.029%, with  $I_{SC}$ ,  $V_{OC}$  and FF being  $0.56 \text{ mA}/\text{cm}^2$ ,  $0.17 \text{ V}$  and 0.30, respectively..

The photovoltaic devices based on polyurethanes viz. PU<sub>1</sub> and PU<sub>2</sub> as host and Rhodamine B dye as guest are fabricated so that the host molecules get well dispersed in polymer matrix to give uniform films. Generally, small organic molecules bear stability issue compared to polymers as their low thermal stability may cause recrystallization or diffusion into one another, owing to repeated heating and cooling condition. The Rhodamine B dye thus will receive better thermal stability when embedded into polyurethane matrix. Moreover, the combination of optically active photoluminescent host polymer with dye molecule (guest) ensures wide range of absorption ability by the active host-guest material over the solar spectrum thereby providing good option to choose photoluminescent host material to fabricate a solar cell device. Thus efficient photon absorption as well as increase in power conversion efficiency in such devices is desired. But power conversion efficiencies shown by both the guest-host system devices are very low. The reason can be explained with the help of energy level diagram shown in the Figure 4.11. The collection of holes at the anode is limited due to high energy barrier ( $> 0.82 \text{ eV}$ ) between low lying HOMO level of polyurethanes and hole injecting PEDOT: PSS level. This will restrict the charge separation and migration to the two opposite electrodes and results in decrease of  $V_{OC}$  and PCE as well. Moreover, it is apparent that the PCE of the device based on PU<sub>1</sub> matrix showed improvement in PCE compared to that of PU<sub>2</sub>. This can also be explained from energy level diagram as HOMO of PU<sub>2</sub> is lying  $0.1 \text{ eV}$  lower to that of PU<sub>1</sub> thereby causing relatively hindered hole migration to hole injecting layer. This shortfall of inefficient charge collection at the anode could be solved by incorporating a layer with intermediate energy level between

the polymer and PEDOT:PSS layer in multilayer solar cell devices. PU<sub>1</sub> or PU<sub>2</sub> with large band gaps does not show any photovoltaic characteristic when used as donor but they viability for thin film preparation by spin casting with Rhodamine B dye as guest material to use in photovoltaic cells.

**Table 4.4:** Photovoltaic parameters of devices based on PU<sub>1</sub> and PU<sub>2</sub> with Rhodamine B

Photoactive layer	$V_{oc}$ (V)	$I_{sc}$ (mA/cm <sup>2</sup> )	FF	PCE, $\eta_e$ (%)
PU <sub>1</sub> + Rhodamine B	0.19	0.81	0.28	0.043
PU <sub>2</sub> + Rhodamine B	0.17	0.56	0.30	0.029

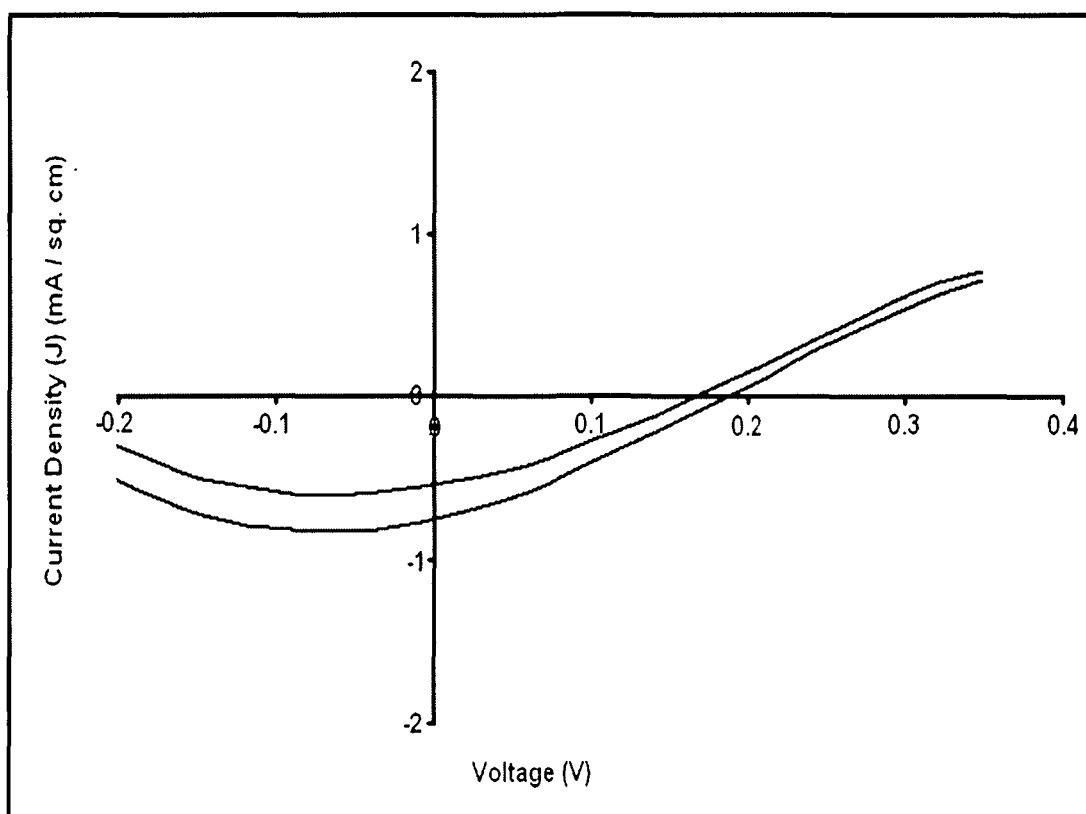


**Figure 4.10:**  $I$ - $V$  Characteristics of (a) PU<sub>1</sub> + Rhodamine B (b) PU<sub>2</sub> + Rhodamine B based photovoltaic devices

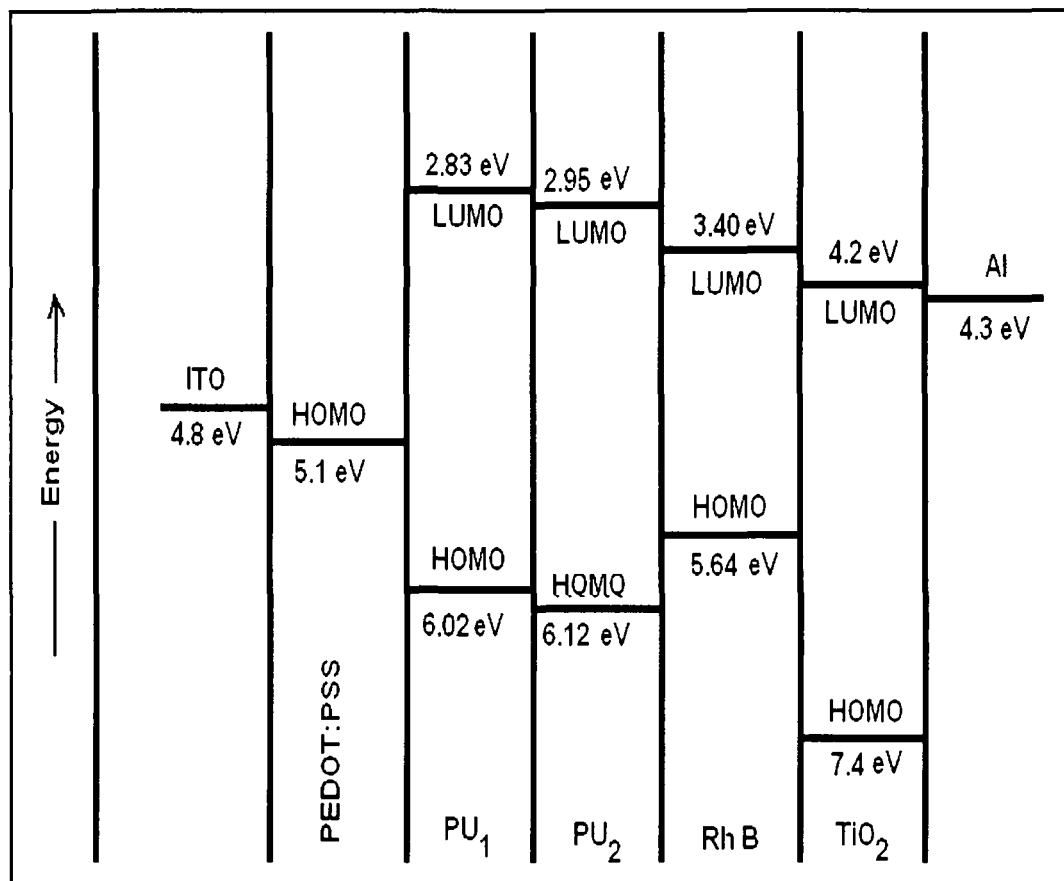


**Figure 4.11:** Schematic energy level diagram for the host-guest system based hybrid heterojunction device, with energy levels in eV relative to vacuum.



#### 4.4. Comparison of power conversion efficiency of devices based on the synthesized polymers

**Table 4.5:** Power conversion efficiency of polymers for different device structures

Polymer	Photovoltaic Device Structure	Power Conversion Efficiency ( $\eta_e$ )
PBTD	Single layer	0.019%
	Bulk heterojunction	0.38%
PPAET	Polymer-TiO <sub>2</sub> hybrid	0.102%
PPABT	Polymer-TiO <sub>2</sub> hybrid	0.125%
PDDC	Polymer-TiO <sub>2</sub> hybrid (Before annealing)	0.11%
	Polymer-TiO <sub>2</sub> hybrid (After annealing)	0.18%
PDDCT	Polymer-TiO <sub>2</sub> hybrid (Before annealing)	0.14%
	Polymer-TiO <sub>2</sub> hybrid (After annealing)	0.24%
PU <sub>1</sub>	Guest-host	0.043%
PU <sub>2</sub>	Guest-host	0.029%

Comparison of photovoltaic device performance of all the polymers with respect to different device architectures is shown in the Table 4.5. The bulk heterojunction solar cell based on PBTD using PCBM as acceptor has shown the highest efficiency of 0.38% among all other devices. This is due to low turn-on potential for p-doping and good absorption ability for PBTD. PPAET and PPABT also hold a promise to be good photovoltaic materials as polymer-inorganic hybrid devices based on these polymers exhibit PCE of 0.102% and 0.125%, respectively. The effect of annealing on improvement of PCE is also witnessed for hybrid devices based on PDDC and PDDCT. The annexed thiophene unit with carbazole derivative in case of PDDCT has immense effect to lower the band gap favoring the quinoid structure of polymer and thus reduces

turn-on potential of p-doping.<sup>13</sup> This structural feature results in receiving higher efficiency for hybrid photovoltaic device based on PDDCT compared to that of PDDC. However, PU<sub>1</sub> and PU<sub>2</sub> shows poor efficiency for their devices with guest-host (rhodamine B dye embedded into polyurethane matrices) architecture where TiO<sub>2</sub> nanoparticles have been used as acceptors. Higher band gap and inability to harvest solar radiation in higher wavelength range are the main causes of the low efficiency for PU<sub>1</sub> and PU<sub>2</sub> based devices. We have successfully demonstrated a few conjugated polymers for photovoltaic applications and optimization of the same to receive the improved power conversion efficiency is not made during this study.

#### 4.5. Conclusion

The synthesized polymers were tested for photovoltaic applications and found that they possess all the concomitant properties to be the photovoltaic materials. The polymers were used as active material in the devices and their performance was calculated with respect to different structures and processing conditions.

- PBDT polymer shows the highest power conversion efficiency of 0.38% for BHJ structure based on organic acceptor PCBM while single layer structure manifested PCE equal to 0.019% only. Efficient charge splitting to respective electrodes due to ultrafast photoinduced electron transfer from polymer to PCBM acceptor is the key factor of increase in PCE in the case of bulk heterojunction solar cell compared to single layer device.

- PPAET and PPABT based polymer-inorganic hybrid solar cells with TiO<sub>2</sub> as acceptor show power conversion efficiency of 0.102% and 0.125%. Use of TiO<sub>2</sub> nanoparticles offers easy and low cost devices apart from other certain advantages.

- PDDC and PDDCT polymer based hybrid solar cells show improvement in PCE on annealing due to better morphological arrangements. The power conversion efficiency for hybrid cell based on PDDC is improved to 0.18% from 0.11% and that of hybrid cell based on PDDCT is found to increase to 0.24% from 0.14% upon annealing at 150°C for 30 minutes.

• PU<sub>1</sub> and PU<sub>2</sub> polymers are used as host material for photovoltaic performance using Rhodamine B dye as guest and showed 0.043% for PU<sub>1</sub> whereas 0.029% for PU<sub>2</sub>. PU<sub>1</sub> or PU<sub>2</sub> with large band gaps does not show any significant photovoltaic characteristic when used as donor but they viability for thin film preparation by spin casting with Rhodamine B dye as guest material to use in photovoltaic cells.

## References

1. Liao, K.-S.; Yambem, S. D.; Haldar, A.; Alley, N.J.; Curran, S.A. Designs and architectures for the next generation of organic solar cells. *Energies* **3**, 1212-1250 (2010)
2. Rockett, A.A. The future of energy-photovoltaics. *Curr. Opin. Solid State Mater. Sci.* **14**, 117-122 (2010)
3. Kippelen, B.; Bredas, J.-L. Organic photovoltaics. *Energy Environ. Sci.* **2**, 251-261 (2009)
4. Krebs, F.C.; Spanngard, H.; Kjaer, T.; Biancardo, M.; Alstrup, J. Large area plastic solar cell modules. *Mater. Sci. Eng. B* **138**, 106-111 (2007)
5. Alstrup, J.; Jørgensen, M.; Medford, A.J.; Krebs, F.C. Ultra Fast and parsimonious materials screening for polymer solar cells using differentially pumped slot-die coating. *ACS Appl. Mater. Interfaces* **2**, 2819-2827 (2010)
6. Peet, J *et al* Efficiency enhancement in low-bandgap polymer solar cells by processing with alkane dithiols. *Nat. Mat.* **6**, 497-500 (2007)
7. Spanggaard, H.; Krebs, F.C. A brief history of the development of organic and polymeric photovoltaics. *Sol. Energy Mater. Sol. Cells* **83**, 125-146 (2004)
8. Hoppe, H.; Sariciftci, N.S. Organic solar cells: an overview. *J. Mater. Res.* **19**, 1924-1945 (2004)
9. Chamberlain, G.A. Organic solar cells: A review. *Solar Cells* **8**, 47-83 (1983)
10. Skotheim, T.A.; Elsenbaumer, R.L.; Reynolds, J.R. *Handbook of conducting polymers* (Marcel Dekker, Inc., New York, 1998)
11. Coakley, K.M.; McGehee, M.D. Conjugated polymer photovoltaic cells, *Chem. Mater.* **16**, 4533-4542 (2004)
12. Bundgaard, E.; Krebs, F.C. Low band gap polymers for organic photovoltaics, *Sol. Energy Mater. Sol. Cells* **91**, 954-985 (2007)
13. Cheng, Y.J.; Yang, S.H.; Hsu, C.S. Synthesis of conjugated polymer for organic solar cell applications, *Chem. Rev.* **109**, 5868-5923 (2009)
14. Helgesen, M.; Søndergaard, R.; Krebs, F.C. Advanced materials and processes for polymer solar cell devices. *J. Mater. Chem.* **20**, 36-60 (2010)

15. Gunes, S.; Neugebauer, H.; Sariciftci, N.S. Conjugated polymer-based organic solar cells. *Chem. Rev.* **107**, 1324-1338 (2007)
16. Dennler, G.; Scharber, M.C.; Brabec, C.J. Polymer-fullerene bulk-heterojunction solar cells. *Adv. Mater.* **21**, 1323-1338 (2009)
17. Nelson, J. Organic photovoltaic films. *Curr. Opin. Solid State Mater. Sci.* **6**, 87-95 (2002)
18. Padinger, F.; Rittberger, R.S.; Sariciftci, N.S. Effects of postproduction treatment on plastic solar cells *Adv. Funct. Mater.* **13**, 85-88 (2003)
19. Arenas, M.C.; Mendoza, N.; Cortina, H.; Nicho, M.E.; Hu, H. Influence of poly3-octylthiophene (P3OT) film thickness and preparation method on photovoltaic performance of hybrid ITO/CdS/P3OT/Au solar cells. *Sol. Energy Mater. Sol. Cells* **94**, 29-33 (2010)
20. Geens, W. *et al* Dependence of field-effect hole mobility of PPV-based polymer films on the spin-casting solvent. *Org. Electron.* **3**, 105-110 (2002)
21. Huang, H.; He, Q.; Lin, H.; Bai, F.; Cao, Y. Properties of an alternating copolymer and its applications in LEDs and photovoltaic cells. *Thin Solid Films* **477**, 7-13 (2005)
22. Marks, R.N.; Halls, J.J.M.; Bradley, D.D.C.; Friends, R.H.; Holmes, A.B. The photovoltaic response in poly(*p*-phenylene vinylene) thin-film devices. *J. Phys. Condens. Matter* **6**, 1379-1394 (1994)
23. Karg, S.; Riess, W.; Dyakonov, V.; Schwoerer, M. Electrical and optical characterization of poly(phenylene-vinylene) light emitting diodes. *Synth. Met.* **54** 427-433 (1993)
24. Antoniadis, H.; Hsieh, B.R.; Abkowitz, M.A.; Jenekhe, S.A.; Stolka, M. Photovoltaic and photoconductive properties of aluminum/poly(*p*-phenylene vinylene) interfaces. *Synth. Met.* **62**, 265-271 (1994)
25. Sariciftci, N.S.; Smilowitz, L.; Heeger, A.J.; Wudl, F. Photoinduced electron transfer from a conducting polymer to Buckminsterfullerene. *Science* **258**, 1474-1476 (1992)

26. Yu, G.; Heeger, A.J. Charge separation and photovoltaic conversion in polymer composites with internal donor/acceptor heterojunctions. *J. Appl. Phys.* **78**, 4510-4515 (1995)
27. Moze, A.J.; Sariciftci, N.S.; Conjugated polymer photovoltaic devices and materials. *C.R. Chimie* **9**, 568-577 (2006)
28. Huang, J.H. *et al* Annealing effect of polymer bulk heterojunction solar cells based on polyfluorene and fullerene blend. *Org. Electron.* **10**, 27-33 (2009)
29. D. Sukeguchi, S. P. Singh, M. R. Reddy, H. Yoshiyama, R.A. Afre, Y. Hayashi, H. Inukai, T. Soga, S. Nakamura, N. Shibata, T. Toru, *Beilstein J. Org. Chem.* **5**, No. 7 (2009); DOI: 10.3762/bjoc.5.7
30. Thompson, B.C.; Frechet, J.M. Polymer-fullerene composite solar cells. *Angewandte Chemie* **47**, 58-77 (2008)
31. Chen, J.; Cao, Y. Development of novel conjugated donor polymers for high-efficiency bulk-heterojunction photovoltaic devices. *Acc. Chem. Res.* **42**, 1709-1718 (2009)
32. Beek, W.J.E.; Wienk, M.M.; Kemerink, M.; Janssen, R.A.J. Hybrid zinc oxide conjugated polymer bulk heterojunction solar cells. *J. Phys. Chem. B* **109**, 9505-9516 (2005)
33. Huynh, W.U.; Dittmer, J.J.; Alivisatos, A.P. Hybrid Nanorod-Polymer Solar Cells. *Science* **295**, 2425-2427 (2002)
34. Sun, B.; Marx, E.; Greenham, N.C. Photovoltaic Devices Using Blends of Branched CdSe Nanoparticles and Conjugated Polymers. *Nano Lett.* **3**, 961-963 (2003)
35. Lin, Y.T. *et al* Efficient photoinduced charge transfer in TiO<sub>2</sub> nanorod/conjugated polymer hybrid materials. *Nanotechnology*, **17**, 5781-5785 (2006)
36. Wu, M.-C. *et al* Nanostructured polymer blends (P3HT/PMMA): Inorganic titania hybrid photovoltaic devices. *Sol. Energy Mater. Sol. Cells* **93**, 961-965 (2009)
37. Beek, W.J.E.; Wienk, M.M.; Janssen, R.A.J. Efficient Hybrid Solar Cells from Zinc Oxide Nanoparticles and a Conjugated Polymer. *Adv. Mater.* **16**, 1009-1013 (2004)

38. Brabec, C.J.; Padinger, F.; Sariciftci N.S., Hummelen, J.C. Photovoltaic properties of conjugated polymer/methanofullerene composites embedded in a polystyrene matrix. *J. Appl. Phys.* **85**, 6866 (1999)
39. Hadziioannou G, van Hutten PF (ed.) *Semiconducting Polymers: Chemistry, physics and engineering*, (WILEY-VCH, Germany, pp554, 2000)
40. Gao, J.; Hide, F.; Wang, H. Efficient photodetectors and photovoltaic cells from composites of fullerenes and conjugated polymers: photoinduced electron transfer *Synth. Met.* **84**, 979-980 (1997)
41. Nunzi, J.-M. Organic photovoltaic materials and devices. *C. R. Physique* **3**, 523-542 (2002)
42. Baran, D. *et al* Processable multipurpose conjugated polymer for electrochromic and photovoltaic applications. *Chem. Mater.* **22**, 2978-2987 (2010)
43. Renz, J.A. *et al* Multiparametric optimization of polymer solar cells: a route to reproducible high efficiency. *Sol. Energy Mater. Sol. Cells* **93**, 508-511 (2009)
44. Song, M.Y.; Kim, J.K.; Kim, D.Y. Temperature effect on photocurrent generation of TiO<sub>2</sub>/conjugated polymer photovoltaic devices. *Synth. Met.* **137**, 1389-1390 (2003)
45. Riedel, I. *et al* Polymer solar cells with novel fullerene-based acceptor. *Thin Solid Films* **451**, 43-47 (2004)
46. Kwong, C.Y.; Djuri, A.B.; Chui, P.C.; Cheng, K.W.; Chan W.K. Influence of solvent on film morphology and device performance of poly(3-hexylthiophene):TiO<sub>2</sub> nanocomposite solar cells. *Chem. Phys. Lett.* **384**, 372-375 (2004)
47. Zeng, T.-W. *et al* A large interconnecting network within hybrid MEH-PPV/TiO<sub>2</sub> nanorod photovoltaic devices. *Nanotechnology* **17**, 5387-5392 (2006)
48. Suresh, P.; Balaraju, P.; Sharma, S.K.; Roy, M.S.; Sharma, G.D. Photovoltaic devices based on PPHT: ZnO and dye-sensitized PPHT: ZnO thin films. *Sol. Energy Mater. Sol. Cells* **92**, 900-908 (2008)
49. Blouin, N.; Michaud, A.; Leclerc, M. A low-bandgap poly(2,7-carbazole) derivative for use in high- performance solar cells. *Adv. Mater.* **19**, 2295-2300 (2007)

50. Leclerc, N.; Michaud, A.; Sirois, K.; Morin, J.F.; Leclerc, M. Synthesis of 2,7-carbazolenevinylene-based copolymers and characterization of their photovoltaic properties. *Adv. Funct. Mater.* **16**, 1694-1704 (2006)
51. Zou, Z.; Gendron, D.; Aïch, B.R.; Najari, A.; Tao Y.; Leclerc, M. A high-mobility low-band gap poly(2,7-carbazole)derivative for photovoltaic application. *Macromolecules* **42**, 2891-2894 (2009)
52. Dierschke, F.; Grimsdale, A.C.; Mullen, K. Efficient synthesis of 2,7-dibromocarbazoles as components for electroactive materials. *Synthesis* **16**, 2470-2477 (2003)
53. Liu, Y. *et al* Synthesis and characterization of conjugated polymers containing, a carbazole moiety. *Polym. Adv. Tech.* **19**, 793-800 (2008)
54. Li, J.; Dierschke, F.; Wu, J.; Grimsdale, A.C.; Mullen, K. Poly(2,7-carbazole) and perylene tetracarboxydiimide: A promising donor/acceptor pair for polymer solar cells. *J. Mat. Chem.* **16**, 96-100 (2006)
55. Morin, J.F.; Drolet, N.; Tao, Y.; Leclerc, M. Syntheses and characterization of electroactive and photoactive 2,7-carbazolenevinylene-based conjugated oligomers and Polymers. *Chem. Mater.* **16**, 4619-4626 (2004)
56. Blouin, N.; Michaud, A.; Gendron, D.; Wakim, S.; Blair, E.; Neagulesu, R.; Belletete, M.; Durocher, G.; Tao, Y.; Leclerc, M. Toward a rotational design of poly (2,7-carbazole) derivatives for solar cells. *J. Am. Chem. Soc.* **130**, 732-742 (2008)
57. Huang, J.H.; Yang, C.Y.; Ho, Z.Y.; Kekuda, D.; Wu, M.C.; Chien, F.C.; Chen, P.; Chu, C.W.; Ho, K.C. Annealing effect of polymer bulk heterojunction solar cells based on polyfluorene and fullerene blend. *Org. Electron.* **10**, 27-33 (2009)
58. Kim, Y. *et al* Composition and annealing effects in polythiophene/fullerene solar cell. *J. Mater. Sci.* **40**, 1371-1376 (2005)
59. JingLu, S. *et al* The effect of annealing treatment on the performance of bulk heterojunction solar cells with donor and acceptor different weight ratios. *Sci. China Ser. G* **52**, 1606-1610 (2009)



60. Luhman, W.A.; Holmes, R.J. Enhanced exciton diffusion in an organic photovoltaic cell by energy transfer using a phosphorescent sensitizer. *Appl. Phys. Lett.* **94**, 153304 (1-3) (2009)
61. Hains, A.W.; Michael, Z.L.; Woodhouse A.; Gregg, B.A. Molecular semiconductors in organic photovoltaic cells. *Chem. Rev* **110**, 6689-6735 (2010)
62. Ruankham, P.; Sae-kung, C.; Mangkorntong, N.; Mangkorntong, P.; Choopun, S. Photoelectrochemical characteristic of ZnO dye-sensitized solar cell with platinum nanoparticle as a counterelectrode *CMU J. Nat. Sci.* **7**, 177-183 (2008)



## Chapter 5

Conclusion and future  
scopes

### 5.1. Conclusions

Conjugated polymers, one of the most studied materials now a day's mesmerize the material scientists in terms of their multiple optoelectronic applications. Amongst different applications, its use in solar cells attracts global importance as it offers potentiality of renewable energy source. In photovoltaics, one of the most critical issues, besides achieving adequate efficiencies and lifetimes, is to reduce the costs associated with achieving economic of scale. Organic solar cells, which can be processed from solution, have great potential to reach the goal of a photovoltaic technology. A large number of different classes of conjugated polymers have been developed such as poly(N-vinylcarbazole)s, poly(fluorine)s (PFs), poly(p-phenylene vinylenes) (PPVs), and poly(thiophenes) (PTs). Polythiophenes and its derivatives are very unique among other polyconjugated systems due to their solubility, environmental stability, fusibility, processibility.

In this thesis, we provide an insight into the synthesis, characterization and concomitant thermal, electrochemical, photoluminescence properties of a few new 1,1'-bis-2-naphthol based polyurethanes, side chain and main chain azomethine linkage containing polythiophene and polycarbazole derivatives. A considerable effort has been devoted to the synthesis of polymers with special emphasis on the solubility, optical and electrochemical properties of  $\pi$ -conjugated polymers. The thesis also provides an account of photovoltaic performances exhibited by the polymers.

The findings of the thesis are described below.

#### (I) Synthesis and characterization of soluble $\pi$ -conjugated polymers

- A series of azomethinic, N-alkyl substituted carbazole derivatives and diol monomers have been synthesised with the yield ranging from 71% to 89%. The formation of monomers was confirmed by FTIR and  $^1\text{H}$  NMR spectroscopy, and CHN analyses.
- The polymers have been prepared by oxidative polymerization using  $\text{FeCl}_3$  and polyurethanes,  $\text{PU}_1$  and  $\text{PU}_2$  have been prepared by condensation

reaction. The polymerization process is slow for oxidative coupling reactions and yields are 51-59%.

- The polymers, PBTD, PPAET, PPABT, PDDC and PDDCT show good solubility in THF, DMF, DMAc, DMSO and NMP due to the presence of alkyl and alkoxy groups as side chain. The reason of good solubility for PU<sub>1</sub> and PU<sub>2</sub> is presence of non-conjugated spacer between the binaphthyl chromophoric groups in the polymer chain.

- The number average molecular weights of polymers are in the range of 3857 to 17647 g/mol. This indicate the prepared polymers are oligomeric in nature.

- Polymers possess good thermal stability with the onset decomposition temperature around 240-305 °C under nitrogen atmosphere, 30-68% weight loss at the temperature of 300-380 °C.

- The polymers exhibit a glass transition temperature (T<sub>g</sub>) in the range of 51-84°C. T<sub>g</sub> of the polymers is established to be side chain dependent. All the polymers possess the suitable thermal properties to receive its applications in photovoltaic devices.

## (II) Study of electrochemical and optical properties of conjugated polymers

- Electrochemical properties of the synthesized polymers are studied from recorded cyclic voltammogram. The polymers bear low oxidation potential compared to reduction potential which indicates that they possess good electron donor ability. HOMO and LUMO energy levels are calculated approximately from the onset oxidation and reduction potential and difference of these level gives band gap of the polymers.

- Electrochemical band gaps of these polymers are found to be in the range of 1.93-3.2 eV. The polymers PU<sub>1</sub> and PU<sub>2</sub> with conjugated-non conjugated system exhibit comparatively higher electrochemical band gaps due to limited conjugation length in the polymer chain.

- The UV-vis absorption spectra of the 0.05% polymer solutions in THF show a broad absorption over the wavelength range of 350-590 nm with

maximum absorption peak at 407 nm, 415 nm and 467 nm ( $\lambda_{\max}$ ), respectively, for PPAET, PPABT and PBTB. This is resulted due to the electronic transition throughout the whole conjugated molecule including both aromatic rings and azomethine (-CH=N-) linkage i.e.  $\pi$ - $\pi^*$  and n- $\pi^*$  transition. PDDC and PDDCT also exhibit absorption maxima at 412 nm and 462 nm. Thiophene moiety attached with 9-dodecyl carbazole unit in PDDCT results in increase of absorption ability.

- The absorptions of the polyurethanes, PU<sub>1</sub> and PU<sub>2</sub> with conjugated-nonconjugated system are found in near blue region. Effective conjugation length in these polymers is restricted by the presence of nonconjugated spacers and thus results decrease in absorption maximum.

- The calculated optical band gaps from onset of absorption spectra are in the range of 2.1-3.4 eV. The polymers exhibit good photoluminescence characteristics in solution. Relative quantum yield with respect to Rhodamine B dye have been calculated and found to be in the range of 0.113-0.846. PBTB exhibited the highest quantum yield whereas PU<sub>1</sub> exhibited the lowest.

- PL characteristic depends on the type of chromophores and conjugation length in the polymers. The PL quenching of the polymers in presence of TiO<sub>2</sub> nanoparticles (or PCBM in case of PBTB) in solution with 1:1 and 1:2 have been observed. This explains the suitability of TiO<sub>2</sub> nanoparticles as electron acceptor in hybrid photovoltaic devices indicating ultrafast electron transfer from donor polymer to acceptor.

### (III) Photovoltaic property evaluation of conjugated polymers

The synthesized polymers were tested for photovoltaic applications and found that they possess all the concomitant properties to be the photovoltaic materials. The polymers were used as active material in the devices and their performance was calculated with respect to different structures and processing conditions.

- PBTB polymer shows the highest power conversion efficiency of 0.38% for BHJ structure based on organic acceptor PCBM while single layer structure manifested PCE equal to 0.019% only. Efficient charge splitting to respective

electrodes due to ultrafast photoinduced electron transfer from polymer to PCBM acceptor is the key factor of increase in PCE in the case of bulk heterojunction solar cell compared to single layer device.

- PPAET and PPABT based polymer-inorganic hybrid solar cells with TiO<sub>2</sub> as acceptor show power conversion efficiency of 0.102% and 0.125%. Use of TiO<sub>2</sub> nanoparticles offers easy and low cost devices apart from other certain advantages.
- PDDC and PDDCT polymer based hybrid solar cells show improvement in PCE on annealing due to better morphological arrangements. The power conversion efficiency for hybrid cell based on PDDC is improved to 0.18% from 0.11% and that of hybrid cell based on PDDCT is found to increase to 0.24% from 0.14% upon annealing at 150°C for 30 minutes.
- PU<sub>1</sub> and PU<sub>2</sub> polymers are used as host material for photovoltaic performance using Rhodamine B dye as guest and showed 0.043% for PU<sub>1</sub> whereas 0.029% for PU<sub>2</sub>. PU<sub>1</sub> or PU<sub>2</sub> with large band gaps does not show any significant photovoltaic characteristic when used as donor but they viability for thin film preparation by spin casting with Rhodamine B dye as guest material to use in photovoltaic cells.

## 5.2. Future scopes

The journey of unconventional optoelectronic devices has started and likely to allure the attention in manufacturing such devices. Here, the electronics must not only bend but also stretch, compress, twist and deform into complex, curvilinear shapes while maintaining levels of performance, reliability, and integration that approach those of well-developed wafer-based systems. Stretchable electronics can be achieved either by use of new structural layouts in conventional materials or development of new materials in conventional lay outs. Any material in sufficiently thin form is flexible, by virtue of bending strains that decrease linearly with thickness. Solution processable conjugated polymers hold the promise of forming thin film by different processing techniques and hence bear suitability of application in stretchable optoelectronics. Stretchable electrodes, LED, Solar cells, offer options for easy carrying and use of these items.

Future directions of study of this present investigation.

1. Theoretical study of band gap and solar cell performance of the polymers
2. Improvement of efficiency of the photovoltaic devices based on the synthesized polymers by multiparametric optimization.
3. Study of these polymers in stretchable solar cells to find its more applicability
4. Study of the synthesized polymers in other optoelectronic devices e.g. LED, electrochromic devices, transistor etc.

## List of Publications

### In Journals

1. **B. Pokhrel**, S. K. Dolui, "Synthesis and characterization of 1,1'-bis-2-naphthol chromophore containing polyurethanes and their electrochemical and photoluminescence properties", *J. Polym. Mater.* 26 (2009) 417-426.
2. J. Maiti, **B. Pokhrel**, R. Boruah, S. K. Dolui, "Polythiophene based fluorescence sensors for acids and metal ions," *Sensors and Actuators B Chemical* 141 (2009) 447-451.
3. S. Konwer, **B. Pokhrel**, S. K. Dolui, Synthesis and Characterization of Polyaniline/Graphite Composites and Study of Their Electrical and Electrochemical Properties, *J. Appl. Polym. Sci.* 116 (2009) 1138.
4. **B. Pokhrel**, S. K. Dolui, Study of hybrid photovoltaic devices based on N-alkyl substituted polycarbazole derivative, *Materials and Manufacturing processes* ( In Press)
5. **B. Pokhrel**, I. R. Kamrupi, J. Maiti, B. Adhikari, "Synthesis, characterization and photovoltaic property evaluation of poly(3-phenyl azomethine alkylthiophene)s", *J. Electron. Mater.* (In press)
6. **B. Pokhrel**, S. Konwer and S. K. Dolui, "Synthesis and photovoltaic properties of conjugated copolymer containing Thiophene-2-carboxyaldehyde and o-Dianisidine" *Thin Solid Films* (Revision submitted)
7. **B. Pokhrel**, S. Konwer, A. Dutta, M. K. Huda, B. Ghosh, S. K. Dolui, "Study of photovoltaic performance of host-guest system comprising optically active polyurethane and Rhodamine B dye", *J. Appl. Polym. Sci.* (Revision submitted)
8. **B. Pokhrel**, S. K. Dolui, "Synthesis, characterization and study of electrochemical behaviour of N-alkyl substituted polycarbazole derivatives" *J. Polym. Mater.* (comm.)
9. I. R. Kamrupi, **B. Pokhrel**, A. Dutta, M. K. Huda, S. Konwer, A. Kalita, M. Boruah, S. K. Dolui, "Synthesis of macroporous polymer particles by suspension polymerization using supercritical carbon dioxide as a pressure adjustable porogen" *Polym. Bull.* (comm.)

### In Proceedings

1. **B. Pokhrel**, S. K. Dolui, "Synthesis and characterization of azomethine based polymer and evaluation of its photovoltaic properties" National Symposium on Photonics and Quantum Structures, Tezpur University, Dept. of Physics, November 2-5, 2009 (Narosa Publishers, In Press)



2. **B. Pokhrel**, S. K. Dolui, "Synthesis and characterization of poly (3-phenyl alkyl azomethine thiophene)s and evaluation of their photovoltaic performance", National Conference on Renewable Energy, Dept. of Energy, Tezpur University, March 23-25, 2010 (Narosa Publishers, In press)

### **Patent(s) Filed**

1. **B. Pokhrel**, S. K. Dolui, "Development of thiophene linked azomethine based polymer for photovoltaic application", (Application no. 1294/KOL/2009 dated 28/10/2009).

### **Conferences Presentation**

1. **B. Pokhrel**, S. K. Dolui, "Synthesis and Characterization of 1,1'-bis-2-naphthol chromophore containing polyurethanes and their electrochemical and photoluminescence properties" International Seminar on Frontier in Polymer Science and Technology (POLY-2007) Guwahati, Assam, India, November 1-3, 2007.
2. S. K. Dolui, Jatindranath Maiti, **Binod Pokhrel**, "Applications of conjugated polymers in electroluminescence and photovoltaic devices", International Conference on Advancement in Polymeric Materials, CIPET Bhubaneswar, Orissa, Feb. 20-22, 2010.
3. **B. Pokhrel**, S. K. Dolui, "Synthesis and characterization of azomethine based polymer and evaluation of its photovoltaic properties" National Symposium on Photonics and Quantum Structures, Tezpur University, Dept. of Physics, November 2-5, 2009.  
(Awarded **Best Poster Presentation**)
4. **B. Pokhrel**, S. K. Dolui, "Synthesis and characterization of poly (3-phenyl alkyl azomethine thiophene)s and evaluation of their photovoltaic performance", National Conference on Renewable Energy, Dept. of Energy, Tezpur University, March 23-25, 2010